

RECOVERY OF VALUE-ADDED PRODUCTS FROM RED MUD AND FOUNDRY
BAG-HOUSE DUST

by

Keegan Hammond

A thesis submitted to the Faculty and the Board of Trustees of the Colorado School of Mines in partial fulfillment of the requirements for the degree of Master of Science (Metallurgical and Materials Engineering).

Golden, Colorado

Date _____

Signed: _____

Keegan Hammond

Signed: _____

Dr. Brajendra Mishra

Thesis Advisor

Golden, Colorado

Date _____

Signed: _____

Dr. Chester VanTyne

Interim Department Head

Department of Metallurgical and Materials Engineering

ABSTRACT

“Waste is wasted if you waste it, otherwise it is a resource. Resource is wasted if you ignore it and do not conserve it with holistic best practices and reduce societal costs. Resource is for the transformation of people and society.”¹

Red mud is a worldwide problem with reserves in the hundreds of millions of tons and tens of millions of tons being added annually. Currently there is not an effective way to deal with this byproduct of the Bayer Process, the primary means of refining bauxite ore in order to provide alumina. This alumina is then treated by electrolysis using the Hall-Héroult process to produce elemental aluminum. The resulting mud is a mixture of solid and metallic oxides, and has proven to be a great disposal problem. This disposal problem is compounded by the fact that the typical bauxite processing plant produces up to three times as much red mud as alumina. Current practice of disposal is to store red mud in retention ponds until an economical fix can be discovered. The danger associated with this current method of storage is immense to the surrounding communities and environment, thus the interest from the Center for Resource Recovery and Recycling (CR³). The purpose of this document is to explain one way to remove the value added materials, primarily iron, from the Jamaican red mud using both pyrometallurgical and hydrometallurgical approaches.

In the beginning, soda ash and carbon roasting were completed simultaneously at 800°C. This type of roasting produced results that were unacceptable. After the soda ash roast was completed independently of carbon roasting, a water wash produced results that separations of alumina at 90%, Iron at 99%, calcium at 99%, titanium at 100%, and sodium by 74%. Smelting produced separations of 97% for alumina, 99% for iron, 87% for sodium, 94% for calcium and 72% for titanium.

TABLE OF CONTENTS

ABSTRACT.....	iii
TABLE OF CONTENTS.....	iv
LIST OF FIGURES	viii
LIST OF TABLES	xi
LIST OF EQUATIONS	xii
ACKNOWLEDGMENTS	xiii
CHAPTER 1	14
INTRODUCTION	14
1.1 Background.....	14
1.2 Motivation for Project.....	14
CHAPTER 2	16
LITERATURE REVIEW	16
2.1 Nature of Bauxite.....	16
2.1.1 Ore Preparation and Mineral Processing	16
2.1.2 Bayer Process Overview	17
2.1.3 Bauxite Preparation and Digestion	18
2.1.4 Impurity Behavior in the Digestion Stage	21
2.1.5 Filtration.....	21
2.1.6 Precipitation.....	22
2.1.7 Calcination.....	22
2.2 Nature of Red Mud	23
2.3 Background of Red Mud.....	24
2.3.1 Previous Red Mud Solution Efforts.....	25
2.3.2 Current Methods of Treatment, Storage and Associated Problems	28

2.3.2.1 Closed Cycle Disposal (CCD)	30
2.3.2.2 Dry Stacking Methods or Thickened Tailings Disposal (TTD).....	31
2.3.2.3 Sea Disposal.....	31
2.3.3 Sources of Red Mud.....	31
2.3.4 Properties of Red Mud.....	32
2.3.5 Applications of Red Mud.....	32
2.4 Red Mud Extraction Processes	34
2.4.1 Initial Plan.....	34
2.4.2 Project Optimization.....	38
CHAPTER 3	39
EXPERIMENTAL PROCEDURES.....	39
3.1 Initial Preparation.....	39
3.1.1 Drying.....	39
3.1.2 Crushing.....	39
3.1.3 Blending and Splitting	39
3.1.4 Thermodynamics.....	40
3.2 Preliminary Sodium Carbonate and Carbon Mixture Roasts.....	41
3.2.1 Roasting Conditions.....	41
3.2.2 Magnetic Separation	42
3.3 Sodium Carbonate Roasts	43
3.3.1 Roasting Conditions.....	44
3.3.2 Thermodynamics.....	44
3.3.3 Water Wash Conditions	44
3.4 Carbon Roasts	46
3.4.1 Roasting Conditions.....	46

3.4.2	Magnetic Separation Conditions.....	46
3.4.3	Thermodynamics.....	47
3.5	Initial Smelting.....	47
3.6	Final Smelting.....	48
3.6.1	Smelting Conditions.....	48
CHAPTER 4		49
RESULTS AND ANALYSIS.....		49
4.1	Initial Sodium Carbonate and Carbon Mixture Roasts	49
4.1.1	Results.....	49
4.2	Sodium Carbonate Roasts	49
4.2.1	Water Wash Results	49
4.3	Carbon Roasts	50
4.3.1	Magnetic Separation Results.....	50
4.4	Final Smelting.....	50
4.4.1	Results by Scanning Electron Microscope (SEM).....	50
4.5	XRD Analysis	50
4.6	QEMSCAN Analysis	52
4.6.1	Elemental Analysis	52
4.6.2	Modal Abundance.....	70
4.6.3	Liberation.....	71
4.7	Economic Analysis	80
CHAPTER 6		82
CONCLUSIONS AND RECOMMENDATIONS		82
5.1	Conclusions.....	82
5.2	Recommendations for Further Work	82

5.3	Contribution to the Field.....	83
	REFERENCES CITED.....	84
	APPENDIX A – PRELIMINARY MAGNETIC SEPARATION.....	88
	APPENDIX B – SODIUM CARBONATE ROASTS WITH WATER WASH	94
	APPENDIX C – CARBON ROASTS AND MAGNETIC SEPARATION	97
	APPENDIX D – FINAL WATER WASH RESULTS.....	100
	APPENDIX E – FINAL MAGNETIC SEPARATION RESULTS	103
	APPENDIX F – FINAL SMELTING PHOTOGRAPHS	104
	APPENDIX G – SCANNING ELECTRON MICROSCOPE RESULTS	106

LIST OF FIGURES

Figure 2-1: The shift from the thermal route (Le Chatelier process) to the hydrometallurgical route (Bayer process)	18
Figure 2-2: Bayer Process Flow sheet	20
Figure 2-3: Locations of Bauxite Mining	32
Figure 2-4: Project Plan	34
Figure 2-5: Bag House Dust QEMSCAN	36
Figure 2-6: Initial Red Mud Extraction Process	37
Figure 2-7: Red Mud Extraction Optimization	38
Figure 3-1: Overall Reaction Stability Diagram $TiO_2+2C+2SiO_2+Na_2CO_3 = Ti+2CO+2NaSiO_2+CO_2$	40
Figure 3-2: Overall Reaction Stability Diagram $Fe_2O_3+2C+Al_2O_3+Na_2CO_3 = 2Fe+CO+2NaAlO_2+2CO_2$	41
Figure 3-3: Temperature vs. Cal/(mol*K) for entire system	43
Figure 3-4: Sodium Carbonate Roasting Stability Diagram	45
Figure 3-5: Carbon Roasting Stability Diagram	47
Figure 4-1: XRD Analysis	51
Figure 4-2: QEMSCAN Image of All Minerals	54
Figure 4-3: QEMSCAN Image of Silicates	55
Figure 4-4: QEMSCAN Image of Carbonates	56
Figure 4-5: QEMSCAN Image of Ilmenite	57
Figure 4-6: QEMSCAN Image of Phosphates	58
Figure 4-7: QEMSCAN Image of Pyrite	59
Figure 4-8: QEMSCAN Image of Chromite	60
Figure 4-9: QEMSCAN Image of AlCaFe Phase	61
Figure 4-10: QEMSCAN Image of FeAlTi Phase	62
Figure 4-11: QEMSCAN Image of FeAl Phase	63
Figure 4-12: QEMSCAN Image of Fe Phase	64
Figure 4-13: QEMSCAN Image of Ti Phase	65
Figure 4-14: QEMSCAN Image of AlMn Phase	66

Figure 4-15: QEMSCAN Image of Al Phase	67
Figure 4-16: QEMSCAN Image of Mn Phase	68
Figure 4-17: QEMSCAN Image of Other Minerals	69
Figure 4-18: Mineral Assay from QEMSCAN	70
Figure 4-19: Overall Liberation	72
Figure 4-20: Al Phase Liberation.....	73
Figure 4-21: AlMn Phase Liberation	73
Figure 4-22: Carbonates Liberation	74
Figure 4-24: Pyrite Liberation	75
Figure 4-27: Ilmenite Liberation.....	76
Figure 4-29: FeAl Phase Liberation.....	77
Figure 4-31: Phosphates Liberation	78
Figure 4-33: FeAlTi Phase Liberation	79
Figure A-1: Preliminary Lower Intensity Magnetic Separation	88
Figure A-2: Preliminary Higher Intensity Magnetic Separation.....	88
Figure A-3: Lower Intensity Magnetic Separation Weights.....	89
Figure A-4: Higher Intensity Magnetic Separation Weights	90
Figure A-5: Lower Intensity Magnetic Separation Test 1 Analysis	90
Figure A-6: Higher Intensity Magnetic Separation Test 1 Analysis.....	91
Figure A-7: Higher Intensity Magnetic Separation Test 2 Analysis.....	92
Figure A-8: Lower Intensity Magnetic Separation Test 2 Analysis	93
Figure B-1: 50% Excess Sodium Carbonate Roast Water Wash Solids Analysis.....	94
Figure B-2: 100% Excess Sodium Carbonate Roast Water Wash Solids Analysis.....	94
Figure B-3: 50% Excess Sodium Carbonate Roast Water Wash Liquids Analysis	95
Figure B-4: 100% Excess Sodium Carbonate Roast Water Wash Liquids Analysis	96
Figure C-1: From Dried Water Wash of 50% Excess Sodium Carbonate Roast and 50% Excess Carbon Roast, Magnetic Fraction	97
Figure C-2: From Dried Water Wash of 50% Excess Sodium Carbonate Roast and 50% Excess Carbon Roast, Non-Magnetic Fraction	97
Figure C-3: From Dried Water Wash of 100% Excess Sodium Carbonate Roast and 50% Excess Carbon Roast, Magnetic Fraction	98

Figure C-4: From Dried Water Wash of 100% Excess Sodium Carbonate Roast and 50% Excess Carbon Roast, Non-Magnetic Fraction	98
Figure C-5: Summary of Carbon Roasts and Magnetic Separation.....	99
Figure D-1: Final Water Wash Liquid Results All Elements	100
Figure D-2: Final Water Wash Liquid Results Excluding Al and Na	101
Figure D-3: Final Water Wash Solids Results All Elements	102
Figure F-1: Final Smelting Top View of Products Broken into Quarters.....	104
Figure F-2: Final Smelting Side View of Products Broken into Quarters	104
Figure F-3: Final Smelting Fe Buttons	105
Figure G-1: Slag SEM XRay Peaks	106
Figure G-2: Iron Button SEM XRay Peaks	107

LIST OF TABLES

Table 1-1: Composition of Dried North Coast Jamaican Bauxite and the Generated Red Mud Compound.....	15
Table 2-1: Typical Phases Present in Red Mud.....	23
Table 2-2: General Properties of Red Mud.....	24
Table 2-3: Recent Red Mud Disasters	29
Table 2-4: Chemical Analysis of Untreated Red Mud.....	33
Table 2-5: Oxides Analysis of Untreated Red Mud.....	33
Table 2-6: Utilization Opportunities for Red Mud	35
Table 2-7: Bag House Dust Analysis.....	37
Table 4-1: Mineral Analysis from QEMSCAN	71
Table 4-2: Reagent Costs for Red Mud Processing	80
Table 4-3: Water and Electric Costs for Red Mud Processing	81
Table 4-4: Final Economics of Red Mud Processing	81
Table D-1: Final Water Wash Conditions	100
Table D-2: Final Water Wash Liquid Results.....	101
Table D-3: Final Water Wash Solid Results.....	102
Table E-1: Final Water Wash Conditions.....	103

LIST OF EQUATIONS

Equation 2-1: Bauxite Calcination.....	21
Equation 2-2: Kaolinite to Sodium Aluminate and Sodium Silicate	21
Equation 2-3: Kalonite Consuming Caustic Reaction	21
Equation 2-4: Calcination of Aluminum Hydroxide	22
Equation 2-5: Overall Red Mud Reduction	35
Equation 3-1: Overall Chemical Equation for Reduction of Red Mud	43
Equation 3-2: Sodium Carbonate Roast.....	43
Equation 3-3: Carbon Roasting.....	46

ACKNOWLEDGMENTS

I would like to thank the CR³ Group for sponsoring this Master's project. I would also like to thank my advisor, Dr. Brajendra Mishra, and my committee members, Dr. Corby Anderson and Dr. Patrick Taylor for their help during the project. I also greatly appreciate the assistance from the graduate and undergraduate students who assisted me throughout graduate school. Last but not least, thank you to my family and friends who have supported and helped me throughout this process.

CHAPTER 1

INTRODUCTION

1.1 Background

Red mud is either a waste or a resource that may one day be a significant source of elements produced from recycling technologies. For the time being however, there have not been enough technological breakthroughs to economically extract the valuables from the red mud. As is apparent in all industrial processes, economics are what drive the industry and determine which technologies will be invested in and will become common practice.

Red mud is a product of the Bayer Process, the primary means of refining bauxite in order to provide alumina. This alumina is then treated by electrolysis using the Hall-Heroult process. The resulting mud is a mixture of solid and metallic oxides, and has proven to be a great disposal problem. This disposal problem is compounded by the fact that typical bauxite processing produces up to three times as much toxic red mud as aluminum. (2,3,6,10,12)

Globally, approximately 44 million tons of primary aluminum are produced annually, by that count there are up to 132 million tons of red mud entering retention ponds and some dry stack tailing areas annually.

1.2 Motivation for Project

The lack of economic solutions to the problem of red mud allows room for significant advancements. With the current price of metals at record highs for most prominent metals, the climate for advancements has never been better. As shown below in Table 1-1: Composition of Dried North Coast Jamaican Bauxite and the Generated Red Mud Compound, red mud is a concentrate of many elements, aluminum especially.

Table 1-1: Composition of Dried North Coast Jamaican Bauxite and the Generated Red Mud Compound

Element	Bauxite (%)	Red Mud (%)
Al ₂ O ₃	56.4	14.7
SiO ₂	0.7	2.6
CaO	1.2	8.8
TiO ₂	4.3	7.2
Fe ₂ O ₃	35.1	60.7
Na ₂ O	0	1.6
Others (P, S, Cr, Mn, Hg, Pb, Zn, Cd, REE, Mg)	2.3	4.4

However, with current ore deposits of iron and aluminum containing relatively high head grades and incredible technological advances in the processing of these ores make for the extraction of iron and aluminum to be economically questionable. Table 1-1: Composition of Dried North Coast Jamaican Bauxite and the Generated Red Mud Compound provides a basic head analysis of a red mud dry stack from Jamaica. Although there are not any elements that produced grades that rival ore deposits, the current price of titanium could make that element in particular economically feasible to extract. Even though the rare earth elements were not analyzed, it was suggested by some experts that other red mud from other areas may be a considerable resource for rare earths. (10)

Since red mud contains such a vast array of elements that are of value to many different industries, the future of research will follow which elements are of the highest value. Currently rare earth magnets are necessary for the advancement of many mineral processing technologies. These will enable the processing of lower grade ores that previously haven't been able to be recovered.

The ability of lower grade ores to be economically mined would signify a new era in the mining industry. These advancements could eventually extend the life of current mines as well as allow for deposits previously thought to be too low in grade to be economically mined.

CHAPTER 2

LITERATURE REVIEW

2.1 Nature of Bauxite

Aluminum is the most abundant metallic element in the earth's crust at approximately 8 wt % (26). Bauxite Ore refers to a deposit of the material that contains high levels of aluminum oxide (Al_2O_3) and low levels of hematite (Fe_2O_3) and silica (SiO_2). This composition makes the ore economically mineable in a variety of locations across the globe. Other potential sources of aluminum include a variety of rocks and minerals including but not limited to, aluminous shale and slate, aluminum phosphate rock and Kaolites (high alumina clays) (27). Bauxite deposits are frequently extremely extensive due to their method of formation over the geological timeline, and thus are found on almost all continents of the world as shown in Figure 2-3: Locations of Bauxite Mining

. Although a worldwide resource, the countries with the largest economically mineable deposits, in order of production, are Australia, Guinea, Brazil, Jamaica and India. The largest consumers of aluminum as of 2002 are The United States of America, Japan and Germany, three countries that do not possess any or very little, bauxite deposits (27).

As the only ore currently being used for the production of aluminum, bauxite consists of multiple hydrous aluminum oxide phases in combination with iron, silicon, titanium oxides and other trace impurities. Gibbsite ($\text{Al}(\text{OH})_3$), boehmite ($(\gamma\text{-AlO}(\text{OH}))$), and diaspore ($(\alpha\text{-AlO}(\text{OH}))$) a form of boehmite that exhibits a more dense state, are the main minerals present in bauxite. Actual hardness of the ore varies dramatically from location to location as friable compacted earth, recemented compacted earth, pisolites (small balls), tubulules (twig like hollow material) have been reported. (10).

2.1.1 Ore Preparation and Mineral Processing

A lack of published literature in the area of mineral processing and ore preparation is largely due to the fact that each ore requires specific processing. The function of this stage in the process is to provide a continuous, consistent and appropriately charged feed to the digesters in the Bayer process to facilitate efficient digestion (10). Generally the material is washed first and screened

to remove irrelevant contaminants such as dirt (29). This procedure is usually completed at the mine site. Particle size is adjusted in the same location where the rest of the Bayer process takes place. A great number of plants now utilize wet grinding mills which are charged with the bauxite ore and a portion of the process solution in order to make a slurry of the material. Completely autogenously mills with diameters over 25 feet are utilizing approximately 8 inch hard bauxite agglomerates as grinding media in Western Australia. (10). Hydrocyclones and screens are used to return the oversize particles to the mill for further grinding. Research has been done on the effects of holding the ground slurry for extended time periods in mechanically agitated tanks to utilize abrasion and finalize particle size reduction (28).

2.1.2 Bayer Process Overview

The Bayer process, named for its developer Karl Josef Bayer in 1888, is still the most widely used method of producing alumina and has had little changes made over the past 125 years.

In 1855, Louis Le Chatelier (1815-1873), the Chief Inspector of Mines in France, invented a process for the recovery of alumina from bauxite. His son, chemist Henri Le Chatelier (1850-1936), is best known for the thermodynamic principle which bears his name. The process involved heating bauxite with sodium carbonate at about 1000°C to form sodium aluminate and then leaching it with water. Aluminum hydroxide is then precipitated from this solution by bubbling CO₂ gas generated during the calcination step. (55)

The process was modified by Karl Josef Bayer (1847-1904) in two stages as seen in Figure 2-1: The shift from the thermal route (Le Chatelier process) to the hydrometallurgical route (Bayer process)

. In 1888, he replaced CO₂ by a seed of aluminum hydroxide on which precipitation took place by vigorous agitation. In 1892, he introduced the pressure leaching step which transformed the process into a fully hydrometallurgical process. This marked the beginning of pressure hydrometallurgy. This process, based on his two German patents, became known as the Bayer process. This process received immediate recognition and is used today in practically the same way as described in the original patents. (55)

The method utilized various techniques including crushing and grinding, high temperature digestion, heat exchangers, clarification, filtration, precipitation, evaporation, rotary kiln and

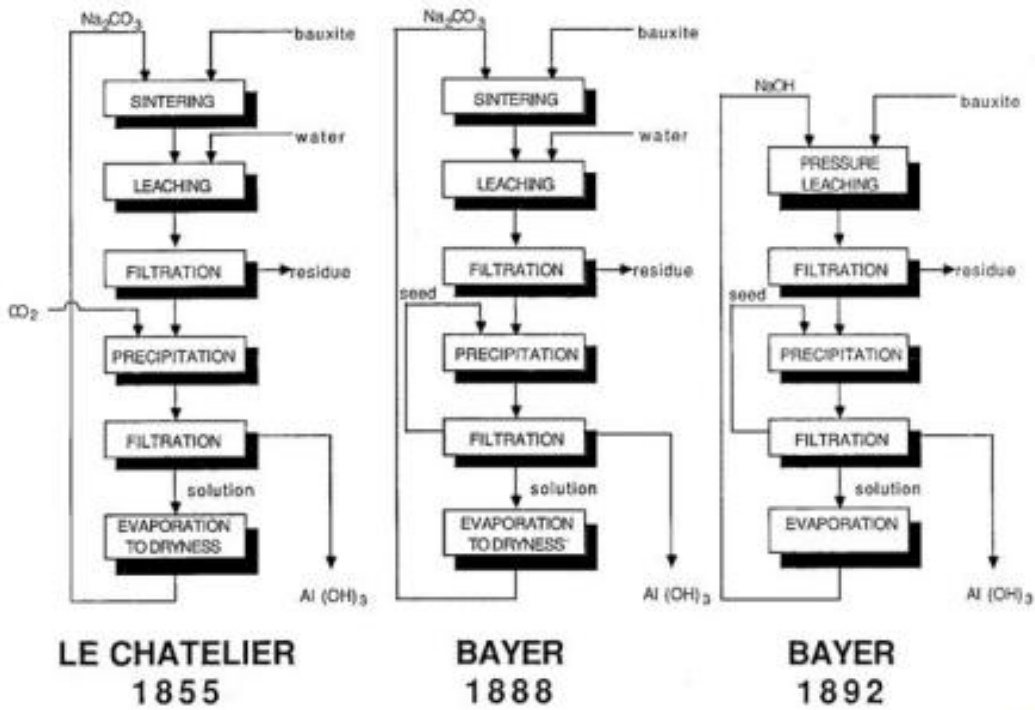


Figure 2-1: The shift from the thermal route (Le Chatelier process) to the hydrometallurgical route (Bayer process)

fluid bed calcinations. A flow sheet of the process is shown in Figure 2-2 (9) above. Since alumina is relatively difficult to reduce it must be void of almost all impurities prior to reduction. If impurities are not removed, when the alumina is reduced by electrolysis to produce aluminum using Hall Héroult Process, most of the impurities are reduced to form metals or metalloids that will allow and contaminate the final aluminum product. Due to this an acceptable alumina contains less than 0.1 weight % of iron, silicon, and titanium oxides (31). The Bayer process provides this level of contaminate elimination, however, during this process approximately three tons of red mud are produced per ton of aluminum metal (30).

2.1.3 Bauxite Preparation and Digestion

Preparing the Bauxite is a process specific to the type of ore being processed. After the washing and screening, the material must then be dried to facilitate further grinding without the formation of agglomerates. Drying must be controlled in order to remove only free water and not the combined water or water of hydration found in the bauxite ore. The digestion process takes advantage of the solubility of amphoteric aluminum oxides in order to form a solution of

aluminate ions that can be removed by filtration leaving the iron and titanium oxides in the solid portion. The next step is calcining that occurs at elevated pressures and temperatures between 135° to 245°C which is determined by the primary mineral form of the ore (Gibbsite or Boehmite) in an effort to encourage the following reaction shown by Equation 2-1 (10).

There are competing incentives for the wide range of variables for concentration and temperature. High concentrations of caustic at high temperatures improve the kinetics of digestions but require more heat exchange equipment and increase the overall digestion operating pressure. In addition, at higher caustic concentrations dilution is required before the precipitation step can occur.

Originally the ground bauxite is mixed with the aqueous sodium hydroxide in the digestion step and then the slurry is pumped into steam jacketed autoclaves and left to react for two to eight hours (32). Although the system is subjected to high sodium hydroxide concentrations, pressured hydrogen embrittlement is not present in the mild steel used. This has been attributed to three factors that protect the steel. First, a tightly adherent scale coating on the steel surfaces, the presence of aluminate ions that reduce the activity of Na_2O , and the presence of iron compounds that cause the caustic solution to become saturated without corroding the reaction vessels (28).

There are two types of impurities found in the digestion stage, soluble in caustic soda (NaOH) or insoluble. The Bayer process removes the ferric oxide and titanium oxide which are unaffected by the caustic solution, and the silica (32). This explains why the resulting residue, red mud, has higher levels of iron, titanium and silica with the iron giving the red mud its coloring. The concentration of caustic is affected by the reaction with other impurities. (10)

Silica is normally found in either the quartz (SiO_2) or kaolinite ($\text{Al}_2\text{O}_3 \cdot 2\text{SiO}_2 \cdot 2\text{H}_2\text{O}$) phases in bauxite. Quartz is insoluble in caustic and reports to the red mud while the kaolinite reacts with sodium hydroxide as shown in Equation 2-2 and Equation 2-3 (28).

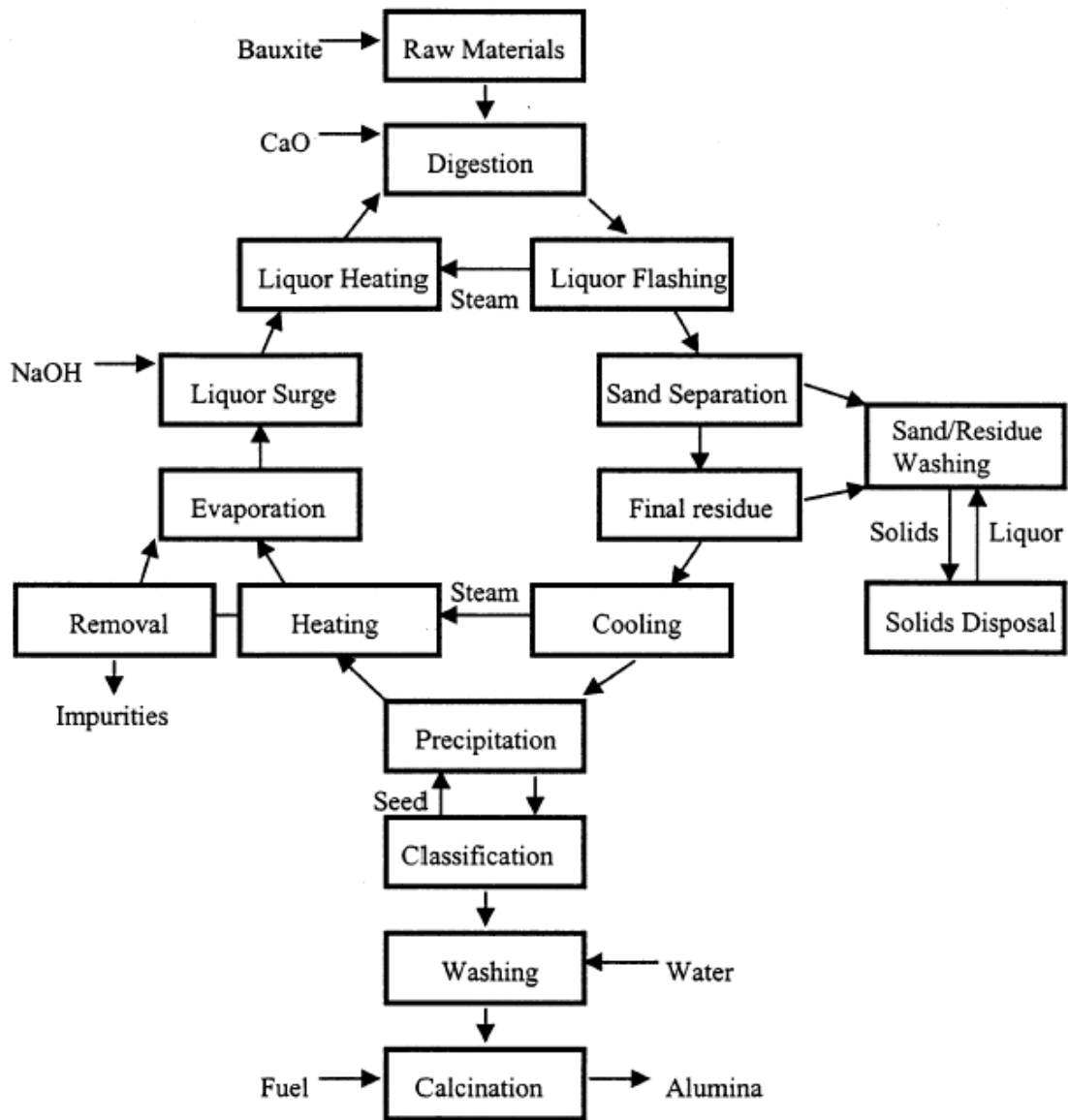
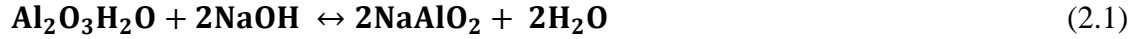
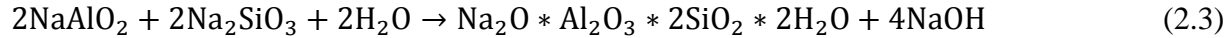
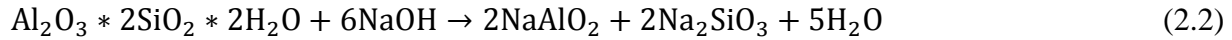


Figure 2-2: Bayer Process Flow sheet



2.1.4 Impurity Behavior in the Digestion Stage



Equation 2-2 Kaolinite to Sodium Aluminate and Sodium Silicate

and above Equation 2-3 Kalonite Consuming Caustic Reaction

show a loss of caustic and alumina reporting to the red mud. Due to this, a complete recovery of aluminum in the bauxite ore is not feasible if there is any silica present. This is the reasoning why there is aluminum in the form of alumina present in the red mud. Silica absorbs approximately equal weights of sodium hydroxide (1kg to 1kg) during the process. The alumino-silicates formed in these reactions is mostly insoluble in the caustion solution although some may dissociate in high sodium hydroxide concentrations. In order to completely precipitate the silica, lime (CaO) is added to the bauxite during fine grinding or digestion to facilitate cancrinite ((Na₂O*Al₂O₃*2SiO₂)*2CaCO₃) formation as this is a less soluble compound. These steps ensure the lowest possible amount of silica reporting to the pregnant liquor as possible. The addition of lime also helps to convert any Na₂CO₃ which is developed by CO₂ being absorbed by the system back into NaOH (10).

Any impurities that enter into the pregnant liquor at this point stay in the solution during the precipitation of aluminum hydroxide (30). These impurities will build up in the system as the caustic is recycled and cause a loss due to the need to bleed off some of the recycled solution to maintain tolerable concentrations of contaminants. As the demand for higher purity products increases, additional processing steps will become necessary.

2.1.5 Filtration

Once the sodium aluminate has entered into a liquid phase, the residual material that did not dissolve must be separated as any solids will contaminate the final product. The pregnant solution is filtered through a system with 100µm pores in order to remove approximately 15% of the overall weight of the residue. This step is completed using liquid solid cyclones or smelting

chambers occasionally. Prior to World War II the pregnant liquor was sent directly to the filtration systems, however current technology and economic drivers have proved flocculation and thickening to be better alternatives. These products are washed in an effort to remove the remaining caustic and reduce the loss of soluble salts. Washed products are discarded with tailings. (10)

The final removal of insoluble material is completed with pressure filtration made of polypropylene fabric or tightly woven wire as to resist corrosion for the caustic solutions. Advancements by Alcoa have suggested using sand as a filtration media. (10)

2.1.6 Precipitation

The filtered pregnant liquor is at a temperature of 100°C and is cooled to approximately 70°C in order for precipitation to occur. Aluminum hydroxide (Al(OH)₃) is mixed with the solution in order to increase the kinetics of precipitation. Temperature has been shown to be extremely influential on the process, as a temperature change of 3 degrees can create extreme reactions. Particles size is also controlled by temperature and is important. Particles that are too small are difficult to handle without excessive dust mediation procedures and particles that are too large can behave erratically and release water during calcination. Precipitates are separated from the caustic solution with caustic being recycled back into the process. (10)

2.1.7 Calcination

Prior to the Hall-Heroult operation calcining is necessary to remove excess water content. The first step is to take the precipitated washed product and calcine typically using a countercurrent vacuum filtration system. The aluminum hydroxide is then turned into aluminum oxide and water as shown in Equation 2-4

by calcining in a rotary kiln, static calcining system or fluid flash calcining systems.



The latter two systems are better for energy recycling as they are essentially a fluidized bed that suspends particles in a cloud of hot gasses. This system is heavily dependent upon particle size for success. (10)

2.2 Nature of Red Mud

A waste created from the production of alumina using the Bayer process, red mud has proven to be difficult to deal with because of its particular characteristics. The complexity is furthered due to the extreme diversity in each red mud product created. There are 22 phases that are typically present in red mud as shown in Table 1-1: Composition of Dried North Coast Jamaican Bauxite and the Generated Red Mud Compound (33) and Table 2-2 (33) shows an overview of the general properties of red mud that make it thixotropic, difficult to settle because of its fine particle size and extremely alkalinity. (10)

The major oxides present in red mud and their weight percents are; Fe_2O_3 (25-70%), Al_2O_3 (13-29%), SiO_2 (3-24%), TiO_2 (4-20%), CaO (0.1-12%), Na_2O (1-10%) with the rest of the 7-13 wt % being made up of V, Ga, P, B, Zn, Cd, K, Sr, Ba, Mg, U, Th, Zr, Hf, As, Sb, Bi, Mn, Cu, Ni, Co, W, Ta, Hg, and Nb. (33)

Table 2-1: Typical Phases Present in Red Mud

Phase	Chemical Composition
Gibbsite	$\text{Al}_2\text{O}_3 \cdot 3\text{H}_2\text{O}; \text{Al}(\text{OH})_3$
Boehmite	$\text{AlO} \cdot \text{OH}$
Diaspore	$\alpha\text{AlO} \cdot \text{OH}$
Kaolinite	$\text{Al}_2\text{Si}_2\text{O}_5(\text{OH})_4$
Sodalites	$3(\text{Na}_2\text{AlSiO}_4)_6 \cdot 2\text{H}_2\text{O}$
Calcium Aluminate	$\text{CaO} \cdot \text{Al}_2\text{O}_3$
Sodium Aluminosilicate	$3\text{Na}_2\text{O} \cdot \text{Al}_2\text{O}_3 \cdot 3\text{SiO}_2 \cdot x\text{H}_2\text{O}$
Hematite	$\alpha\text{Fe}_2\text{O}_3$
Magnetite	$\gamma\text{Fe}_3\text{O}_4$
Goethite	$\alpha\text{FeO} \cdot \text{OH}$
Maghamite	Fe_2O_3
Siderite	FeCO_3
Calcite	CaCO_3
Calcium Alumino Silicates	
Alumogeoithite	$\alpha\text{FeAlO} \cdot \text{OH}$
Anatase	TiO_2
Rutile	TiO_2
Sodium Titanate	Na_2TiO_3
Cancrites	$\text{Na}_6\text{CaCO}_3(\text{AlSiO}_4)_6 \cdot 2\text{H}_2\text{O}$
Quartz	SiO_2
Ca(Mg,Al,Fe) titanate	
Manesite	MgCO_3

Table 2-2: General Properties of Red Mud

Property	Range
Specific Gravity	2.6-3.1
pH Value	11.0-12.5
Pulp Density (g/cm ³)	1.1-1.3
Initial % of Solids in Slurry	8.0-36.0
Settling Rate	1.0-3.0
% Solids after 24 hours	25-36
Particle Size	<10 mm 60-90 <1 mm 10-20

2.3 Background of Red Mud

Extensive research was done approximately 20 years ago and prior. At the time research was done the focus was on the recovery of aluminum and iron. Attempts were also made to develop a safe material from red mud that could be used for building materials. There has been successful implementation of this in Jamaica with a building constructed of pseudo-geopolymers created using red mud. Built in Jamaica almost 20 years ago, this shows that the recycling of red mud has been researched for many years. One possibility for this lack of current research is that, in general, research has moved away from iron and aluminum recycling to things of more value such as precious metals and rare earth element extraction. Perhaps the difficulty of working with the red mud, due to extensive silicates and liberation problems, are the reason that previous research did not provide any economic answers to the problem. (10)

Because the modern high grade deposits of the Bauxite ore are no longer in developed countries, they are now being mined in developing countries such as Papua New Guinea, China, India, Yugoslavia, and Russia. These countries are not as conscious about the environment and thus there is no push for public research to continue. Therefore, most recent research has been completed by the aluminum companies themselves. Because of this, the research has been proprietary and not shared with the academic community thus current information is extremely lacking and inadequate. (9)

It appears that the thesis completed at CSM in 2002 was among the last major research project in developed countries. There have been various other papers and smaller research projects that

can be found on the redmud.org website. This research is primarily focusing on the extraction of rare earth elements as well as the development of construction materials from red mud.

Although there had previously been research and successful applications of construction materials, it is unclear if this is an oversight and research is being duplicated or if advancements are being made. (10)

The goal of this research is to develop a process that will effectively and economically extract the iron and alumina from red mud using Pyrometallurgy. Although hydrometallurgy is historically less expensive, it has been determined that Pyrometallurgy will be the most effective methods of extraction. (10)

Figure 2-4: Project Plan

shows the flow sheet that CR³ is attempting to improve upon. This flow sheet shows the most current proposed way to extract the iron and alumina from the red mud. This current proposed method is expensive and time intensive way to extract the iron and aluminum. Rare earth element concentration will also be investigated; however as can be seen in section 2.1.3, this particular sample lacks the necessary grade to make this a viable solution.

It has been suggested that there are four main parts of previous research that are lacking and should be thoroughly investigated; a complete elemental and mineralogical analysis needs to be done, solid state reductions for magnetic separation feasibility tests, smelting reduction feasibility work for metal slag separation, and finally non magnetic and slag analysis for phase II recovery of elements. This research has not been previously completed and would greatly add to the knowledge of red mud and could possibly lead to breakthroughs in technology that could revolutionize the industry.

2.3.1 Previous Red Mud Solution Efforts

Limited application of red mud has been tried as a constituent in industrial construction aggregates, such as bricks, road surface material, and cement, in combination with other waste products such as fly ash, and it has also been tried as a soil modifier. These applications do not add value but can serve as a valid route for waste utilization after metal extraction. Careful consideration is required for addressing the vastness of the problem via construction material

applications. The extraction of Fe, the main constituent in red mud, has been the focus of several previous research efforts. One investigator suggests separating the red mud (in slurry form) using high intensity magnetic separation. The resulting magnetic product can be used as an ingredient for iron making or as a pigment for pottery making. The nonmagnetic portion can be applied in building materials or supplemented back into the Bayer process.

Another investigator reduces the Fe with chlorocarbons before magnetic separation and uses the resulting magnetic portion as feed for iron making. (22) Another research suggests drying the red mud, blending with lime and ground coal and feeding the mixture into a machine that agglomerates it into ½-in. diameter balls. Subsequently, the balls are pre-reduced at high temperatures in a circular grate. The balls are then fed into a submerged arc electric furnace for smelting and transported to a basic oxygen furnace, where high-quality steel is produced. The final product yields about 98-99% pure Fe. (23, 24). Another process entails mixing the red mud with $\text{Fe}_2(\text{SO}_4)_3$. This solution removes the Na from the mud, leaving behind material eligible for iron making. Simultaneous recovery of Al and Na is performed by mixing the red mud with a solution of caustic soda and lime at 300C at pressures of 4-9MPa. This solution is supplemented into the Bayer process for increased alumina recovery. One approach utilizes the amphoteric characteristics of Al by extracting it via treatment with sulfuric acid. It also attempts to extract the Al through biological leaching using sewage sludge bacteria. (10)

An additional process that emphasizes Ti recovery converts the red mud into sodium-aluminum fluoride compounds. The red mud is mixed with hydrochloric and hydrofluoric acid to obtain a silicic acid, which is then separated out. Evaporation leaves behind a material close to cryolite. The remaining material is mixed with the residual liquor, which dissolves the Fe and Al. The Ti-rich solid remaining can be further processed via chlorination. (8) Synchronous recovery of Al, Fe and Ti is investigated by a number of researchers. One method utilizes chlorination combined with fractional distillation to extract Fe and Ti from red mud. The red mud can be leached prior to this to retrieve Al. (7) A novel technique is being investigated where the red mud is carbothermically reduced in an electric arc furnace to produce pig iron and a fiberized wool material from slag. (9)

After looking at the previous creative attempts made to deal with red mud there are many limitations that must be addressed and solved before anything useful can be made. Red mud is generated and currently stored where processing for alumina recovery from bauxite ore (Bayer process) is done. Any recovery process from red mud that would require the transport of red mud (fine material with 20-30% water) to far distances, iron making operations, will likely be cost prohibitive. Thus, any conversion scheme that is adopted needs to be located near the bauxite processing facility. Whether an electric arc furnace or a rotary hearth type of process is used, it must be collocated. Solid-state carbothermic reduction of red mud to recover Fe and its separation from the remaining oxides via any physical means is difficult due to the mineralogy of red mud where fine iron oxide is intimately associated with other oxides and does not allow the separation of reduced Fe in a concentrated form. This is a major limitation which forces the carbothermic smelting of red mud. A solid Fe-rich product, such as direct reduced Fe, is unlikely. However, a solid product with reduced metallic Fe amenable to steelmaking remains a possibility. Injection of red mud, with or without pre-reduction, into a blast furnace through the tuyeres, is an interesting concept. However, the high alumina content is a problem for the slag fluidity and volume in the blast furnace and the high alkali content is not compatible with the refractory and alkali accumulation. While lime, silica and titania additions from red mud are acceptable to the blast furnace, alumina and alkali oxides must be removed before any injection. This concept will also require transportation adding to commercialization challenges. Removal of alumina via soda-ash roast and water leaching can produce a liquor that can be reverted back to the Bayer process, thus generating a residue that will be very low in alumina and alkali metals—a material now suitable for Fe production by any viable process. Alumina can be a recoverable commodity at this stage. Once alumina and alkali metals are removed by soda-ash roast and Fe is reduced by carbon, the resulting material may be smelted to produce pig-iron and a slag now rich in calcium titanate. Titanium could be considered a product from this slag stream. However, the process suitable for Ti recovery is the sulfation method developed by the US Bureau of Mines¹⁴. The Kroll process is unsuitable due to the high lime content of the slag. Based on these considerations, Figure 2-4: Project Plan

shows the flow sheet that CR3 is attempting to improve upon. There appear to be more valuable materials in red mud than the Fe and Al, such as Ti and rare earth elements. (25)

2.3.2 Current Methods of Treatment, Storage and Associated Problems

Due to the unusual chemical and mineralogical complexities associated with red mud investigations for treating, disposing of and utilizing red mud have produced limited advancements. With no environmentally friendly and economical way of disposing of red mud, companies are forced to figure in disposal fees in their final bottom line, a cost that is passed down to the end consumer. In an era where low costs and environmental friendliness are crucial, economically viable options of treatment are imperative (10).

Space requirements for storage of red mud are one of the largest constant problems facing the aluminum industry to date.

There are two current methods of storage. The first is to simply pump the red mud into holding ponds. However, this method takes up a considerable amount of land. The other way to store the mud is to first dry it and then dry stack it upon a special liner. Once there is sufficient red mud the dry stack is then covered with topsoil. This method still alleviates some of the issue of land use however; the land cannot be used for farming or to live on. Farming cannot occur due to the fact that red mud is extremely basic due to the large amounts of sodium used in the original processing of aluminum that is left in the byproducts. Although there have not been any reports of leaching from the red mud through the liners there is still the risk of caustic soda leaching into groundwater. Another risk is the heavy metals such as lead, cadmium and mercury leaching into the groundwater. (1,3,6,10,12)

Perhaps one of the most well documented tragedies associated with red mud occurred on October 4, 2010 in Hungary. The dam wall of the Ajka refinery collapsed and approximately one million cubic meters of red mud flowed into the surrounding countryside. (1) Nine people were killed in the disaster, 122 people were injured and the contamination included 40 square kilometers. The nearby Marcal River was reported to have suffered a loss of all living organisms, and within days the contamination had reached the Danube River as well. (4,6)

This, however, is hardly the only incident of contamination caused by red mud. Table 2-3 discusses 17 other incidents in the past 10 years. It appears that aside from the direct contamination of the red mud, the next largest concern has been the dust that is produced from the drying of the red mud.(1,5) A vast majority of the red mud is sub 10µm, and this material is too fine to ever completely settle out. Also, this tiny particle size means that any slight breeze will easily disrupt the dry stacks if they are not properly covered after each addition.(1,6)

Table 2-3: Recent Red Mud Disasters

Date	Company	Country	Incident
1966-Present	Rio Tinto	France	Red mud discharge into ocean
6-May-2002	Alcoa	Australia	Disposal of red mud onto local farmland
14-May-2006	Alcoa	Australia	Poisonous dust emission
6-Apr-2007	Rio Tinto	Canada	49 tonnes released into Saguenay River
21-Feb-2008	KAP Aluminum	Montenegro	Fine dust contamination
20-Aug-2008	Rio Tinto	Canada	Red mud discharge into river
27-Apr-2009	Norsk Hydro	Brazil	Red mud discharge into Murucupi river
1-Feb-2010	Rusal	Jamaica	Clouds of toxic dust
27-Jun-2010	Vedanta	India	Fine dust contamination
4-Oct-2010	MAL Hungarian	Hungary	Dam break
22-Oct-2010	Alcoa	United States	Fine dust contamination
3-Mar-2011	Rusal	Ukraine	Fine dust contamination
16-May-2011	Vedanta	India	Pollution after heavy rain
2-Jun-2011	Rusal	Italy	Spills of red mud
17-Oct-2011	Venezolana de Guayana	Venezuela	Red mud discharge into Orinoco River
10-Dec-2011	Alcoa	Virgin Islands	General pollution
12-Jan-2012	Rusal	Ireland	Fine dust contamination
26-May-2012	Guangxi Huayin	China	Leaking of disposal pond

2.3.2.1 Closed Cycle Disposal (CCD)

As the most prominently used method for storage this method consists of first washing red mud in order to remove as many water soluble elements as possible including caustic and sodium aluminate. Even after effective washing is completed in a countercurrent decantation apparatus the liquid contained in the solid fraction still can have a pH of 12 or higher (28). Because of this, the slurry (10-30% solids) cannot come in contact with ground water and must be pumped to impoundment ponds outfitted with special liners to inhibit contamination (33). Once the material is in the ponds it is subjected to two types of treatment, settling using flocculants or the drying and evaporation of water (DREW) process. DREW greatly reduces the time needed to ensure settling has occurred using perforated drain pipes at the bottom of the ponds under layers of sand and gravel. The high cost of construction can be prohibitive? even though the process improves the probability of a high density stabilized mud field forming (10).

Numerous problems are associated with this process as outlined below (33)

- High cost of land: the typical alumina plant utilizing traditional CCD methods require 0.2 square meter per year per ton of aluminum oxide capacity as red mud can only effectively be dewatered to 37% solids at a depth of 1.5m (35) resulting in large amount of water storage
- High cost of construction, maintenance, and constant monitoring of the impoundment ponds and dikes
- Seepage of caustic soda and other hazardous elements, as a multitude of alkaline and toxic elements have the potential to seek through the membranes lining the ponds thus contaminating soil and possibly ground water
- High cost of recycling pond water, due to the low amount of solids in the slurry large amounts of water must be recycled back into the Bayer process
- Difficulty to reclaim and rehabilitate land used. Both due to aesthetic damage to the surrounding areas due to dust and because of the caustic toxic nature of red mud make re-vegetation difficult (10)

2.3.2.2 Dry Stacking Methods or Thickened Tailings Disposal (TTD)

This process involves the removal of excess water from the red mud until water content below 45% is reached typically being done using drum filtration systems. Dewatered material then needs to be transported to its final destination typically at higher costs (35). Once at the final location, one of two final dewatering techniques are used; either solar drying or sloped stacked TTD methods.

In the solar drying method, the partially dewatered slurry is spread to a height of approximately 3 inches on a slight grade. Sloped stacked methods consist of pumping the material and allowing it to form a conical shape that will use gravity to flatten. In both of these methods the mud is then allowed to dry and harden until heavy equipment can be used to level the area, usually taking two to three weeks depending on environmental conditions. (10, 33)

These methods decrease the land usage by up to four times when compared to the CCD method, and create a storage bed with a stable base and excellent compressive strength. The downside however is that any rain water must be collected as it can leach through the stack and dissolve the soluble substances; also this area cannot support plant life without considerable modifications (28). To prevent dust hazards, common soils are spread on top and plant life can begin re-vegetation of the areas after organic fillers and fertilizers are added. (10, 35)

2.3.2.3 Sea Disposal

Environmental irresponsibility and potential catastrophic effects make this method practically extinct. Only done as a last remaining option this procedure is closely monitored by the environmental governing body. (10)

2.3.3 Sources of Red Mud

As a byproduct of the aluminum industry, red mud is a worldwide problem as shown in Figure 2-3. (10)



Figure 2-3: Locations of Bauxite Mining

2.3.4 Properties of Red Mud

Although a byproduct, there are still enough value added constituents present to warrant research into extraction of the valuables. The most abundant metal is iron, as seen in Table 2-4 which is almost five times as high as the next element, aluminum. The oxides of iron and aluminum make up almost 80% of the present material as seen in Table 2-5. Because of that the focus of this thesis's research was in the extraction of iron and aluminum.

2.3.5 Applications of Red Mud

Currently there are no effective uses for red mud. As shown in the section Motivation for Project, if red mud is stored in retention ponds it risks the dam breaking and contaminating and destroying anything nearby. Efforts have been made to utilize dry stack tailings however the small particle size has created a dust problem. Any small gust has been reported to send a toxic cloud of tiny red mud particles into the air, thus decreasing the quality of life for residents around the area.

Table 2-4: Chemical Analysis of Untreated Red Mud

Element	Weight %
Aluminum	7.630
Cadmium	0.011
Calcium	6.315
Carbon	1.085
Cerium	0.077
Chromium	0.165
Dysprosium	0.009
Erbium	0.006
Europium	0.003
Gadolinium	0.000
Holmium	0.000
Iron	35.450
Lanthanum	0.070
Lutetium	0.000
Magnesium	0.163
Manganese	0.913
Mercury	1.000
Neodymium	0.043
Praseodymium	0.010
Samarium	0.019
Scandium	0.013
Silicon	1.470
Sodium	1.065
Terbium	0.003
Thorium	63.000 (mg/kg)
Thulium	0.001
Titanium	3.655
Ytterbium	0.005
Yttrium	0.087
Zinc	0.080

Table 2-5: Oxides Analysis of Untreated Red Mud

	Compound wt %					
	Fe ₂ O ₃	Al ₂ O ₃	TiO ₂	CaO	SiO ₂	Gangue
Red Mud Head Sample	67.7	11.7	7.1	6.6	2.5	4.4

2.4 Red Mud Extraction Processes

Two steps were involved in the red mud extraction process. The first was to determine what the initial plan should be and test those ideas. Following that project optimization would be done to further increase the success of the project.

2.4.1 Initial Plan

This project had three main components as seen in Figure 2-4: Project Plan

below. The industry processes (construction aggregate, etc.) and soil products were only to be briefly investigated as noted in Figure 2-4: Project Plan

(10) , where the bulk of the work was to be done on the recovery of value added products.

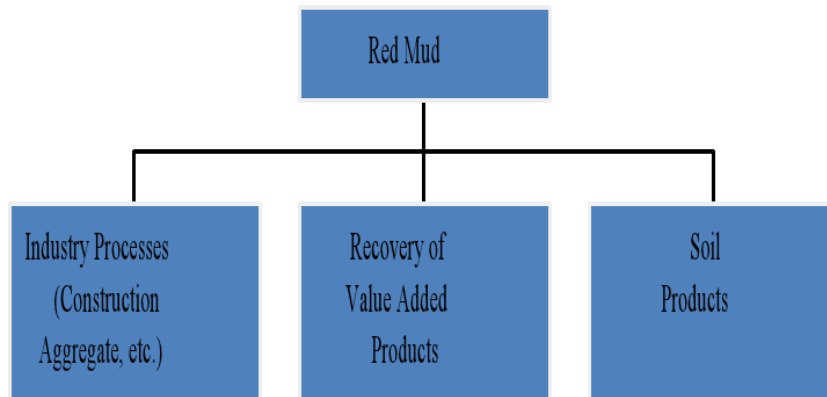


Figure 2-4: Project Plan

In the original project plan for recovery of value added products, foundry bag house dust was to be used as a carbon source, and sodium carbonate would be acquired from commercially available sources. This carbon source would enable the conversion of alumina and sodium into a water soluble compound, Equation 2-5

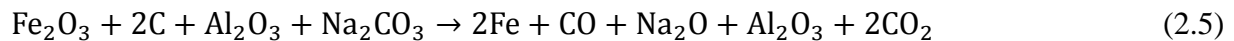


Table 2-6: Utilization Opportunities for Red Mud

<p>I. Constructional uses (Civil and Municipal Applications (12,13,14))</p>	<ol style="list-style-type: none"> 1. Construction blocks 2. Stabilized blocks 3. Light weight aggregates 4. Road/dyke construction 5. Additive to cements, cement mortars, concretes 6. Raw material for special cements 7. Glazed/unglazed roof, floor and wall tiles 8. Prefabricated structures 9. Land/mine fill
<p>II. Composites/Reinforced Products (39)</p>	<ol style="list-style-type: none"> 1. Red mud plastic (RMP) roofing sheets, door panels, pipes, fittings 2. Red mud rubber products 3. Red mud metal composites
<p>III. Treatment of Industrial/Municipal Effluents (40,41)</p>	<ol style="list-style-type: none"> 1. Adsorbent for toxic elements/compounds and waste gases 2. Cation exchanger 3. Filter aid 4. Treatment of liquid wastes
<p>IV. Ceramic Raw Material (27,28)</p>	<ol style="list-style-type: none"> 1. Pottery 2. Sanitary waste 3. Special glasses 4. Special refractories 5. Ferrites
<p>V. Metallurgical Raw Material (19, 20, 22, 23)</p>	<ol style="list-style-type: none"> 1. Iron and steel production 2. Sinter aid for iron ores 3. Flux in steel making 4. Titania recovery 5. Recovery of minor constituents, ex. Vanadium oxide and rare earth elements 6. Recovery of alumina and alkali
<p>VI. Miscellaneous and Soil Products (24,25,26)</p>	<ol style="list-style-type: none"> 1. Neutralizer for acidic soils 2. Soil amendment 3. Fertilizer additive (micronutrient) 4. Pigments and paints 5. Catalyst for coal, hydrogenation, hydroliquification, and others

Previous work was completed by Brandon Dugan in his thesis titled “Recycling of Bag-House Dust from Foundry Sand Dust from Foundry Sand Through Chemical and Physical Beneficiation.” From Mr. Dugan’s work we were able to work we were able to establish an understanding of the phases present in the bag house dust using QEMSCAN EDS, using QEMSCAN EDS, energy dispersion X-ray Spectra. In Figure 2-5, Figure 2-5: Bag House Dust QEMSCAN

the pink represents quartz, green bentonite clay, blue is other clays, and the black sections represent the iron metal present. (13)

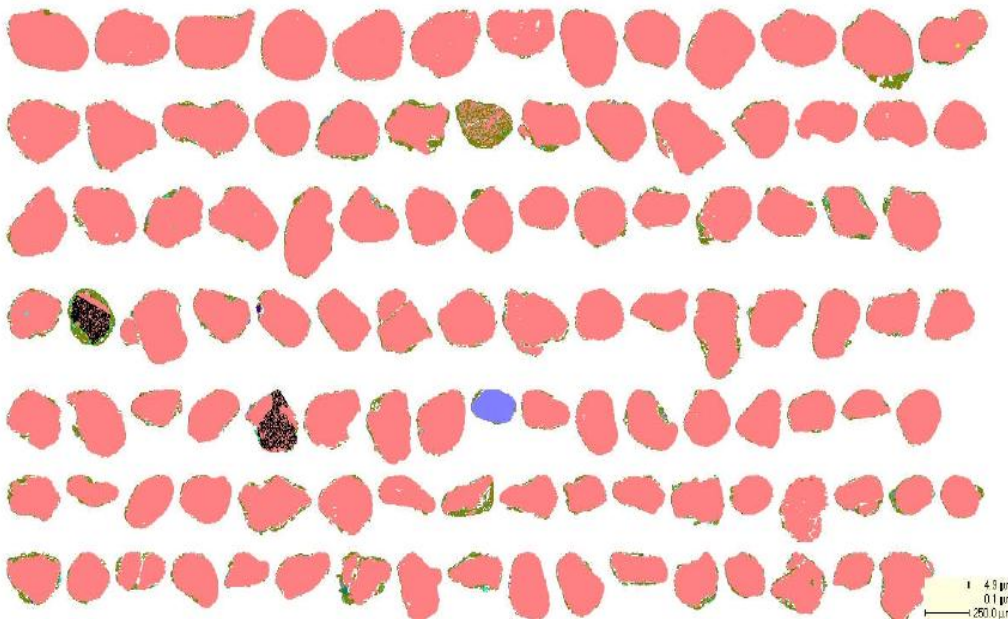


Figure 2-5: Bag House Dust QEMSCAN

It is evident from the above figure that the bag house dust is predominantly quartz while the other minerals have limited liberation. This is rather surprising considering that according to other work done by Dugan the quartz mineral only makes up 22 weight percent of the dust sample shown, with the vast majority reporting to the smectite and illite clay portions. (13)

The portion that is of interest to this work is the carbonates, as the bag house dust was one of the options for the carbon source needed for transformation of hematite to magnetite.

Although the initial carbonate is low in the bag house dust Dugan’s thesis uses, it shows ways to upgrade the dust enough to be a viable carbon source. Using that information the Figure 2-6 shows proposed work to be completed. (13)

Table 2-7: Bag House Dust Analysis

Mineral	Bag-House Dust (wt %)
Quartz	22
Smectite/Illite Clay	60
Plagioclase Clay	6
Carbonate	4
Chlorite	3
K-Feldspar	1
Iron Metal	0
Other	3

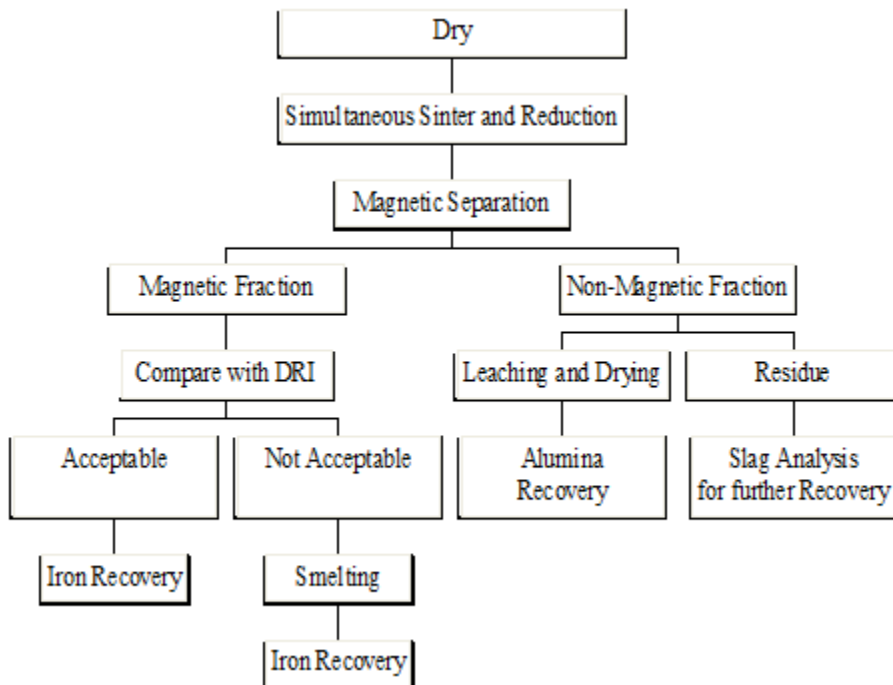


Figure 2-6: Initial Red Mud Extraction Process

2.4.2 Project Optimization

As will be explained in later sections, it was discovered that the process showed marked improvement if the soda ash and carbon roasts were separated. Figure 2-7: Red Mud Extraction Optimization

shows how the test work was optimized to exhibit the most effective results. Excess amounts of soda ash and carbon were used to ensure that the system was not starved. The varying amounts of water were used in an effort to conserve water if possible since many of the areas in which red mud is stored have limited water access.

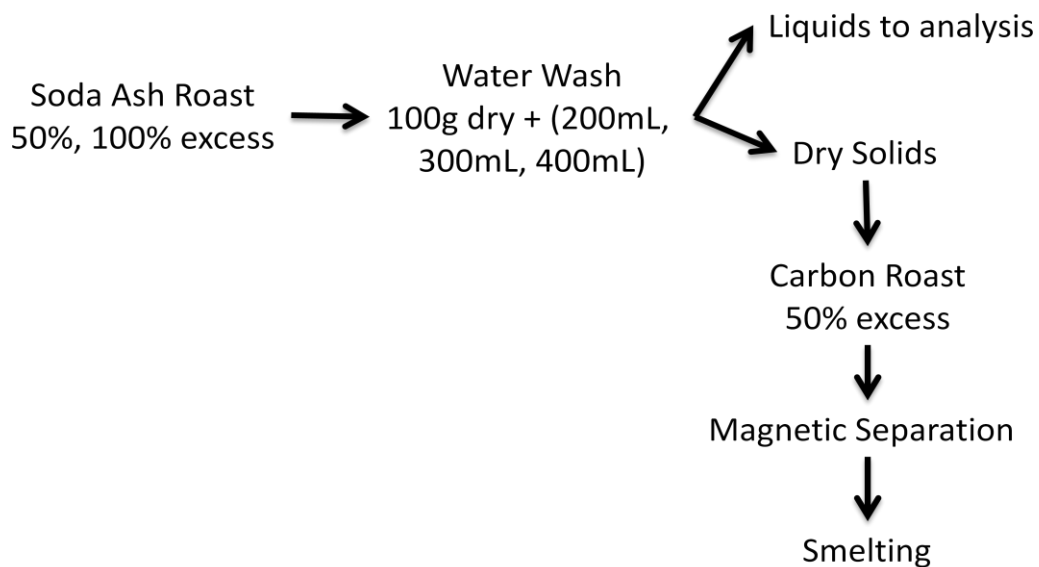


Figure 2-7: Red Mud Extraction Optimization

CHAPTER 3 EXPERIMENTAL PROCEDURES

3.1 Initial Preparation

Before any test work could begin, sample preparation needed to happen to ensure that any subsequent samples were as non-biased as possible.

3.1.1 Drying

Jamaican red mud was received in a five gallon bucket that was still relatively damp. In order to more effectively handle the sample it was separated into pans and dried at 75°F overnight to drive off any moisture present and help prevent future agglomerations and variances in weight due to moisture losses during roasting.

3.1.2 Crushing

Using a jaw crusher, all material that was above ¼ inch was crushed to 100% passing the ¼ inch screen. This was done to ensure a more uniform size distribution from this point forward. ¼ inch was determined to be industrially feasible as most operations have the ability to crush to that size without an extensive amount of energy being expended.

3.1.3 Blending and Splitting

In order to ensure the most unbiased head sample possible, the dried and crushed material was then blended using a cone and quarter method. Due to the large amount of material, the riffle splitters available at the time were not large enough to accommodate the sample. The cone and quarter method is where the sample is split into four approximately equal amounts that are then randomly put on top of each other in a conical shape. Once a cone of all material has been formed, the cone is flattened into a pancake shape and then split into four approximately equal sections and the process begins again. This was done four times in order to effectively blend the head sample and reduce any bias present.

In order to achieve an accurate head sample, one quarter was then taken from the last cone and quarter and that was put through a riffle splitter multiple times until only approximately 20 grams remained. These 20 grams were used as the head sample that was sent for analysis. The remaining quarter was used for subsequent test work. When the remaining quarter was used, the left over head sample was again cone and quartered to produce more unbiased sample to be used for the remainder of the project. It was deemed necessary to continue the cone and quarter process due to the large amount of fines present in the sample and the concern with them settling to the bottom of the container.

3.1.4 Thermodynamics

Shown in Figure 3-1 and Figure 3-2 .

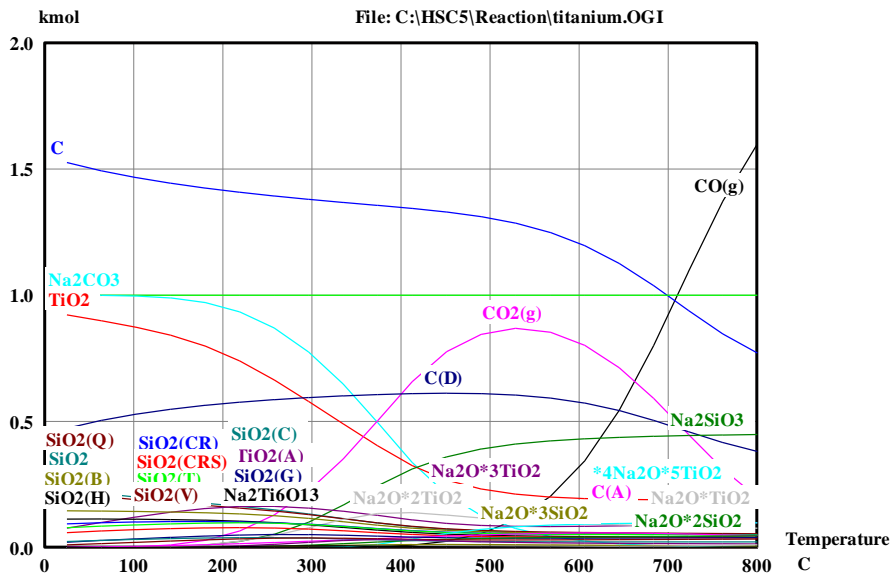


Figure 3-1: Overall Reaction Stability Diagram $\text{TiO}_2 + 2\text{C} + 2\text{SiO}_2 + \text{Na}_2\text{CO}_3 = \text{Ti} + 2\text{CO} + 2\text{NaSiO}_2 + \text{CO}_2$

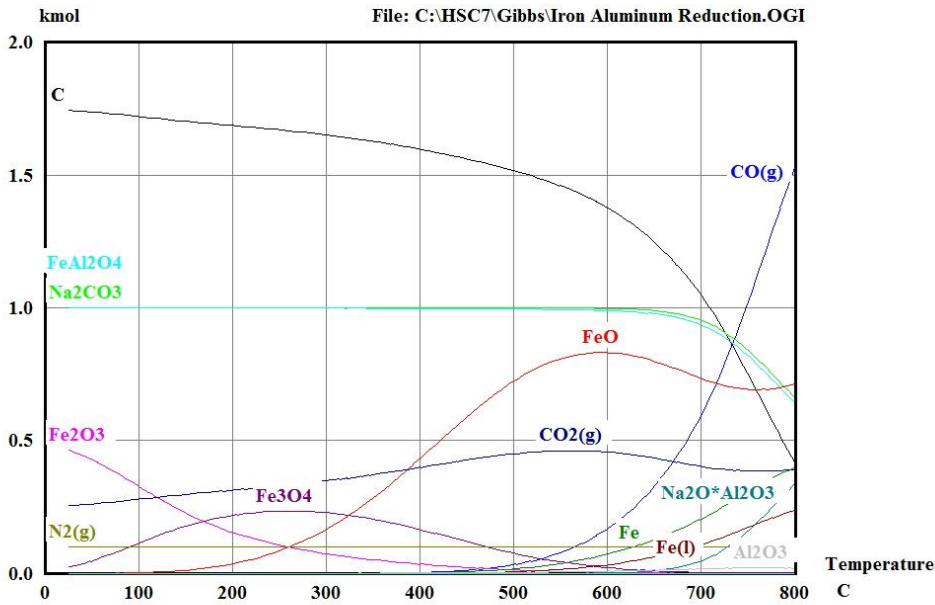


Figure 3-2: Overall Reaction Stability Diagram $\text{Fe}_2\text{O}_3 + 2\text{C} + \text{Al}_2\text{O}_3 + \text{Na}_2\text{CO}_3 = 2\text{Fe} + \text{CO} + 2\text{NaAlO}_2 + 2\text{CO}_2$

3.2 Preliminary Sodium Carbonate and Carbon Mixture Roasts

Originally it was believed that the sodium carbonate, also known as soda ash, and carbon roasts could occur at the same time using the bag house dust as half of the carbon source. The other half of the carbon needed would come from petroleum coke.

3.2.1 Roasting Conditions

Zirconium crucibles were chosen as the container for the roasting due to the high temperatures that were needed for the reactions to occur. Alumina was not used as it was a possibility for the crucible to react with the alumina already present in the untreated red mud and give a false result once analytical analysis was completed.

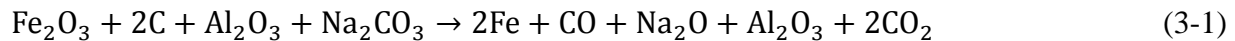
Untreated red mud in the amount of 250 grams was used so that there would be ample sample left for further processing. The desired amount of soda ash and carbon (50 or 100% molar excess) were added to the red mud and then the mixture was stirred and shaken in a Ziploc bag to

ensure proper mixing of the constituents. The mixture was then separated into the appropriate amount of crucibles with each receiving a thin layer of lime (CaO) on the top to prevent off gas as much as possible.

These tests were to be completed at 1000°C with a ramp up temperature of approximately 250°C per hour and then held at temperature for 2 hours before being allowed to furnace cool overnight. Test that were completed using these conditions produced agglomerates that could not successfully be separated from the crucible or broken apart to be used in further test work.

It was determined that the cause of these agglomerations was the bag house dust carbonate. The carbonates were in the form of coal that has the tendency to break down into coke near 1000°C resulting in a fusion of the surrounding material making it almost rocklike. Subsequent tests were lowered in temperature to 800°C and petroleum coke was used as the carbon source to ensure test work could be completed without any fusion of material. Future test work can be done using upgraded bag house dust as a carbon source keeping in mind the temperature restrictions due to the presence of coal.

As shown in Equation 3-1



It was the original hope to be able to combine the sodium carbonate and carbon roasts in an effort to conserve energy, thus lowering costs, and to save time. It was determined that although the thermodynamics showed this as a viable option, the liberation and perhaps kinetics inhibited this reaction. Complete reduction to pure iron was only expected to occur after smelting, as higher temperatures were needed to make that separation.

In the Gibbs plot shown below in Figure 3-3, the necessary reactions can take place at the lower 800°C temperature for roasting.

3.2.2 Magnetic Separation

After the joint sodium carbonate and carbon roasts, it was confirmed that the hematite had been converted to magnetite. Magnetic separation was then completed using hand-held magnets in

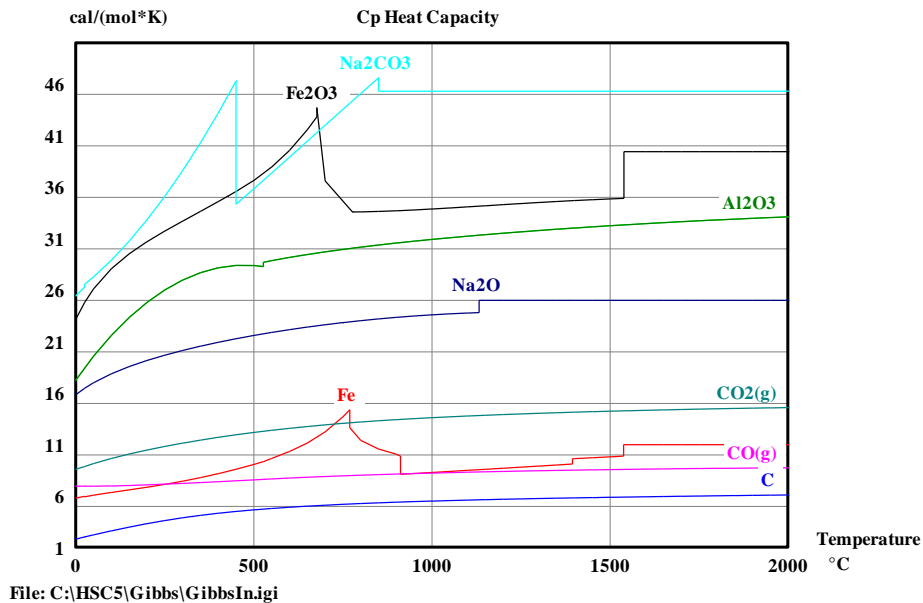


Figure 3-3: Temperature vs. Cal/(mol*K) for entire system

both dry and wet conditions as shown in Appendix A, Figure A-1 and Figure A-2. Test 1 and test 2 both dry and wet conditions as shown in Appendix A, Figure A-1 and Figure A-2. Test 1 and 2 were performed using 50% excess sodium carbonate and 100% excess sodium carbonate in the roasts respectively. Both tests were roasted using 100% excess carbon in the form of half bag house dust and half petroleum coke.

3.3 Sodium Carbonate Roasts

The decision was made to separate the sodium carbonate and carbon roasts in an effort to extract the water soluble elements, primarily aluminum, sodium, and calcium in a 70°C water wash after a sodium carbonate roast. Equation 3-2 expresses the goal of the sodium carbonate roast.



Sodium was the main element of concern being as smelters will not be as likely to take solids that are above 0.7 weight % sodium (10), and thus any benefit may be undone by the penalties charged for a high sodium product.

3.3.1 Roasting Conditions

It was determined that the extraction of sodium and calcium were not adequate so the next step was to separate the sodium carbonate and carbon roasts in order to more effectively be able to separate the water soluble elements, alumina and sodium, from the bulk material. Two bulk sodium carbonate roasts were completed, one at 50% excess and one at 100% excess. The roasted material was then split out and subjected to water washes. Each water wash consisted of 100g dried material being mixed with distilled water heated to 70°C and then agitated for 1 hour before being filtered. There were three varying amounts of water used, 200mL, 300mL, and 400mL. Since most bauxite mines are located in areas of the world with limited water supplies, the lowest water consumption was a desirable aspect of the research. Results from these tests can be found in Appendix B.

As is obvious from the graphs, the water wash was extremely effective at providing a liquid without iron or titanium. However there is still a noticeable amount of alumina and sodium remaining in the solids portion. This problem will need to be further investigated.

3.3.2 Thermodynamics

According to the thermodynamic models developed by HSC software, there is no reason why the reactions should not occur as seen in Figure 3-2: Overall Reaction Stability Diagram

$$\text{Fe}_2\text{O}_3 + 2\text{C} + \text{Al}_2\text{O}_3 + \text{Na}_2\text{CO}_3 = 2\text{Fe} + \text{CO} + 2\text{NaAlO}_2 + 2\text{CO}_2$$
The fact that there is still limited extraction of both the alumina and sodium could be due to the high amount of excess sodium carbonate being added to the system or to the lack of liberation in the system.

3.3.3 Water Wash Conditions

Two types of water washes were performed. Each type was done after the sodium carbonate roast product had been split into 100g dry samples. Then water that had been preheated to 70°C was added to the 100g dry solid samples in three volumes; 200mL, 300mL, and 400mL. In the first type of water wash, the system was enclosed in a bottle and placed on a shaking table for one hour. Although this caused the system to cool slightly, the latent heat loss was less than

originally expected. These bottles were then filtered first using a Whatman #3 filter paper and then using a Millipore filter with a 0.25 μ m pore size. Double filtration was used to ensure that all solids were removed from the filtrate before being analyzed.

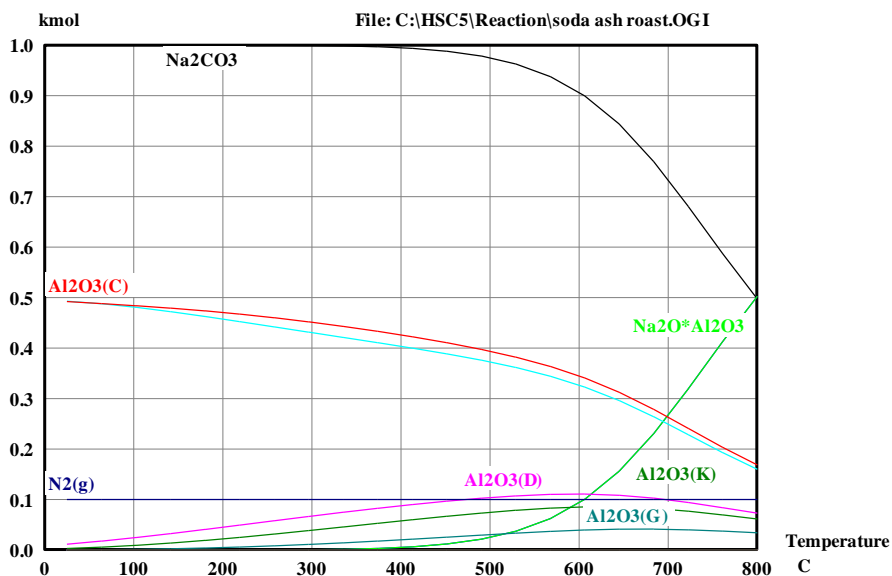


Figure 3-4: Sodium Carbonate Roasting Stability Diagram

After the first type of water wash was determined to lack the desired results, variable speed overhead mixers were ordered as agitation was thought to be one of the problems inhibiting full leaching. The most effective water washes were then repeated using agitation and temperature for three varying times. One samples was removed from the testing at 60 minutes as to have a control to compare to the previous tests, the next was removed at 90 minutes and the final at 120 minutes. The sample size was decreased to 10g of sodium carbonate roast product, and the amount of 70°C water was kept the same as the most effective tests, 40mL. Mixers were placed in the bottles that were suspended in a water bath of 70°C to ensure the slurry was kept at temperature. An agitation of 20 rpm proved to be adequate to keep all solids suspended without creating too much of a vortex within the slurry. After being agitated in the water bath for the desired amount of time, the samples were filtered only using the Millipore 0.25 μ m pore size filter under vacuum. The Whatman filter paper was not used due to the smaller sample size.

3.4 Carbon Roasts

Carbon roasts were completed separately from the sodium carbonate roasts using only petroleum coke as the carbon source at this point of the test work. As stated previously, petroleum coke was used to inhibit agglomeration issues, and was proven by previous work to be 96% carbon. The purpose of the carbon roasts was to convert, by reduction, the hematite to elemental iron which is magnetic so that the iron could then be concentrated using magnetic separation as seen in . The magnetic section of this would then go to smelting to produce a pure iron button, Equation 3-3.



3.4.1 Roasting Conditions

Dried solids from the sodium carbonate roast and water wash were then subjected to a carbon roast using a mixture of petroleum coke and foundry bag house dust as the carbon sources. This roast occurred at 800°C for 2 hours. Temperature was lowered from the sodium carbonate roasts due to the melting of coal and the agglomeration that ensued at 1000°C. Carbon roasted material was then separated using a Frantz magnetic separator. Conditions for magnetic separation were as follows, pulsar range of 3, mili amps at 25 (equal to 0.25 Gauss). Results from these tests can be found in Appendix G.

From the graphs it is apparent that there is still a significant aluminum and sodium contamination. This will be addressed in further work.

3.4.2 Magnetic Separation Conditions

Magnetic separation was done using a Frantz dry magnetic separator. At the beginning of the project, magnetic separation was done on material that had been roasted using both excess sodium carbonate and excess carbon at the same time. These experiments were performed at 1000°C for 2 hours and then allowed to furnace cool overnight. 5.00g dry material was separated and then subjected to two intensities of magnetic fields. Lowest intensity was determined to be 20 mili-amps or 0.2 Gauss. The maximum intensity was determined to be 30

mili-amps or 0.3 Gauss. It was discovered that anything with a higher intensity than 30 mili-amps lead to the sample sticking to the mechanisms and inhibiting a complete separation. Results from these tests can be reviewed in Appendix A.

3.4.3 Thermodynamics

As seen in Figure 3-5.

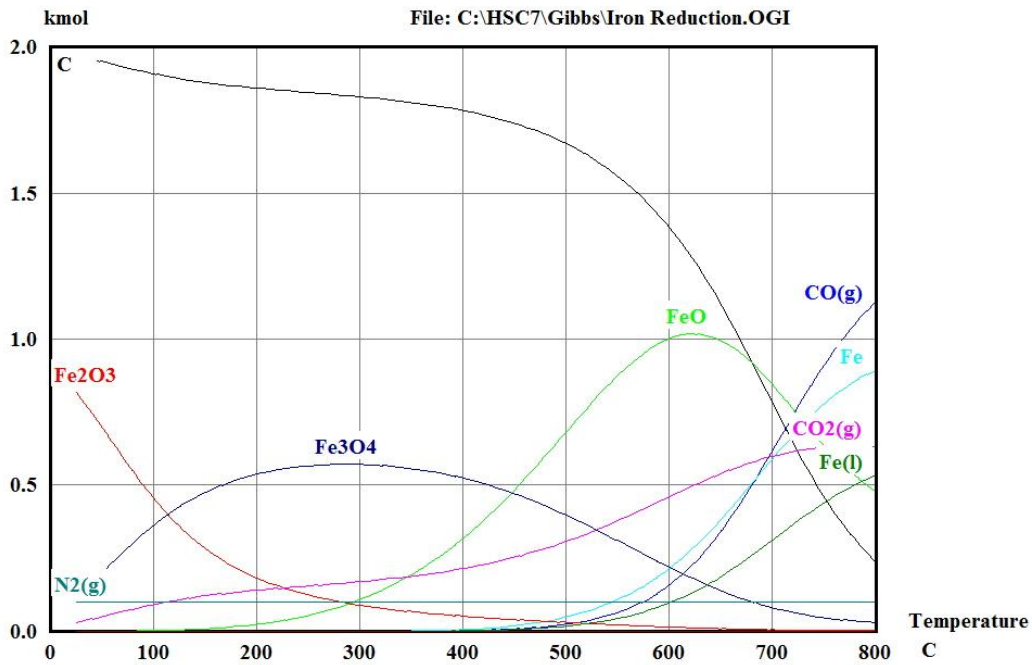


Figure 3-5: Carbon Roasting Stability Diagram

3.5 Initial Smelting

Smelting was tried on the magnetic fraction of the material that had experiences simultaneous sodium carbonate and carbon roasting. This material was to be heated to 1500°C in an argon atmosphere. Unfortunately due to thermal shock, the zirconium crucible failed during the test causing the test to need to be aborted before temperature could be reached. This test was not repeated.

3.6 Final Smelting

Smelting was performed after magnetic separation, using the Frantz dry magnetic separation machine, had occurred on material that had previously undergone sodium carbonate roasting, water washing, filtration, drying, and carbon roasting. It was believed that the magnetic fraction would have a higher concentration of iron than the non magnetic fraction and thus would result in less material needing to be treated at extremely high temperatures.

3.6.1 Smelting Conditions

Magnetic separation using the Frantz was performed on the dried water washed materials using the second method of water washing using agitation and sustained temperature. Conditions were similar to those done on the previous magnetic separations with a pulsar range of 3, milliamps to 25 which corresponds to 0.25 gauss. It was again determined that anything with a stronger magnetic field caused sticking in the machine and resulted in an incomplete test.

These magnetic fractions from the six tests were then combined to create enough material to send to smelting. The material was mixed with 25 weight percent lime and then placed in a zirconium crucible. Lime was spread over the top of the mixture, 2.33 grams, and then an alumina plate was placed on top of the crucible.

In an oxygen deficient environment the temperature was raised at 150°C per hour until a temperature of 1450°C was reached. The sample was then held at 1450°C for two hours and then the furnace was cooled down at a rate of 150°C per hour until the temperature reached 700°C. At 700°C the furnace was turned off and was allowed to furnace cool until approximately 110°C at which time the furnace door was cracked open to expedite the cooling process.

CHAPTER 4

RESULTS AND ANALYSIS

4.1 Initial Sodium Carbonate and Carbon Mixture Roasts

Initially, sodium carbonate and carbon roasting was to be completed together in an effort to conserve energy thus minimizing energy costs, this however was not effective.

4.1.1 Results

Results from the initial combined sodium carbonate and carbon mixture roast were not what was expected, as can be seen in Appendix A. The separations that were made were inadequate at best with the water wash section being a subpar. These results, Figures A-1 to A-8, lead us to the conclusion that the sodium carbonate and carbon roasts should be separated in an effort to improve the separations of the value added products that we were aiming for and thus further work was needed as no clear separation was made using this approach

4.2 Sodium Carbonate Roasts

Once it was determined that roasting with sodium carbonate and carbon simultaneously was not effective, the roasts were separated.

4.2.1 Water Wash Results

As shown in Appendix C, the final water wash results were still not what we were expecting, Figures B-1 to B-4. Final conditions are found in

Table D-1. Although the alumina has been reduced to an acceptable level in the solids, the sodium is still at a level that is too high to send to a conventional smelter. Liquid analysis provided information that was excellent with only sodium and alumina being present as shown in Appendix C. This problem will need to be resolved if these products are expected to be used in further processing.

4.3 Carbon Roasts

Once it was determined that roasting with sodium carbonate and carbon simultaneously was not effective, the roasts were separated.

4.3.1 Magnetic Separation Results

Magnetic separation showed limited success due to liberation problems. The six final water wash solids were the feed for the magnetic separation and showed similar weight distributions, seen in Appendix D Figures D-1 to D-3, however there was not a clear distinction of iron concentration.

4.4 Final Smelting

After magnetic separation, the magnetic portion was collected and combined to create the sample that was used in the final smelting step.

4.4.1 Results by Scanning Electron Microscope (SEM)

As shown in Appendix E, final smelting was a success. Two small buttons of iron were produced that weighed a total of 9.4907g which is approximately 31% of the total initial weight of 30.8712g that was initially put into the smelting process, as shown in Figure F-23: . These buttons were analyzed by SEM-EDX to determine their purity as was the slag that was produced on top of the buttons as seen in Figure G-24: and Figure G-25: .

4.5 XRD Analysis

XRD (X-Ray Diffraction) analysis was completed in an effort to confirm the initial form of iron was in the hematite form, as seen in Figure 4-1: XRD Analysis Figure 4-1. XRD analysis did not provide results that were extremely clear due to the fact that the sample is very amorphous. It can be deduced however from the data that hematite is present.

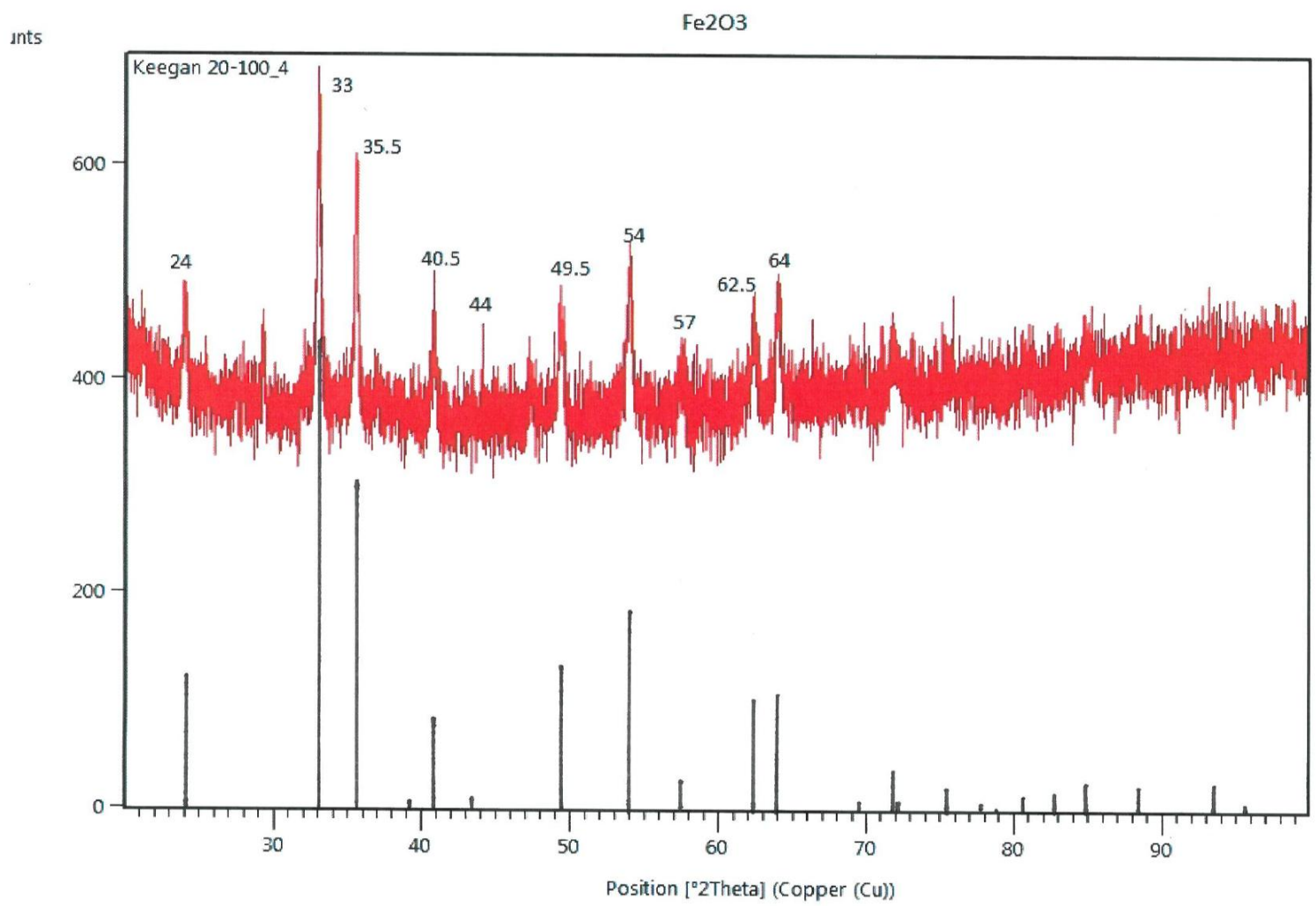


Figure 4-1: XRD Analysis

4.6 QEMSCAN Analysis

QEMSCAN technology was used to create a detailed analysis of the unroasted red mud head sample. The sample was mounted in a traditional epoxy mount and then polished. The results showed a serious liberation problem across all elements and compounds as can be seen in Appendix A. Appendix B shows the locking and liberation graphs for each of the major elements and compounds. Appendix C shows the modal abundance of each element and compound. The overall average liberation across all elements and compounds is approximately 5%, the midlings makes up 20% and the locked portion makes up approximately 75% of the sample.

4.6.1 Elemental Analysis

The following figures show the amount of the selected element present in the sample. Each color represents a different mineral or element. Some of the selected minerals show limited liberation and thus are more difficult to reach without grinding to a smaller particle size.

Figure 4-2 represents all minerals together shows a liberation concern as there does not appear to be any particles of a solid color.

The silicates are represented in an orange color in Figure 4-3 and are sporadically located throughout the particles. Silica creates a problem when attempting to leach value added products due to its high resistivity to leaching.

Figure 4-4 shows the carbonates represented by blue are incredibly abundant however not very well liberated throughout the sample.

Ilmenite (FeTiO_3) is represented by red in Figure 4-5. Ilmenite is a faintly magnetic mineral, which is greatly overpowered in magnetic strength by magnetite. Although titanium is a value

added product clearly present in the red mud, it is difficult to separate due to its limited liberation.

Phosphates are shown in magenta in Figure 4-6. This mineral catch has varying different types of phosphates due to the fact that each individual phosphate is too low in amount to be effectively shown.

The absence of pyrite (FeS_2) shown in Figure 4-7 is a benefit because the lower the sulfur levels the more effective the roasting conditions are. Sulfur has the potential to bind with some of the other elements present and either inhibit full transformation or off gas into undesirable compounds.

Figure 4-8 shows limited amounts of chromite present in teal. This aligns with the chemical analysis that was previously completed on the untreated head sample showing only 0.165 weight percent present.

Maroon represents the aluminum-calcium-iron phase in Figure 4-9. Although extremely copious the liberation is again the issue facing complete separation of this phase.

Another promising phase is the iron-aluminum-titanium shown in light blue in Figure 4-10. With these elements being the most abundant metals present, this phase would be the most valuable for extraction. However the locked nature of the phase makes it near impossible without further mechanical or chemical cracking of the particles.

Figure 4-11 represents the iron and aluminum phase in the lime color. The large amount of the mineral present corresponds to the fact that iron and aluminum are the two most abundant elements present in the sample.

Plum represents the iron phase in Figure 4-12. Although one of the most abundant elements in the head sample, the lack of liberation makes it difficult to effectively extract the iron from its other constituents.

Free titanium in Figure 4-13 is located in incredibly sporadic and locked places within almost all of the particles.

Figure 4-14 shows the aluminum and manganese phase in dark teal. With some smaller particles appearing to be fully liberated this may be an element that can be separated in small quantities.

Dark gray represent the free aluminum in Figure 4-15. Aluminum is one of the more liberated minerals and this image shows promise for the hope of extraction without the need for smaller particle sizes in order to liberate and then separate the mineral.

Manganese is represented in Figure 4-16. Since it is an essential trace element for plant and human life, this would be an element that would be useful as a micro nutrient in the fertilizer industry. Yet as the chemical analysis and the QEMSCAN results confirm the low amount present.

Various other minerals are present in Figure 4-17 that represents all other minerals that are in too small of an amount to be effectively analyzed using the QEMSCAN technology at this time.

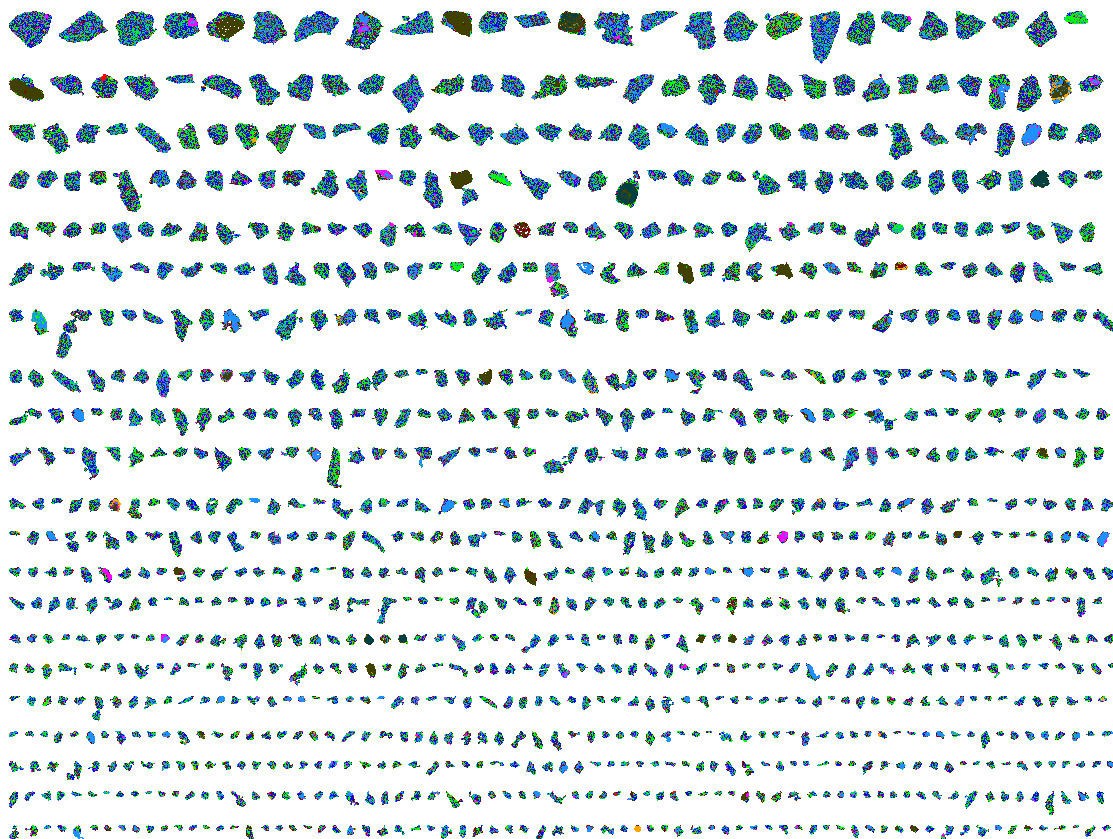


Figure 4-2: QEMSCAN Image of All Minerals





Figure 4-3: QEMSCAN Image of Silicates



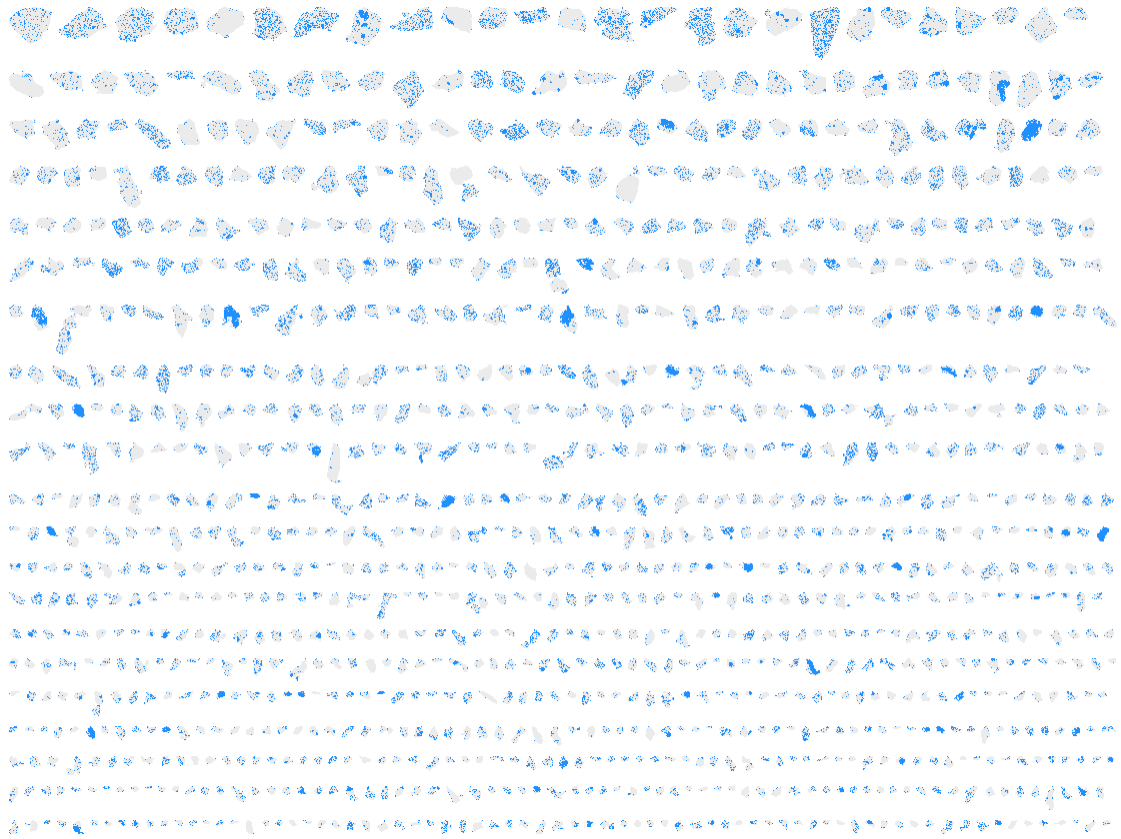
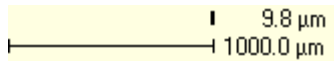


Figure 4-4: QEMSCAN Image of Carbonates



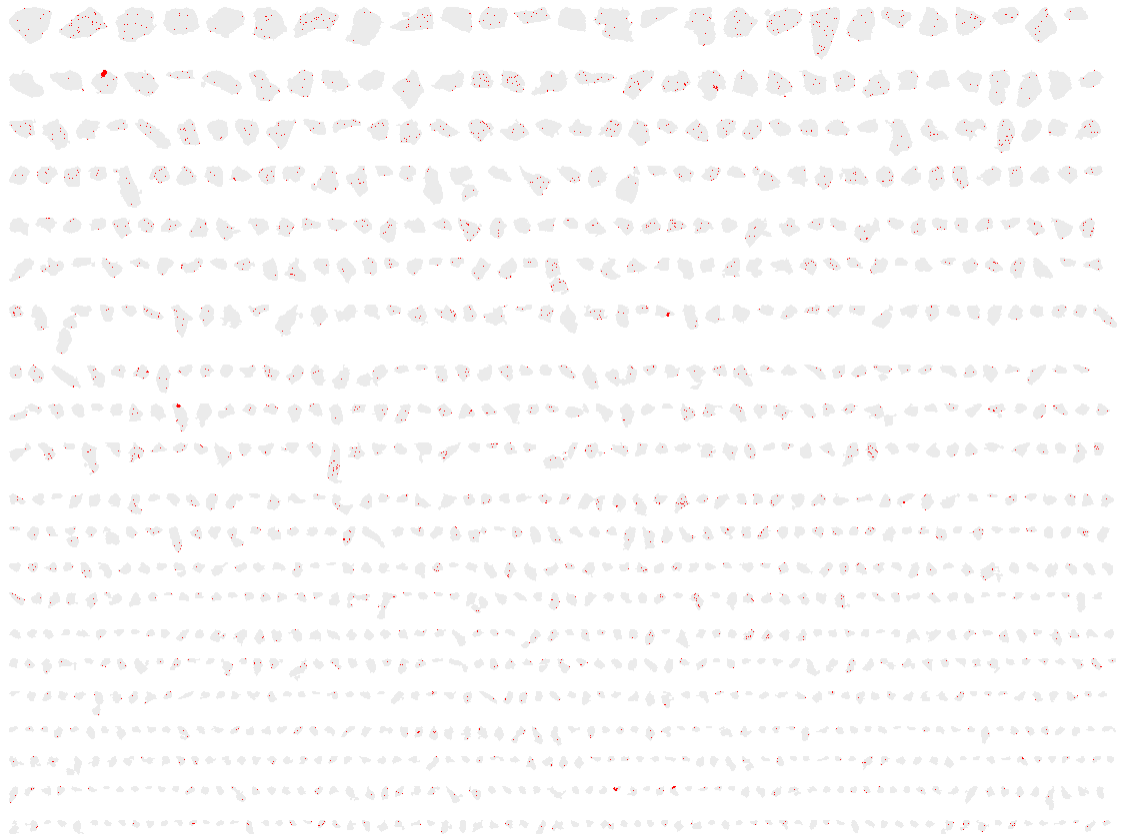
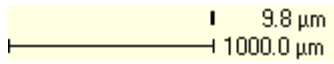


Figure 4-5: QEMSCAN Image of Ilmenite



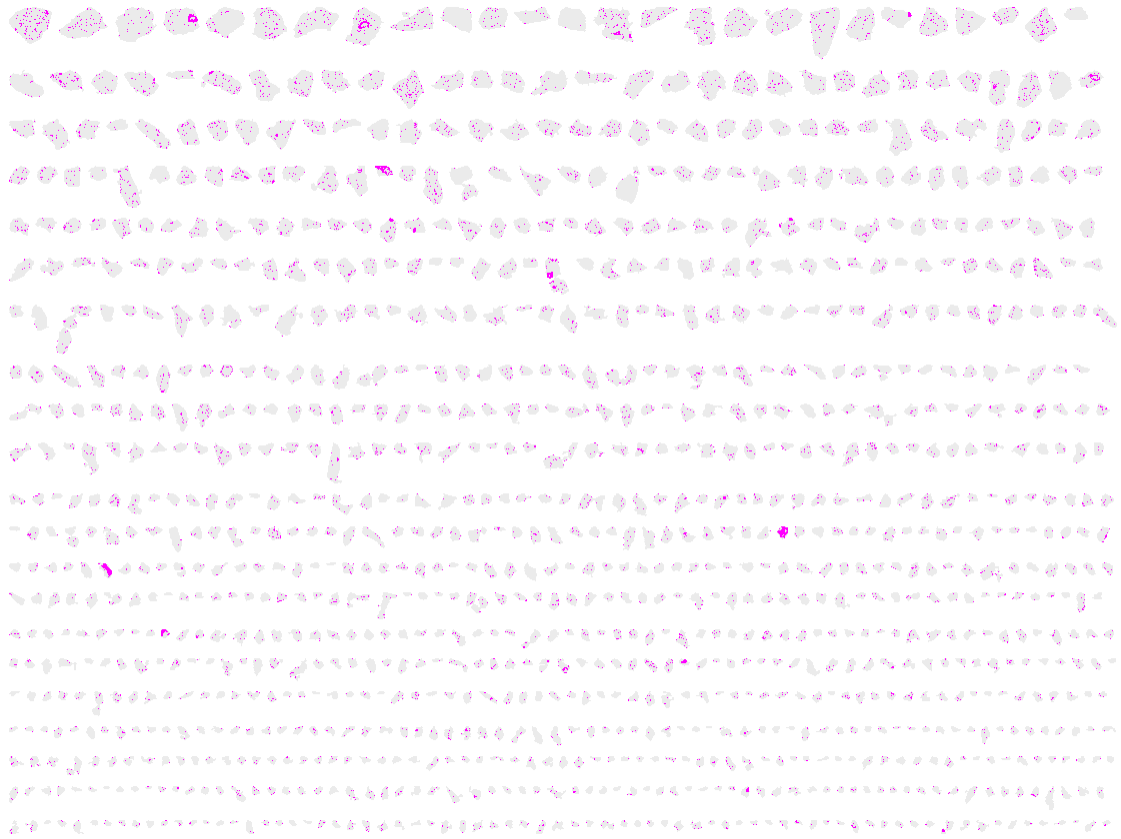
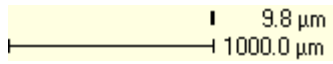


Figure 4-6: QEMSCAN Image of Phosphates



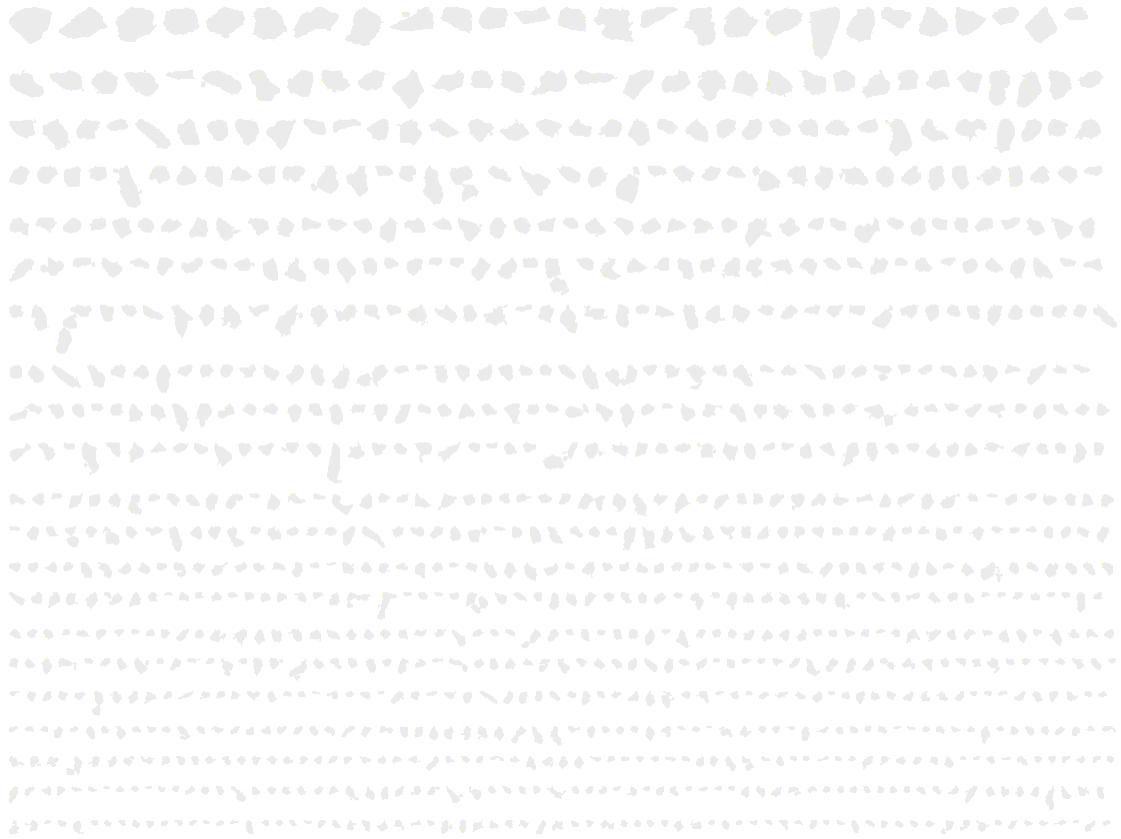
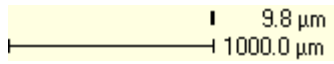


Figure 4-7: QEMSCAN Image of Pyrite



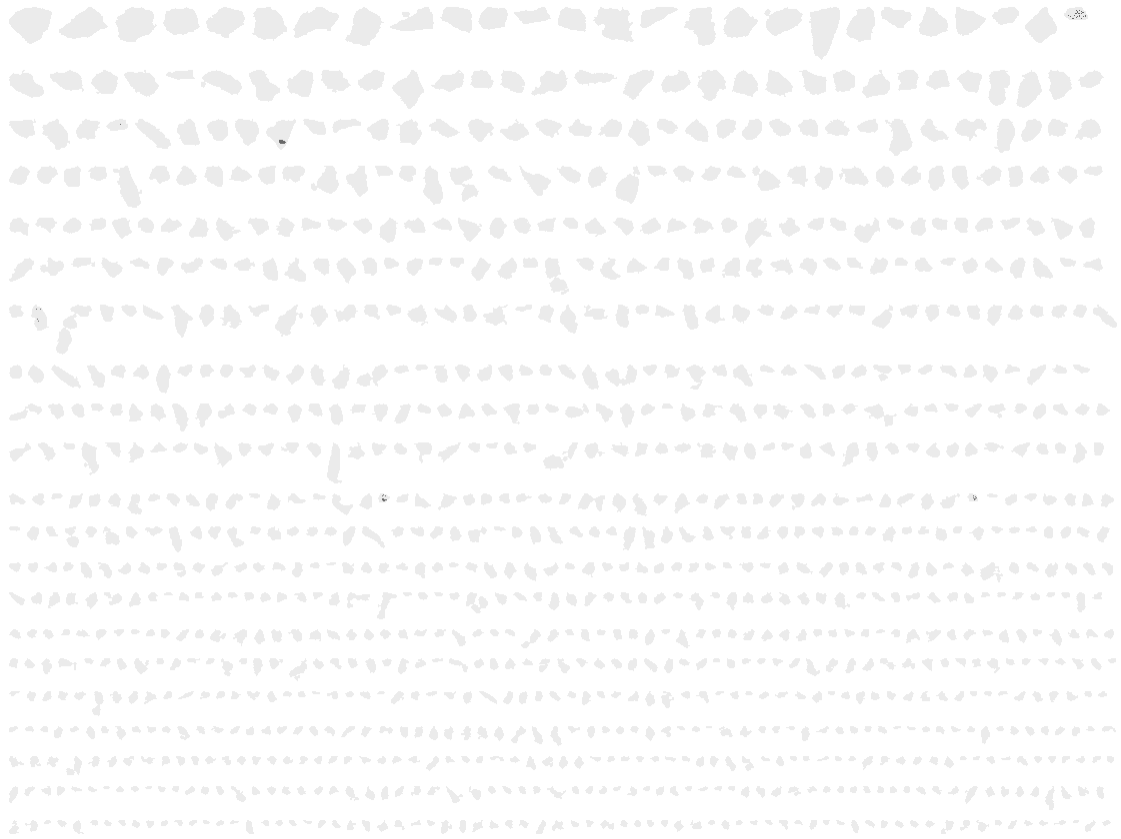
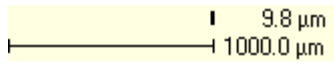


Figure 4-8: QEMSCAN Image of Chromite



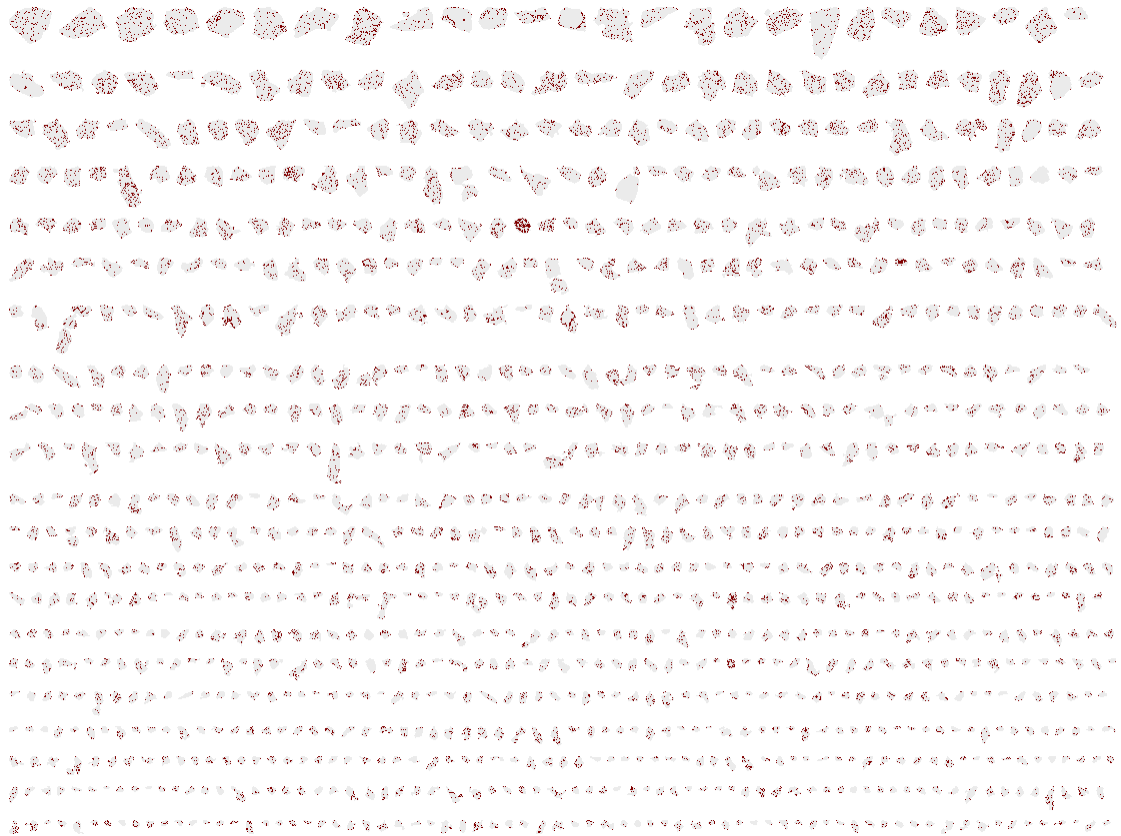
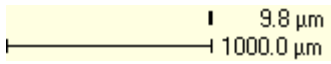


Figure 4-9: QEMSCAN Image of AlCaFe Phase



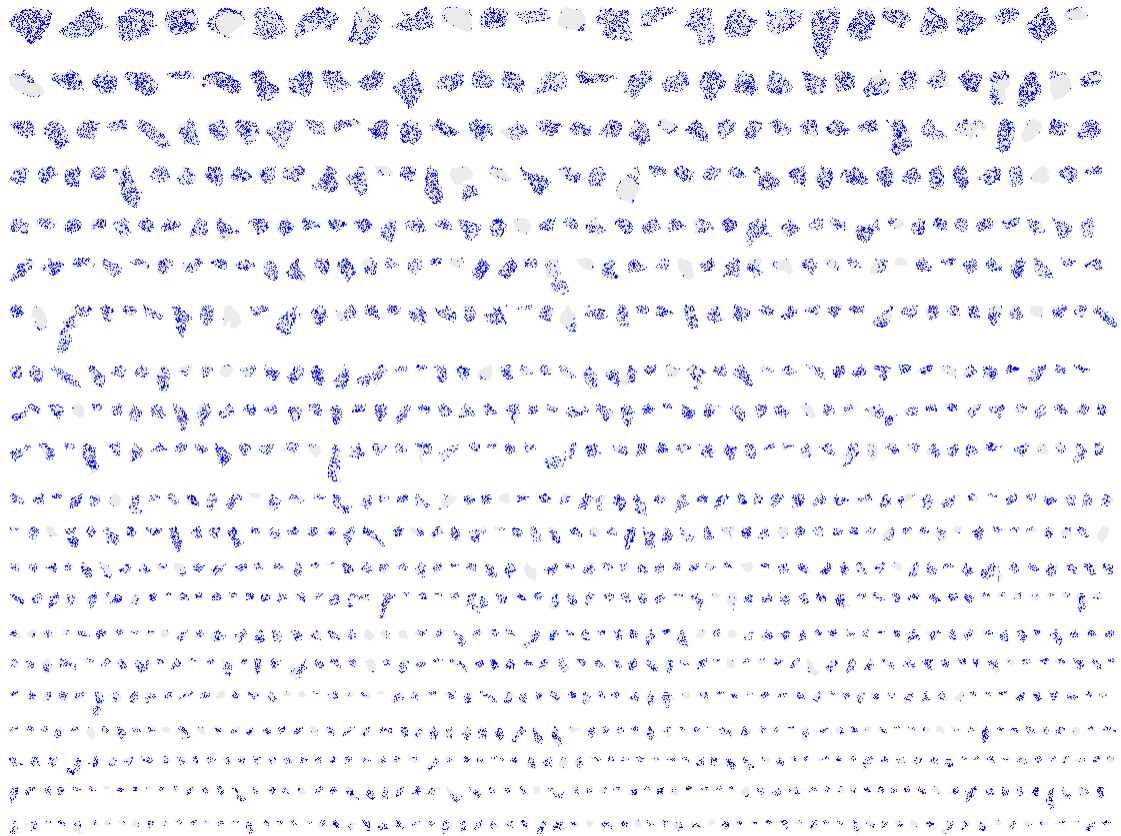
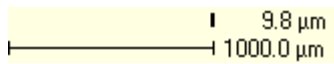


Figure 4-10: QEMSCAN Image of FeAlTi Phase



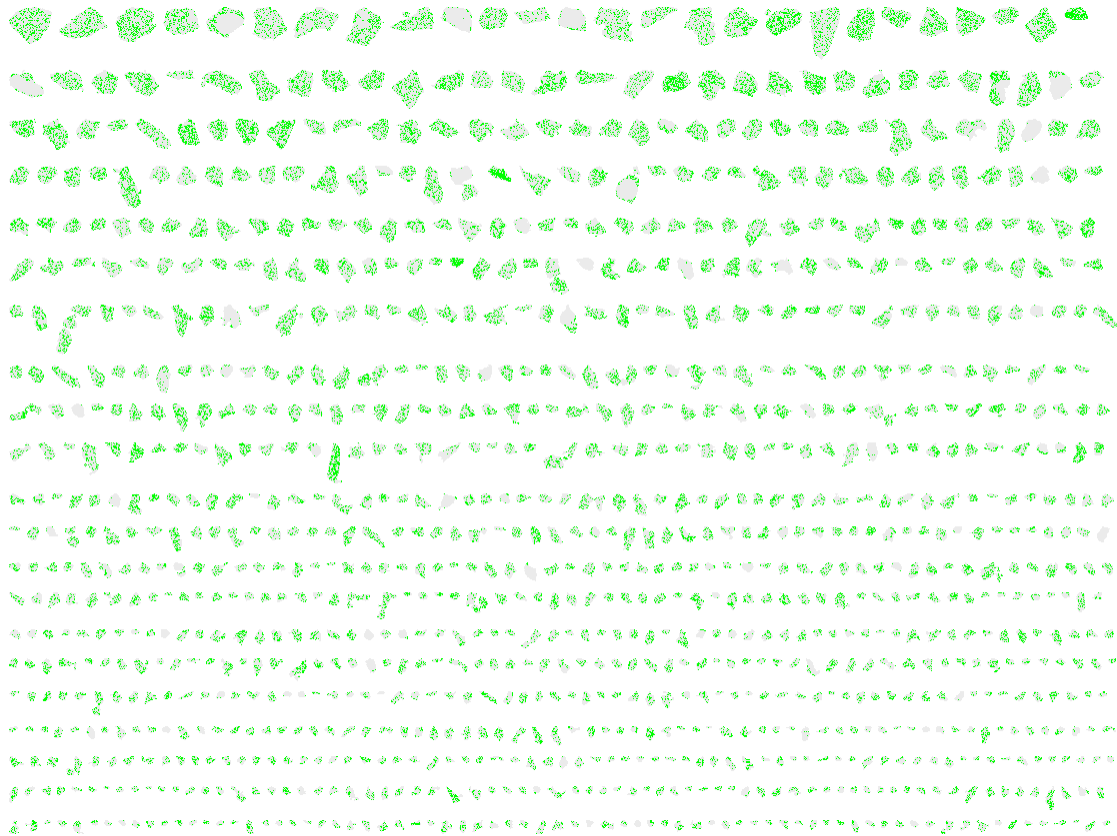


Figure 4-11: QEMSCAN Image of FeAl Phase





Figure 4-12: QEMSCAN Image of Fe Phase





Figure 4-13: QEMSCAN Image of Ti Phase

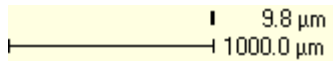




Figure 4-14: QEMSCAN Image of AlMn Phase



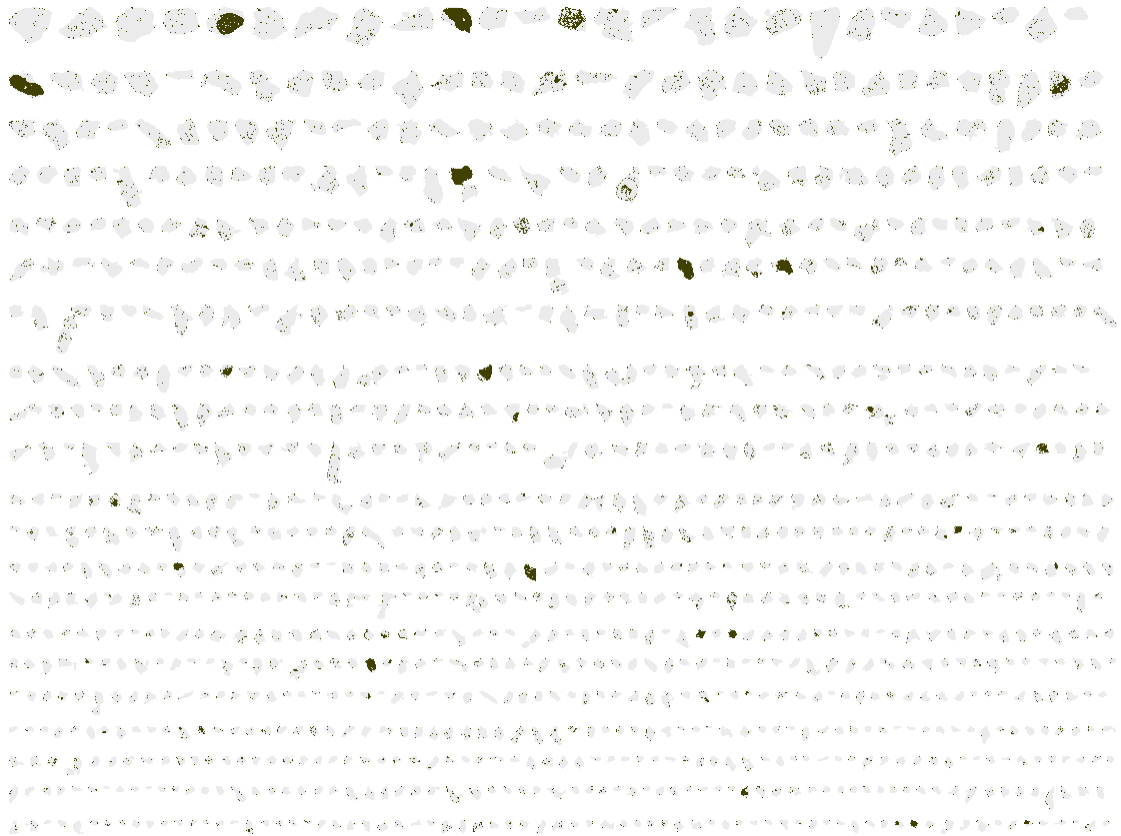


Figure 4-15: QEMSCAN Image of Al Phase

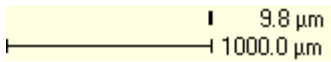
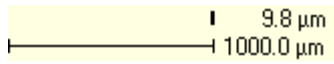




Figure 4-16: QEMSCAN Image of Mn Phase



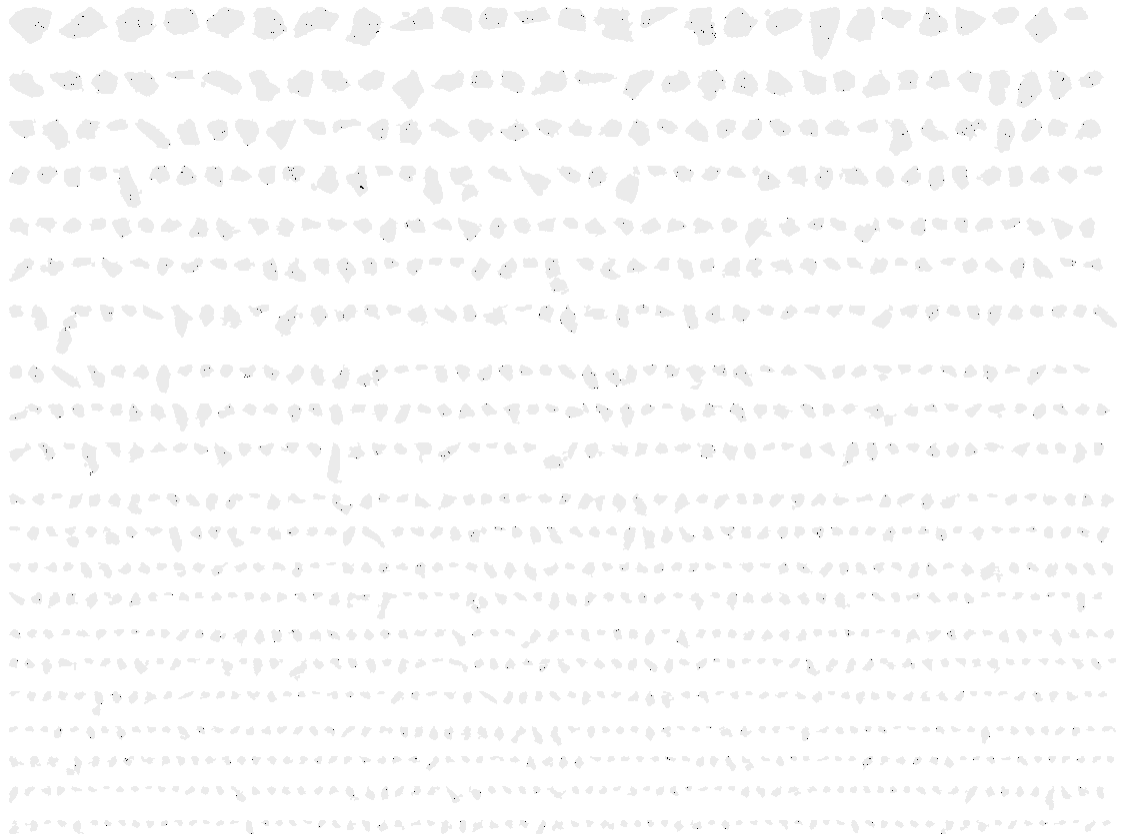


Figure 4-17: QEMSCAN Image of Other Minerals



4.6.2 Modal Abundance

Figure 4-18 shows the minerals as they make up the volume percentage of the whole sample. Colors coordinate with those representing the elements in the previous figures. Minerals represent only the volume percent that they occupy, not as a total to that point. Individual percentages are broken down and shown in Figure 4-18.

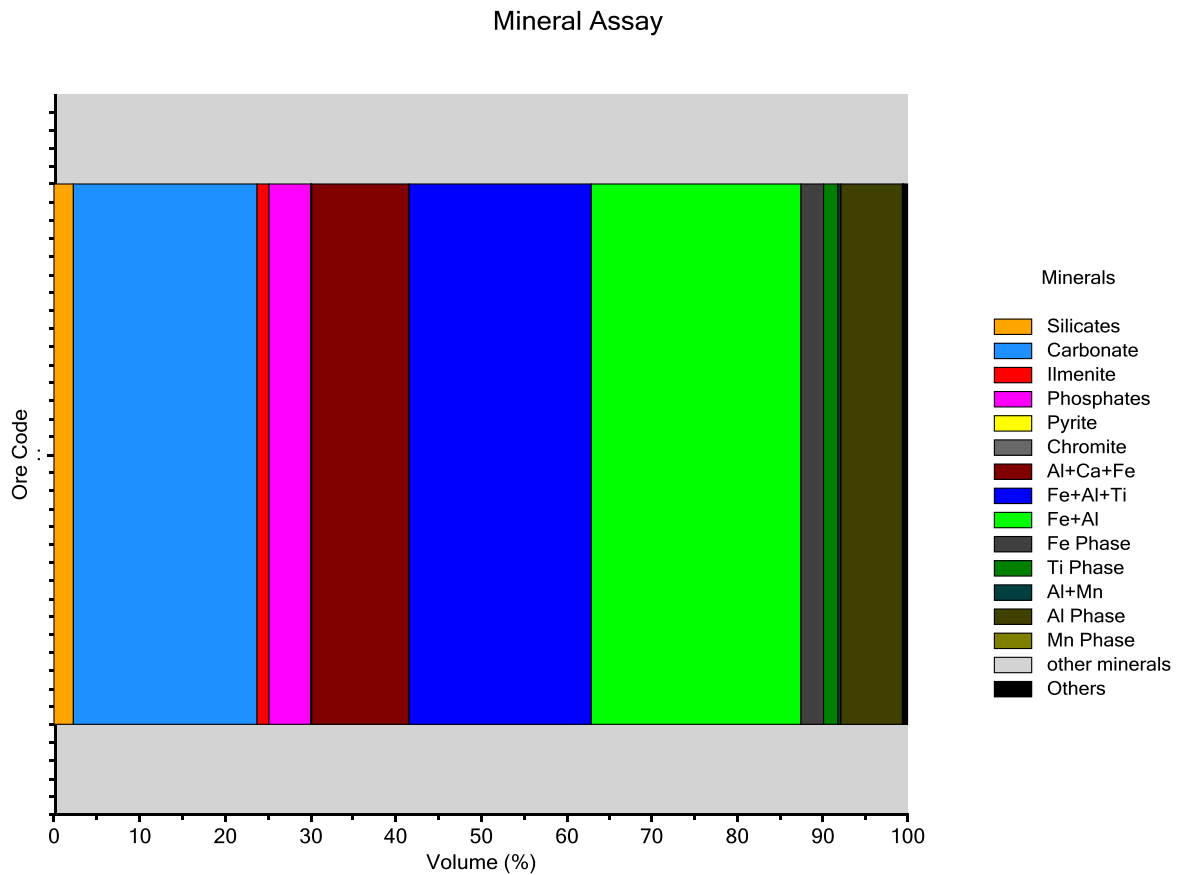


Figure 4-18: Mineral Assay from QEMSCAN

Table 4-1: Mineral Analysis from QEMSCAN

Mineral Name	Area Percent (Mineral)
Silicates	2.27
Carbonate	21.52
Ilmenite	1.39
Phosphates	4.88
Pyrite	0.10
Chromite	0.03
Al+Ca+Fe	11.41
Fe+Al+Ti	21.35
Fe+Al	24.56
Fe Phase	2.65
Ti Phase	1.68
Al+Mn	0.34
Al Phase	7.21
Mn Phase	0.08
other minerals	0.07
Others	0.45

4.6.3 Liberation

As discussed in the previous elemental analysis section, liberation issues have plagued the project. Without the proper amount of liberation, it is impossible to effectively separate the value added components needed to make this effort economically feasible. As shown in Figure 4-19, with an over 70% locked result further crushing or work in chemically fracturing the outside of the particles is necessary in order to achieve a higher recovery of the value added materials. As with the elemental analysis, each mineral cache is broken down into the amounts that are classified as liberated, midlings, or locked components. Liberated means that greater than 90% of the particle being examined is the desired mineral, and locked means that less than 30% of the particle being the mineral in question. The midlings represent all minerals that fall between 30 and 90% purity.

The two phases of the most interest are the aluminum and iron phases as shown in Figure 4-20 and Figure 4-28 respectively, neither of these phases have much liberated material. Aluminum

only has 7% liberated while the iron phase is below 1% liberation. Chromite is the phase with the least liberation, Figure 4-23, at 100% locked, while the aluminum and manganese phase, Figure 4-21, have the least amount of the sample being locked with 25% however almost all of the remaining material is in the middling portion. Pyrite,

Figure 4-24, an element of little interest and small quantity is the most liberated with 20% reporting to the liberated section. Carbonates, Figure 4-22, are split? relatively equally across the locked and middling at 51% and 45% respectively. Silicates which make digestion in acid for analysis difficult show 84% of the mineral being locked, Figure 4-25. Titanium, Figure 4-26, is an element that could prove to be very useful if the 98% locked section could be overcome and economically extraction was discovered. Ilmenite follows suit with elemental iron and titanium at 94% locked as shown in Figure 4-27. Phosphates, Figure 4-31, and the aluminum calcium iron phase, Figure 4-32, have similar liberation characteristics at 89% and 87% locked particles. Iron aluminum, Figure 4-29, manganese, Figure 4-30, and iron aluminum titanium Figure 4-33, show slight liberation improvements at 53%, 68% and 67% locked particles respectively.

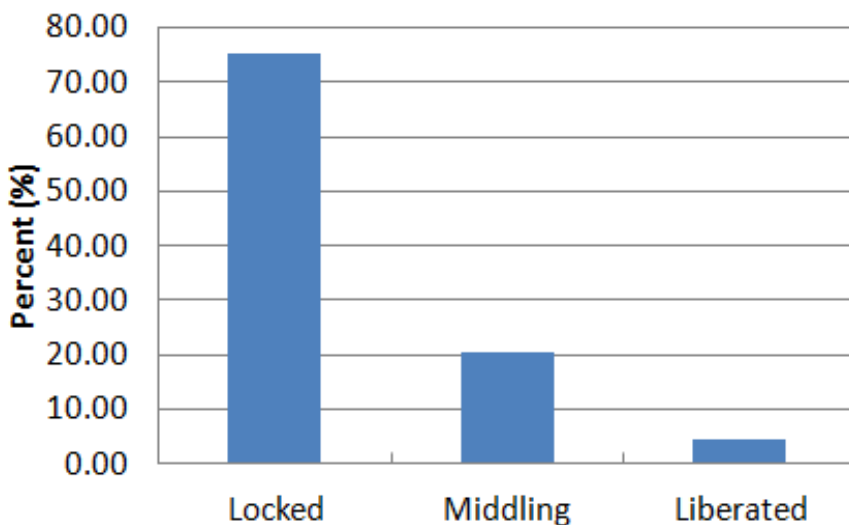


Figure 4-19: Overall Liberation

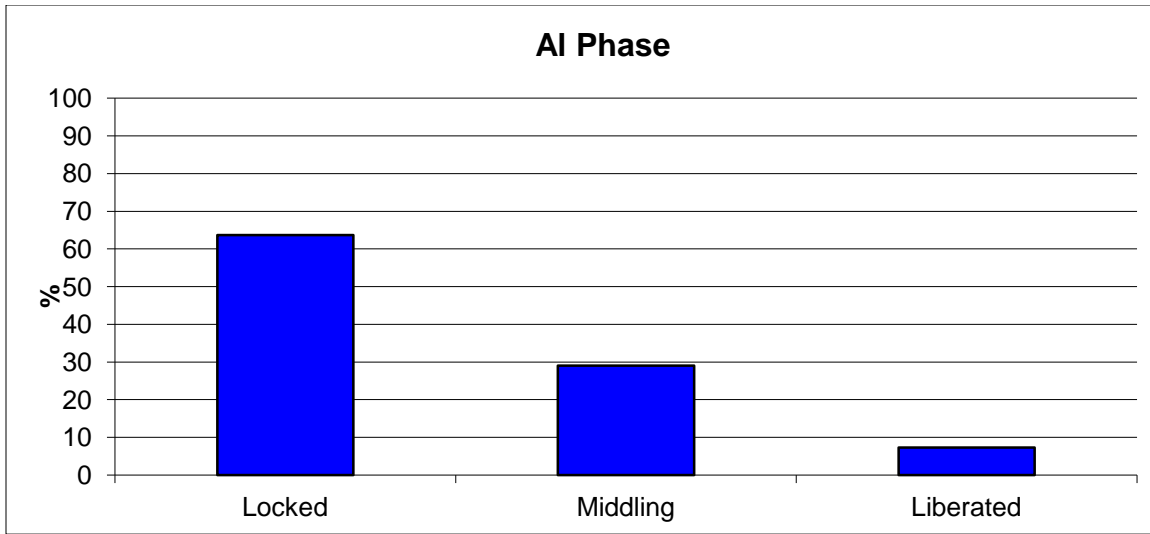


Figure 4-20: Al Phase Liberation

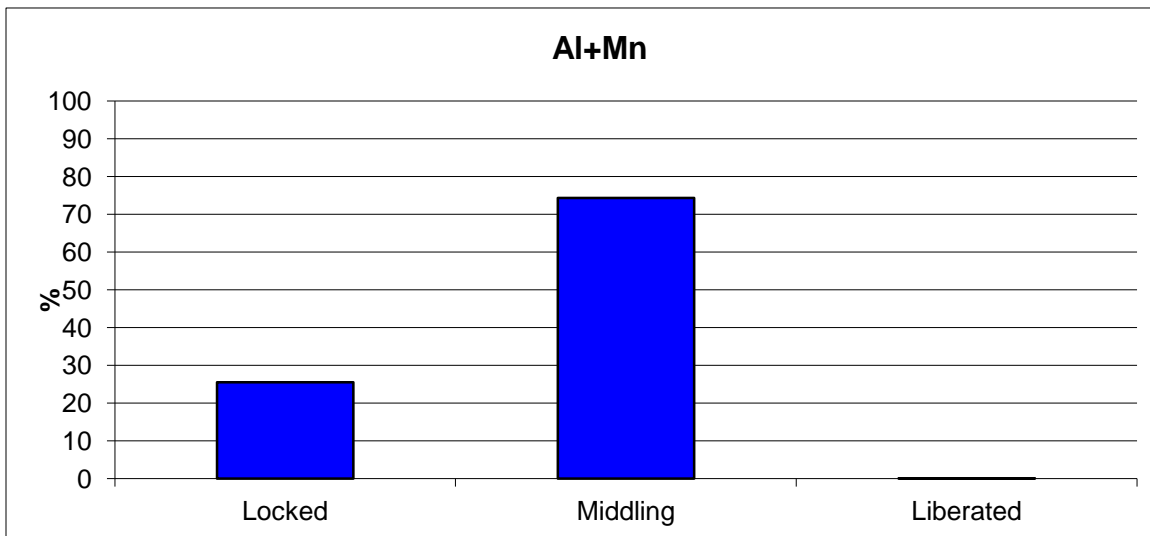


Figure 4-21: AlMn Phase Liberation

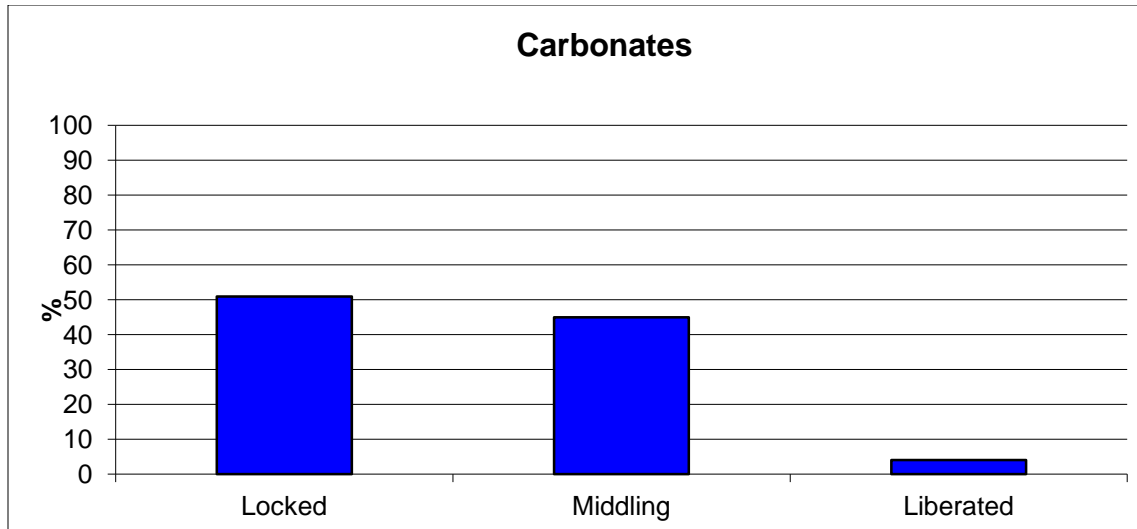


Figure 4-22: Carbonates Liberation

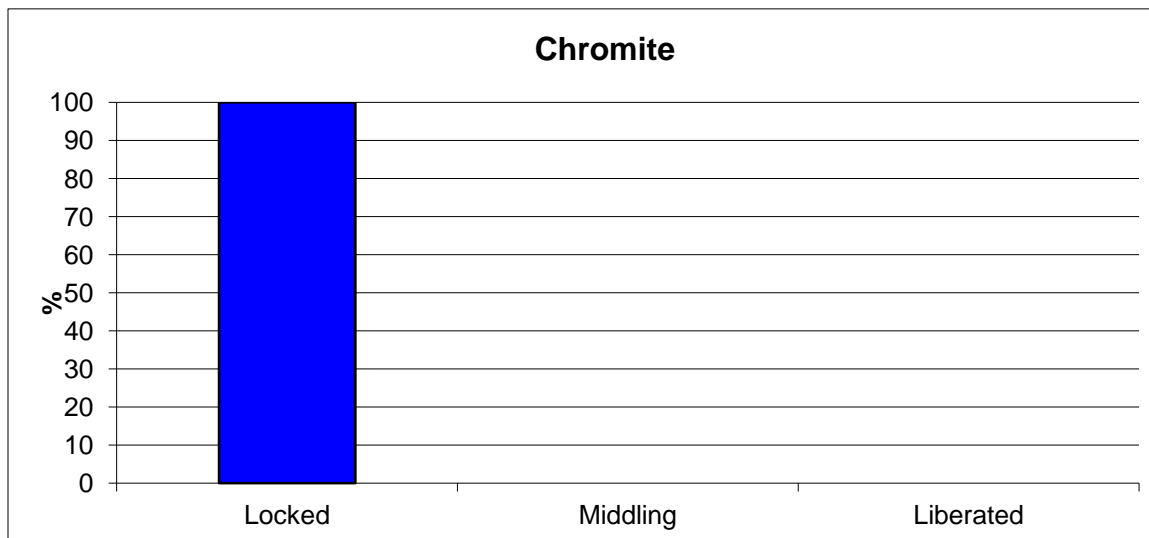


Figure 4-23: Chromite Liberation

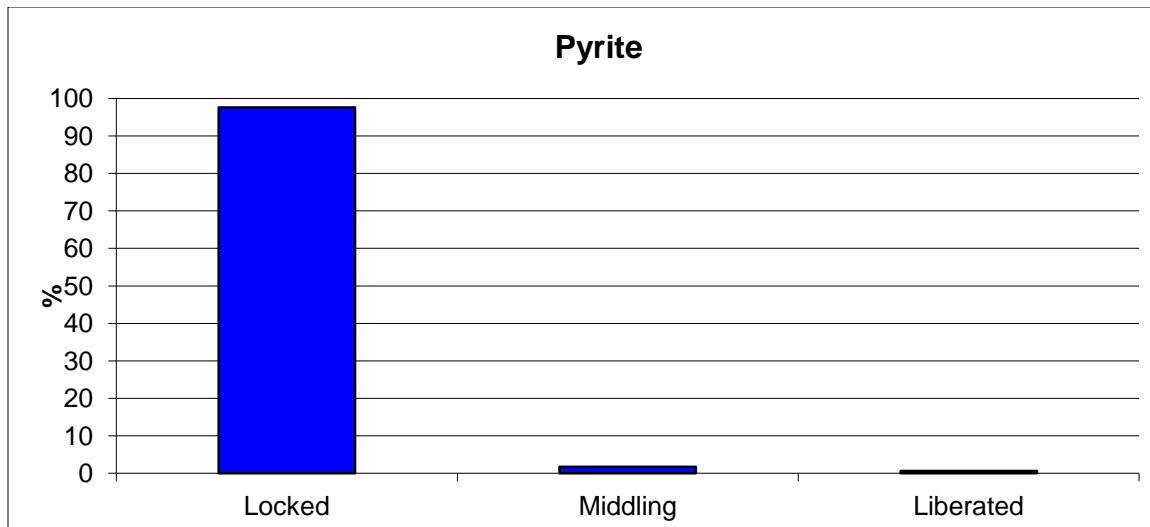


Figure 4-24: Pyrite Liberation

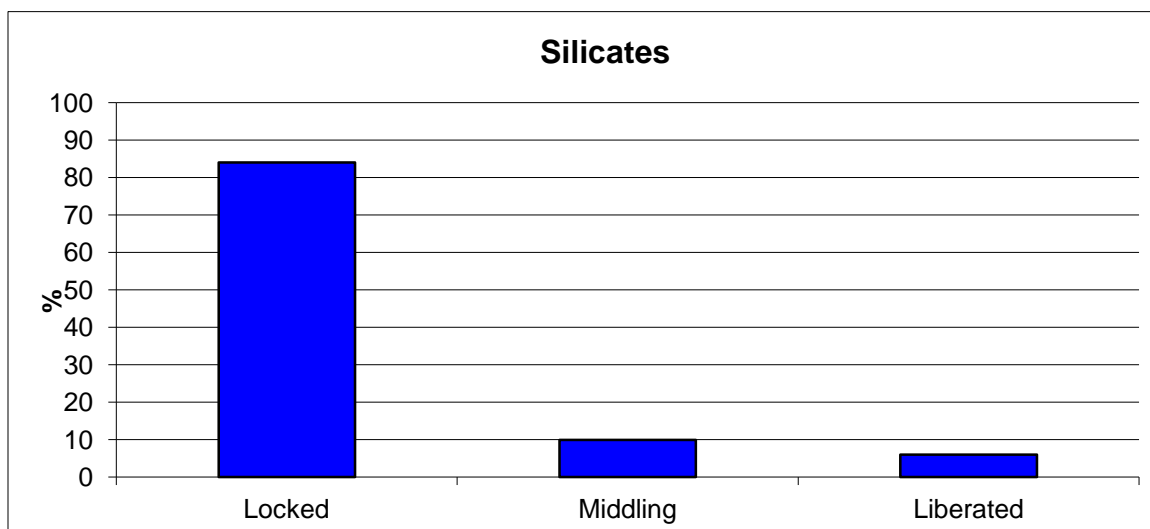


Figure 4-25: Silicates Liberation

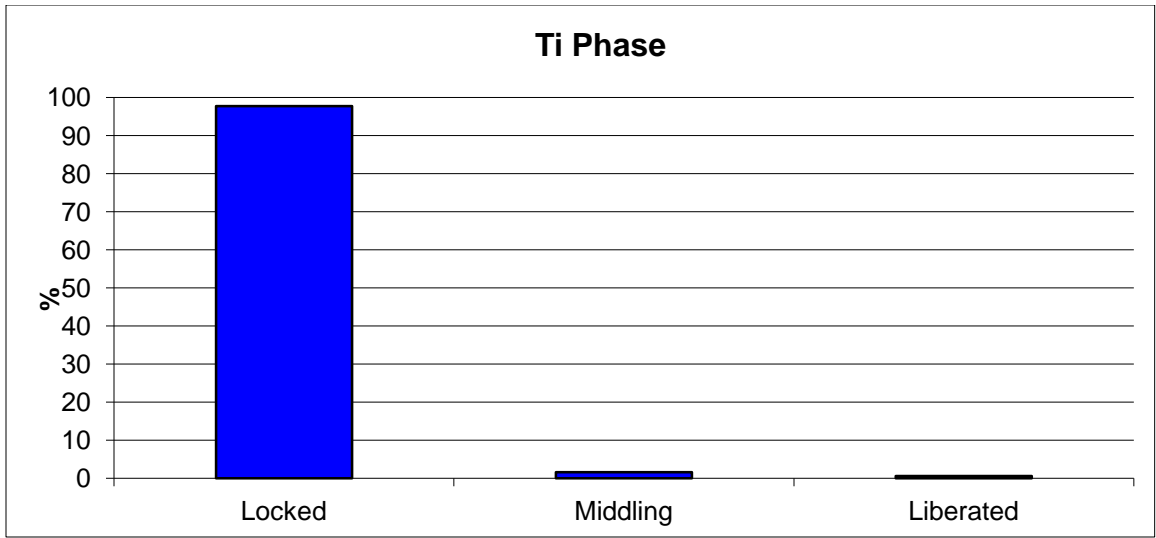


Figure 4-26: Ti Phase Liberation

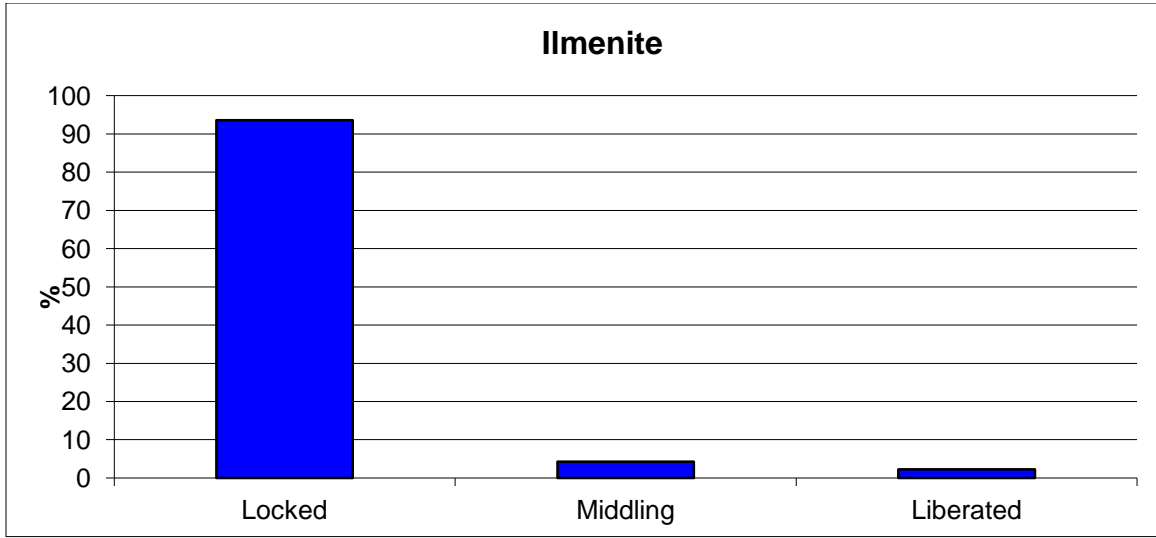


Figure 4-27: Ilmenite Liberation

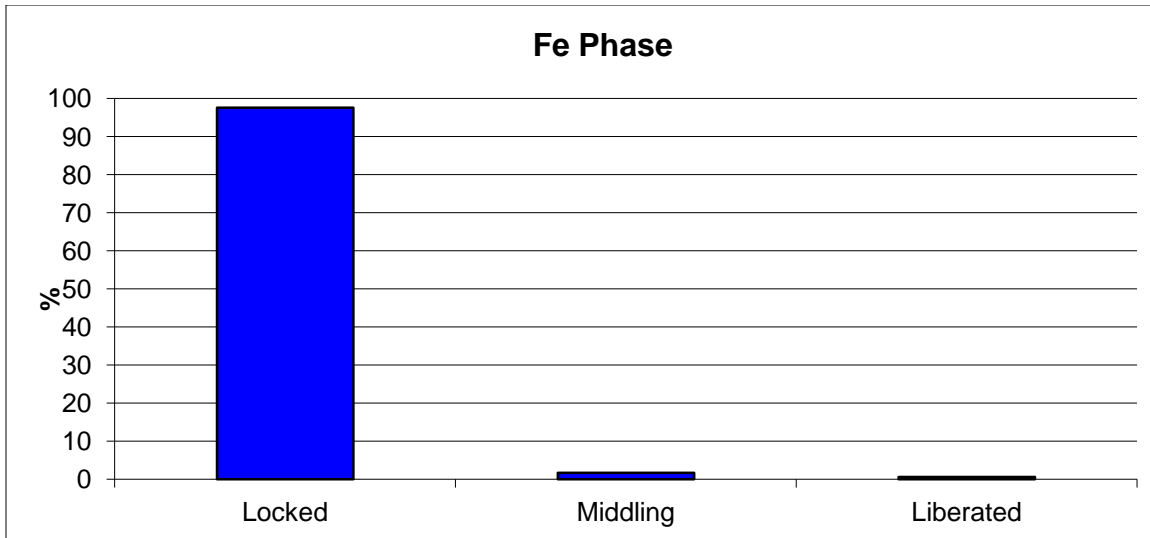


Figure 4-28: Fe Phase Liberation

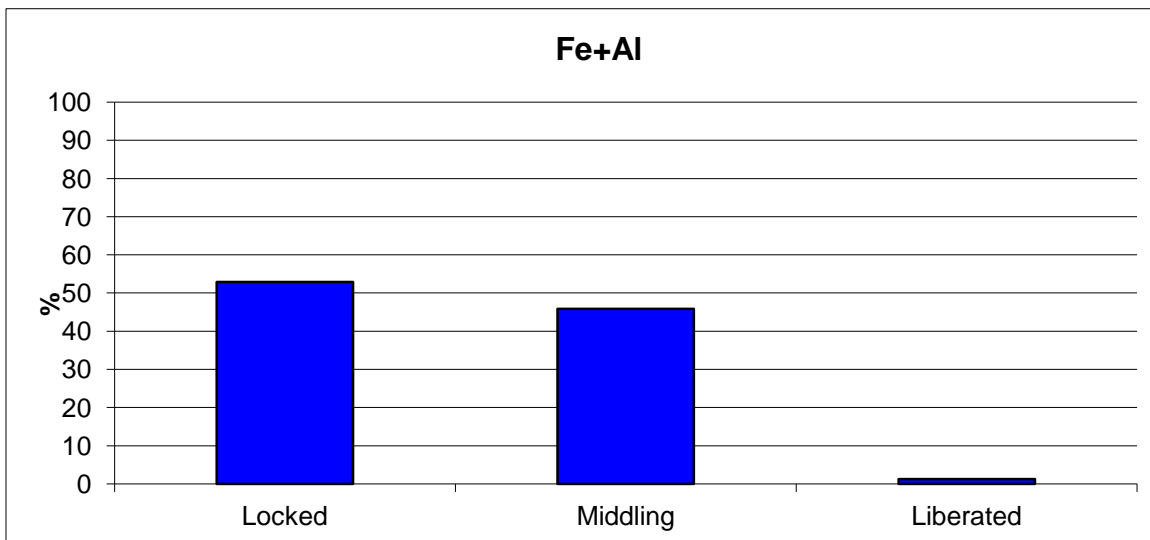


Figure 4-29: FeAl Phase Liberation

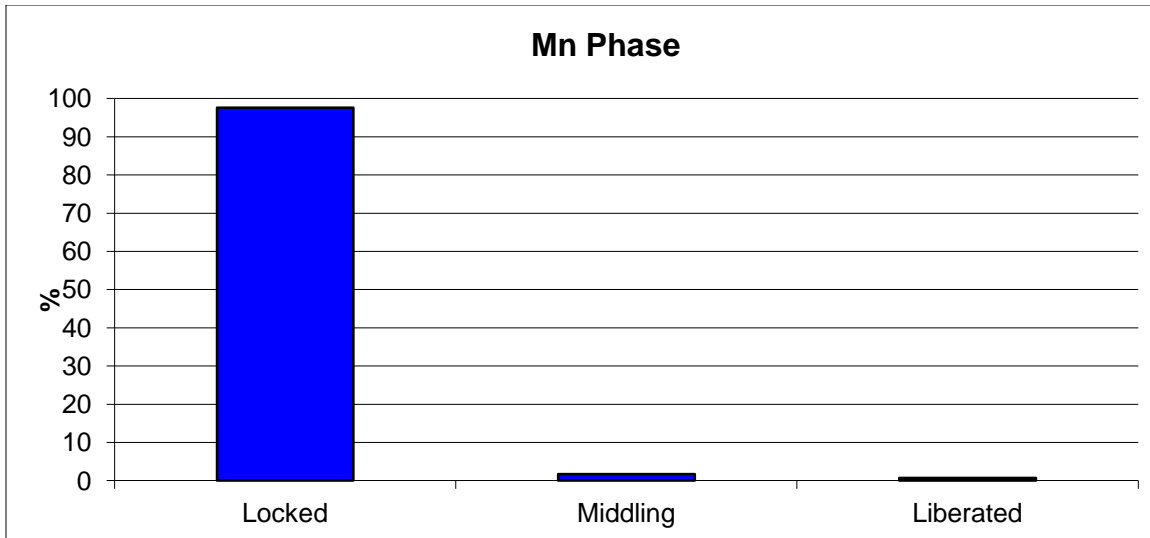


Figure 4-30: Mn Phase Liberation

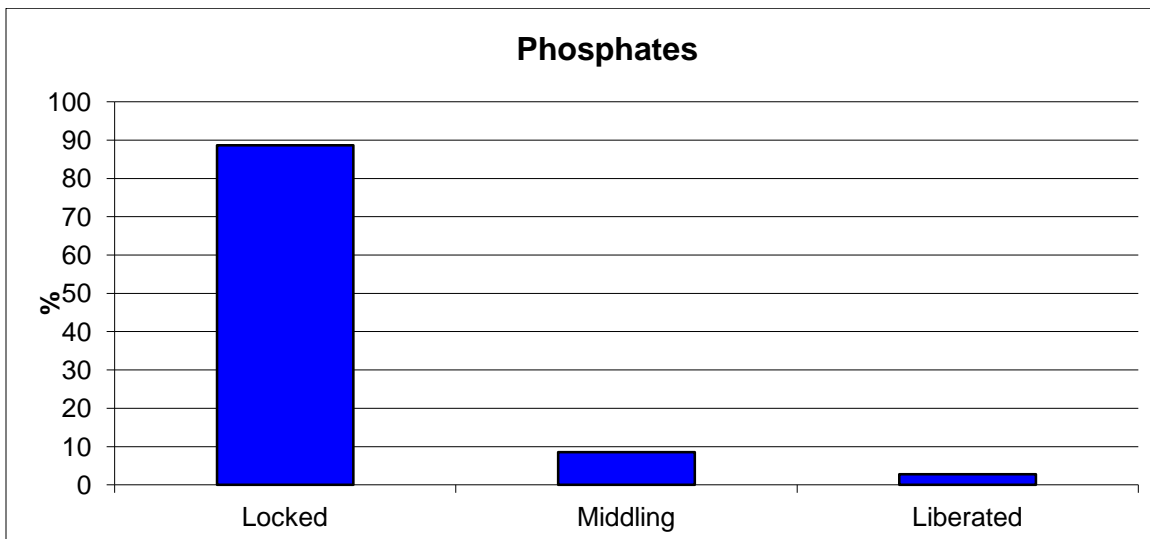


Figure 4-31: Phosphates Liberation

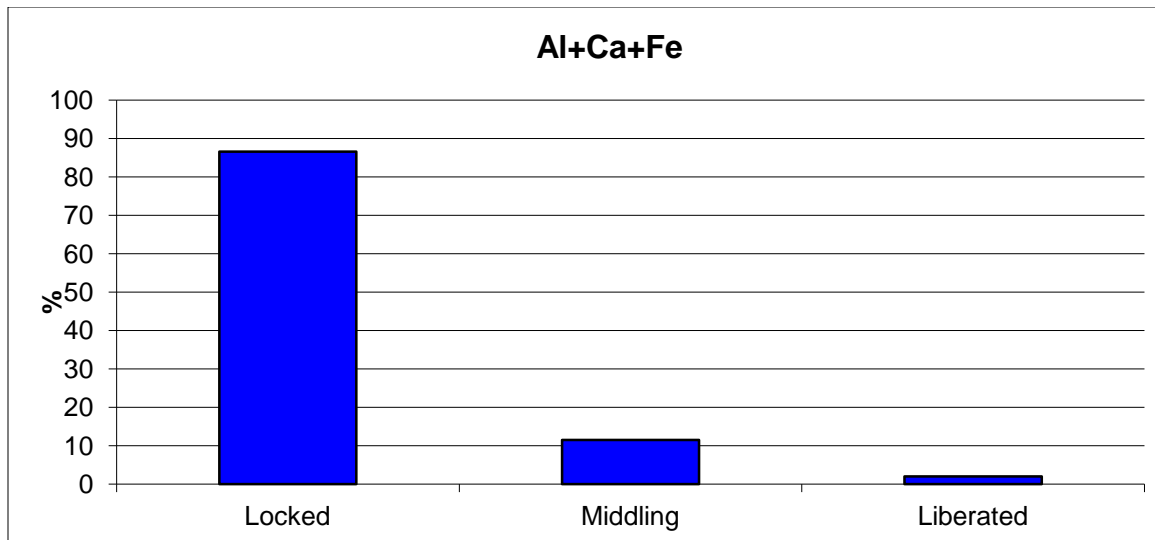


Figure 4-32: AlCaFe Phase Liberation

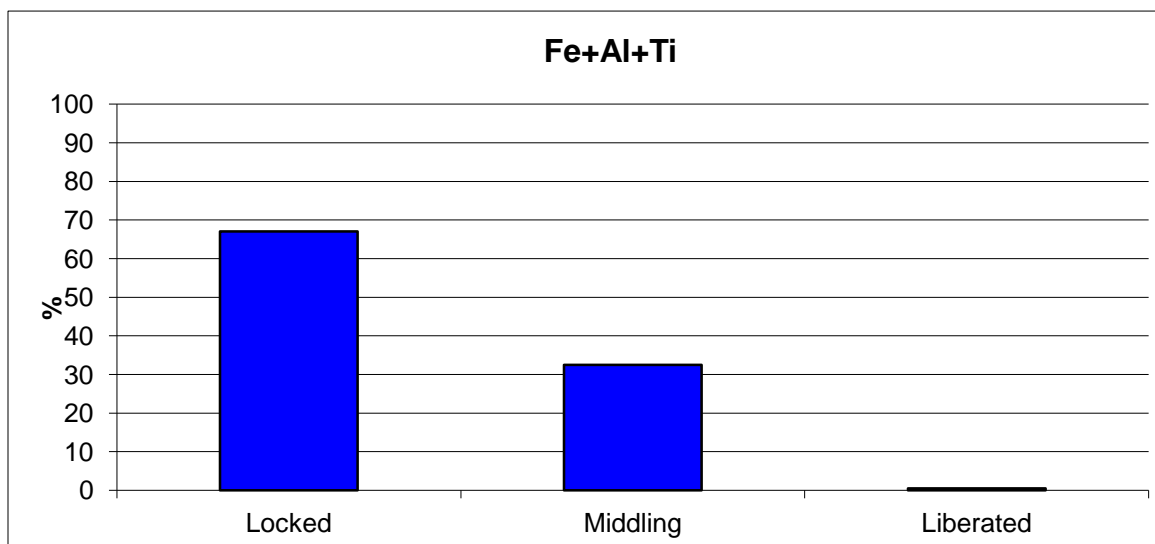


Figure 4-33: FeAlTi Phase Liberation

4.7 Economic Analysis

A general economic analysis was done only on the process cost estimate. This included only the materials, reagents and energy costs. Things not included are labor, transportation, equipment, or maintenance of equipment. This example assumes a zero cost for red mud, and the only benefits being alumina and iron at a 95% recovery rate per kilogram of red mud as seen in Table 4-2.

Table 4-2: Reagent Costs for Red Mud Processing

Reagent Name	Amt in 250g RM	Cost	Amount (g)	cost/g	Total Cost per 250g roast	Total Cost per kg Red Mud
Red Mud	250	0	0	0	0	0
Na ₂ CO ₃ 50% excess	159	185	1000000	0.000185	0.029415	0.11766
CaO	10	112.5	1000000	0.0001125	0.001125	0.0045
Petroleum Coke 50% excess	11.2	579	907185	0.000638238	0.007148	0.028593
Total Reagent Costs					0.037688	0.150753

The cost for sodium carbonate, calcium oxide, and petroleum coke were determined from the alibaba.com website on November 19, 2013. There was a range in cost per ton with the low being \$238 USD and the high being \$920 USD, an average of \$579 USD/ton was used for the calculation of petroleum coke.

The prices for water needed were taken from North Table Mountain Water and Sanitation District's current residential prices. These prices may also be high as commercial water rates were not available at this time. The price per kilowatt hour was used from eia.gov on November 16, 2013 and the values were based on the published commercial rates for Colorado. Depending on the area, these costs could increase or decrease. The results are shown in Table 4-3: Final Economics of Red Mud Processing

. With the benefits of alumina and iron reported in Table 4-3: Final Economics of Red Mud Processing

Prices are reported for November 16, 2013. Alumina was reported from indmin.com/MarketTracker and Iron prices were reported from chemicool.com/elements/iron. Taking into account the costs and benefits, as shown below this process is not currently economically viable.

Table 4-3: Final Economics of Red Mud Processing

	Reagents	Energy	Costs	Benefits	Total
Iron Bulk	0.150753065	1.75531512	1.91	0.222775	-1.68

CHAPTER 5

CONCLUSIONS AND RECOMMENDATIONS

5.1 Conclusions

Five main conclusions can be drawn from the test work and results. First, roasting with both sodium carbonate and carbon are not beneficial, roasts need to be done individually in order to more effectively separate the water soluble elements. Roasting with foundry bag house dust cannot be done above 800°C or an agglomerate forms due to the fusion caused by the presence of coal. Water washes are effective at removing some but not all of the alumina and sodium from the roasted material. Liberation is an ongoing problem that needs further investigation. Finally, more work needs to be done to optimize conditions

5.2 Recommendations for Further Work

Although the original goal of producing an iron button was completed, the current process leaves room for improvement. The most important part of this project that needs to be understood is the liberation problem. More mineralogical work needs to be done to determine if the phases can be economically separated enough to create enough liberation to separate elements effectively.

Once liberation and mineralogy are fully understood, optimization of both sodium carbonate and carbon roasts need to be done. Sodium carbonate roasts need to be optimized in order to achieve a clean separation of alumina and sodium in the water wash step, without lowering the sodium levels this process cannot go to commercial smelting.

Water washing of the sodium carbonate roasts should be done using various agitation speeds and impeller types. The impeller types and speeds may affect the type of shear forces that the slurry experiences, thus improving or inhibiting the leaching of the water soluble elements.

Carbon roasting should be done using upgraded foundry bag house dust according to the procedure introduced in Brandon Dugan's Master's Thesis. This step will determine if it possible to utilize another waste product to possibly decrease the overall reagent cost for the project.

Magnetic separation will benefit greatly from more complete mineralogical understanding. This understanding will determine if it is possible to separate the magnetite from the other elements or if it a wasted step.

Although smelting was a success, it should be done at varying temperatures and times in an effort to reduce the overall energy consumptions and thus overall cost of the project.

5.3 Contribution to the Field

Red Mud is a worldwide problem with hundreds of millions of tons sitting waiting for a solution. This project contributed by demonstrating that a separation can be made to produce iron that could then be sold in an effort to make the process economically feasible. Although more work needs to be done to optimize the process, it is a good start to show what does and does not work for this particular processing scheme.

REFERENCES CITED

1. Boily, Robert, Ph.D. Twenty Cases of Red Hazard, An Inventory of Ecological Problems Caused by Bauxite Residue from Alumina Production. Larval, Quebec, Canada: Inforex, 2012. Print.
2. Chandra, Satish. Waste Materials Used in Concrete Manufacturing. Westwood, N.J., U.S.A.: Noyes Publications, 1997. Print.
3. Fly Ash. Fly Ash. N.p., n.d. Web. 01 Dec. 2012. <<http://www4.uwm.edu/cbu/>>.
4. Gura, David. "Toxic Red Sludge Spill from Hungarian Aluminum Plant 'An Ecological Disaster'" October 5, 2010.
5. Hungarian Chemical Sludge Spill Reaches Danube. BBC. October 7, 2010.
6. Kogel, Jessica Elzea. Industrial Minerals & Rocks: Commodities, Markets, and Uses. Littleton, CO: Society for Mining, Metallurgy, and Exploration, 2006. Print.
7. Mohan, D.; Pittman, CU. (Apr 2007). "Arsenic removal from water/wastewater using adsorbents--A critical review". J Hazard Mater 142 (1-2): 1-53.
8. Peretti, Daniel. The Modern Prometheus: The Persistence of an Ancient Myth in the Modern World. N.p.: Indiana University, 2008. Print.
9. Pontikes., Y. "Red Mud Applications." Red Mud Project, 14 Mar. 2005. Web. <<http://www.redmud.org/Applications.html>>.
10. Staley, Anthony K., Ph.D. An Investigation Into the Pyrometallurgical and Electrometallurgical Extraction of Iron from "red Mud" Generated in the Processing of Bauxite Ores. Golden, CO: Colorado School of Mines, 2002. Print.
11. The Kolontár Red Mud Dam Failure (Hungary). The Kolontár Red Mud Dam Failure (Hungary). N.p., n.d. Web. 3 Sept. 2012. <<http://www.wise-uranium.org/mdafko.html>>.
12. Zhang-long, YU, Chen Yong-jian, Wang Yong-xia, and Wan Ping-yu. Red-mud Treatment Using Oxalic Acid by UV Irradiation Assistance. School of Science, Beijing University of Chemical Technology, Department of Mineral Resource and Metallurgical Materials, PR China, Beijing General Research Institute for Non-Ferrous Metals, The Nonferrous Metal Society of China, n.d. Web. 2 Oct. 2012.
13. Dugan, Brandon. Recycling of Bag-House Dust From Foundry Sand Through Chemical and Physical Separation. Golden, CO: Colorado School of Mines, 2011. Print.

14. “Aluminum,” US Geological Survey, Mineral Commodity Summaries (Washington, D.C., USGS 2012), minerals.usgs.gov/minerals/pubs/commodity/aluminum/mcs-1012-alumi.pdf.
15. J. Fursman, J.E. Mauser, M.O. Butler, and W.A. Stickney, ‘Utilization of Red Mud Residues From Alumina Production’, U.S. Bureau of Mines Report of Investigations 7454 (1970).
16. R. Piga, F. Pochetti, and L. Stoppa, JOM, 45 (35) (1993), pp. 55–59.
17. W. Braithwait, GB patent 2078211-A (January 1982).
18. Agency of Ind. Sci. Tech., J. patent 52152896-A (December 1977).
19. S. Guccione, Eng. Min. J., 172 (34) (1971), pp. 136–138.
20. N. Dakatos, M. Miskei, and J. Szolnoki, DE patent 2,747,436 (May 1978).
21. M. Cresswell, and D.J. Milne, AU patent 88102 (September 1981).
22. R. Vachon, R. Tyagi; J-C. Auclair, and K.J. Wilkinson, Environ. Sci. Technol., 28 (26) (1994), pp. 26–30.
23. E. Balomenos, I Gianopoulou, D. Panias, and I. Paspaliaris, “A Novel Red Mud Treatment Process” (Paper presented at the 3rd Intl. Conf. on Industrial & Hazardous Waste Management, Crete, Greece, 2012).
24. B. Mishra, A. Staley, and D. Kirkpatrick, Recycling and Waste Treatment in Mineral and Metal Processing: Technical & Economic Aspects: Vol.2, ed. B. Björkman, C. Samuelsson, and J.-O. Wikström (Warrendale, PA: TMS, 2002), pp. 567–576.
25. K. Hammond, B. Mishra, D. Apelian, and B. Blanpain. JOM, 65 (28) (2013), pp. 340-341.
26. W.G. Rumbold; Bauxite and Aluminum; 1925; Imperial Institute, London; Hazell Watson & Viney Ld., London.
27. Various Websites: Company Sites from Alcoa, Nabalco, Renyolds Kaiser, US Geological Serveys Site, and the Mineral Council of Australia.
28. A.R. Burkin. Production of Aluminum and Alumina. 1987. Published on behalf of the Society of Chemical Industry by John Wiley & Sons. Chichester, New York, Brisbane, Toronto, Singapore.
29. F.King; Aluminum and its Alloys; Ellis Hornwood Limited; Chichester, West Sussex, England; 1987.

30. Fathi Habashi. A Textbook of Hydrometallurgy. 1993. Métallurgie Extractive Québec, Canada.
31. Junius David Edwards, Francis C. Faray, Zay Jeffries. Aluminum and its Production. 1930. McGraw-Hill Book Co., Inc. New Yourk and London.
32. Robert J. Anderson. The Metallurgy of Aluminum and Aluminum Alloys. 1925. Henery Carey Baird & CO., Inc. New York, New York.
33. P.M. Prasad; Maneesh Singh; Problems in the Disposal and Utilization of Red Muds; The Banaras Metallurgist, Vol. 14 & 15, 1997: pp. 127-140.
34. February 2000. Technology Roadmap Bauxite Residue Treatment and Utilization. Summary of Workshop Prepared by Energetics, Inc.
35. Luigi Piga; Fausto Pochetti; Luisa Stoppa; Recovering Metals from Red Mud Generated During Alumina Production; Journal of Metals, pp. 54-59; November 1993.
36. P.M. Prasad; J.M. Sharma; V. Vishwanathan; A.K.Nandi; Maneesh Singh; Production of Bricks/Stabilized Blocks From Red Mud; Department of Metallurgical Engineering, Institute of Technology, Banaras Hindu University, Varanasi 221005; Proceeding of Interactive Meeting on the Bauxite and Alumina (BAUXAL-96); Feb 1996, Allied Publishers New Delhi, pp. 387-396.
37. P.M. Prasad; S.N. Upadhayay; Maneesh Singh; Preparation of a Iron Rich Cements Using Red Mud; Cement and concrete research, volume 27, No. 7, pp. 1037-1046, 1997, Pergamon, Elsevier Science Ltd.
38. Maneesh Singh; S.N. Upadhayay; P.M. Prasad; Preparation of Social Cements from Red Mud; Waste Management, Volume 16 No. 8, pp. 665-670, 1970; Pergamon, Elsevier Science Ltd.
39. Anonymous; Red Mud Door Panel; Project Profile; Reg. Res Lab.; Bohpal (1993).
40. L. Schmidt et al.; DD Patent 239345-A; September 24th, 1986.
41. H. Bruhne; DE Patent 3436085-A; March 10th, 1986.
42. Funke, Armin, H. Wetzel, and G. Buhler; Rubber Fillers from Red Mud to Produce Aluminum-Iron Coagulant and Si-Stoff; Sov. J. Non-Ferrous Met.; 25 (30) 1964; pp 64-65.
43. I.V. Nikolaev et al.; Comprehensive Treatment of Red Mud to Produce Aluminum-Iron Coagulant and Si-Stoff; Sov. J. Non Ferrous Met.; 25 (30) 1964; pp 64-65.

44. Land, G.W.; Controlling Sulfur Dioxide Emissions from Coal Burning; Nat. Eng. 73(26): 6-8, 1969.
45. E.I. Kanzantsev, E.K. Stephanenko, and A.N. Gerasimenko (USSR); Removal of Arsenic from Waste Waters by Sorption; Tsvet. Metal 45(26): 18-20, 1972 (Russia).
46. F.G. Shultz and J.S. Berber; Hydrogen Sulfide Removal from Hot Producer Gas with Sintered Absorbents; J. Air Pollut. Contr. Ass. 20(27): 93-96, 1970.
47. H. Forester; Concrete Color Composition; DD Patent 57543; August 20th, 1967.
48. K.O Hahnel; Red Mud as a Raw Material for Colored Glass; Glasstech. Ber 76 (1953); pp. 174-175.
49. Ramanujam, S.; Bauxite Residues as Corrosion Inhibitive Primers; Paintiudia 12, 22-34, 1962.
50. G. Bayer and E. Cherdron; Red Mud Flocculant for Waste Water Treatment; Fer Offen. 2,242,822. 9pp. March 14, 1974.
51. Ellis Edward II; Chlorinated Copper as Treatment of Sewage at Kingston-on-Thames; Surveyor, 106, 195-196, 1947.
52. Agency of Industrial Science Technology; J Patent 52152896-A; December 19th, 1977.
53. Fursman, Oliver C.; Mauser, James E.; Butler, M.O.; and Stickney, W.A. 1970. Utilization of Red Mud Residues From Alumina Production; U.S. Bureau of Mines Report of Investigations RI 9397. I 28.23:7454.
54. A.E. Peterson, M.B. Shirts, and J.P. Allen. 1992. Production of titanium Dioxide Pigment from Perovskite Concentrates, Acid Sulfation Method. U.S. Bureau of Mines report of Investigations RI 9397. I 28.23:9397.
55. Habashi, Fathi. "Karl Josef Bayer and His Time* - Part 1." Proc. of International Committee for the Study of Bauxite, Alumina, and Aluminum (ICSOBA), National Aluminum - Magnesium Institute, Saint Petersburg, Russia. N.p.: n.p., 2004. N. pag. Print.

APPENDIX A – PRELIMINARY MAGNETIC SEPARATION

Lower intensity magnetic separation was performed using the following set up. The magnetic strength in Gauss is shown on the right.

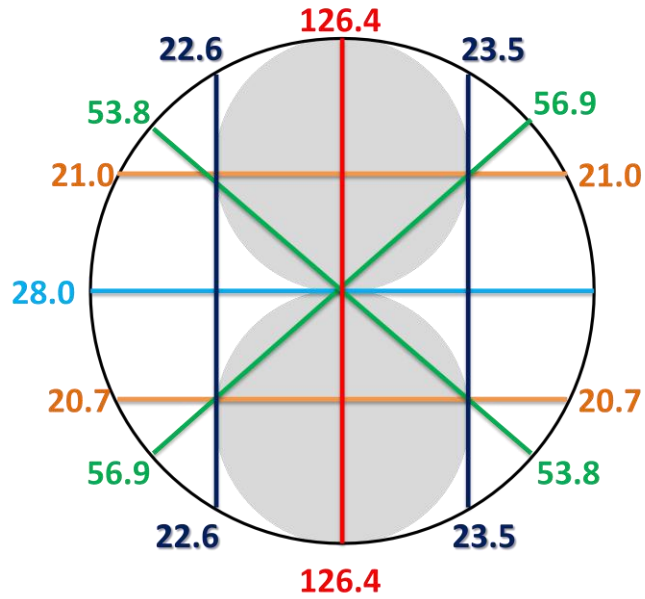


Figure A-1: Preliminary Lower Intensity Magnetic Separation

Higher intensity magnetic separation was performed using the following set up. The magnetic strength in Gauss is shown on the right.

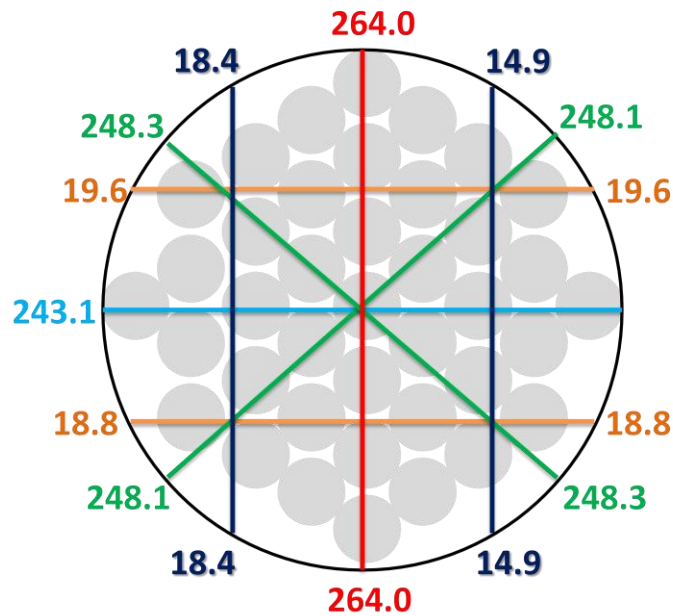


Figure A-2: Preliminary Higher Intensity Magnetic Separation

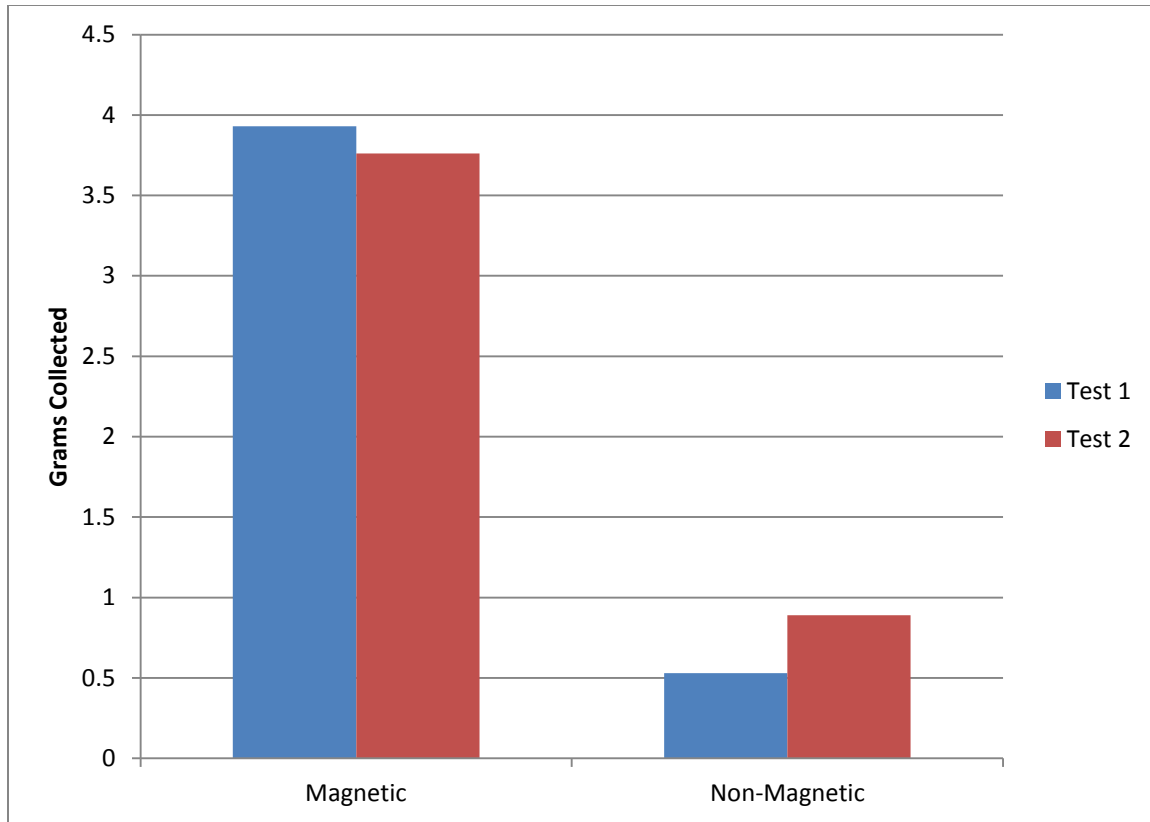


Figure A-3: Lower Intensity Magnetic Separation Weights

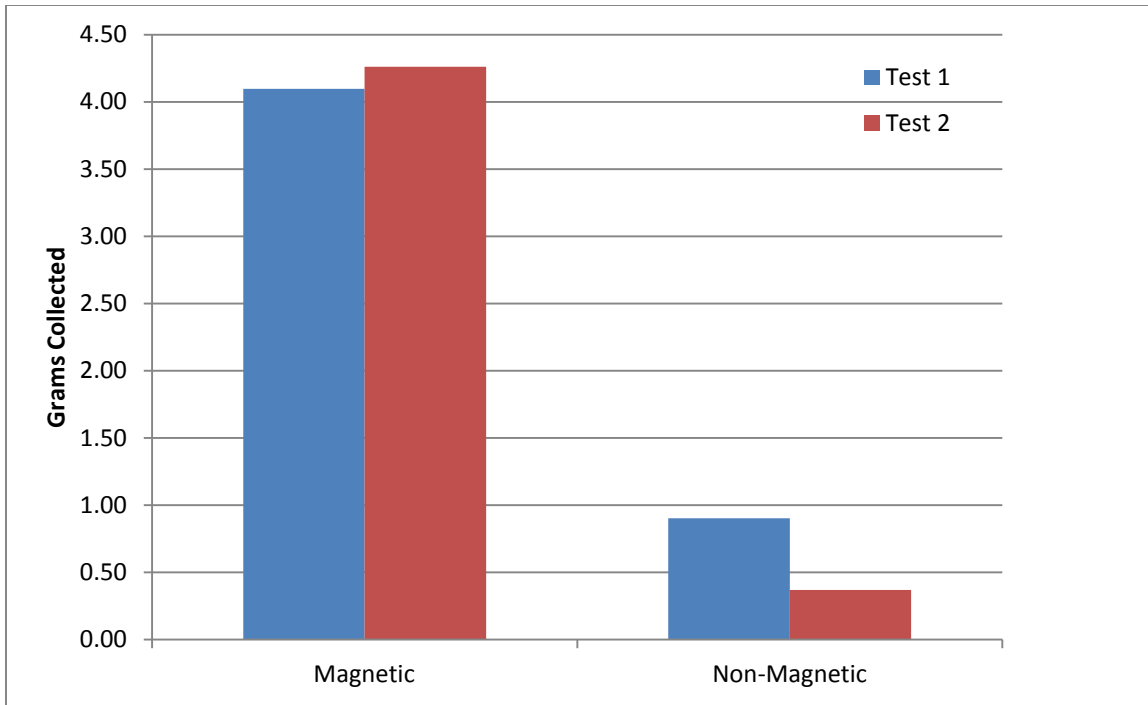


Figure A-4: Higher Intensity Magnetic Separation Weights

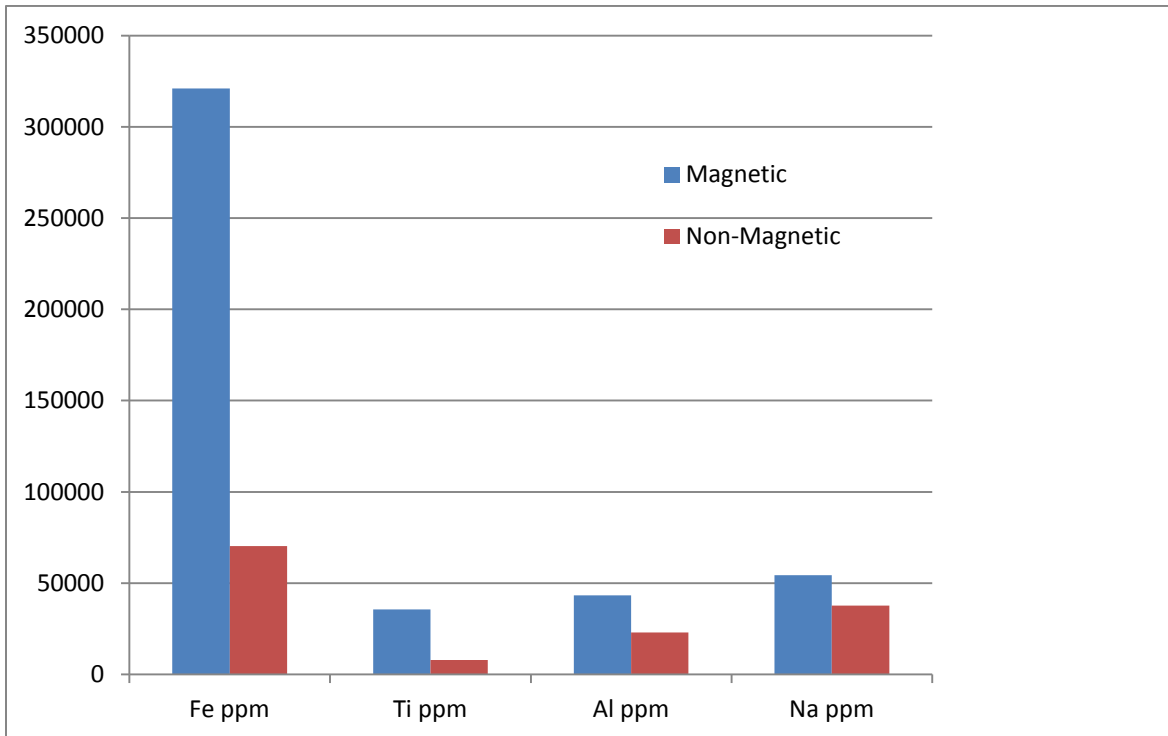


Figure A-5: Lower Intensity Magnetic Separation Test 1 Analysis

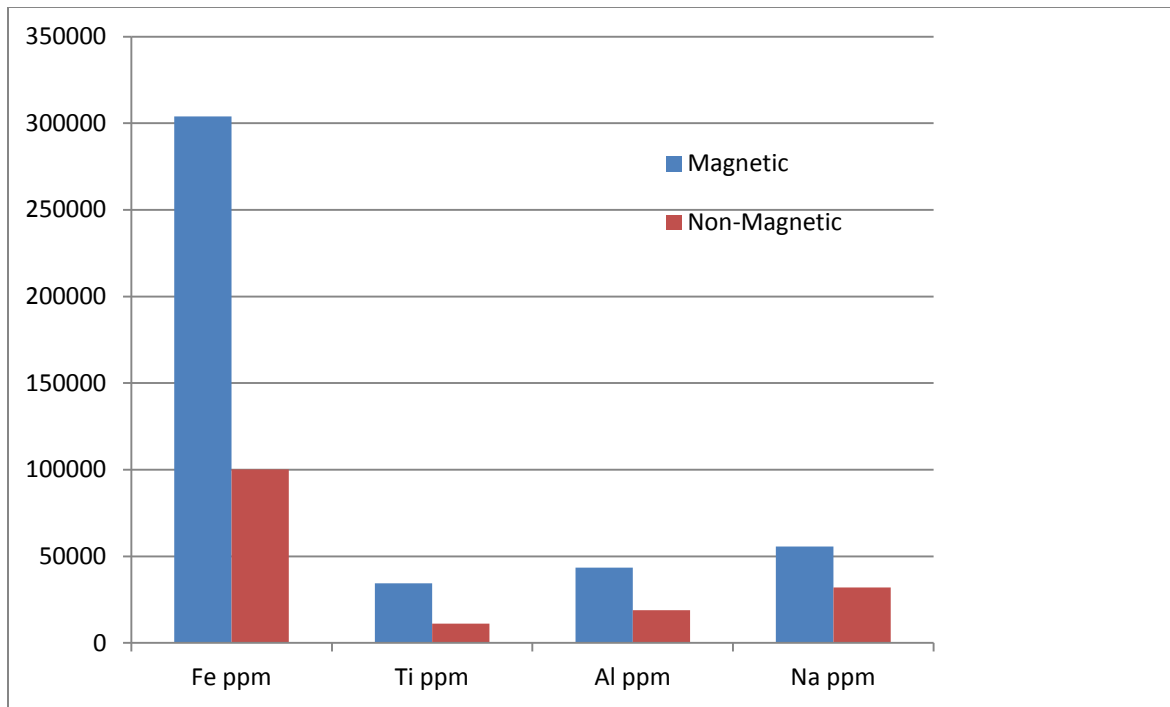


Figure A-6: Higher Intensity Magnetic Separation Test 1 Analysis

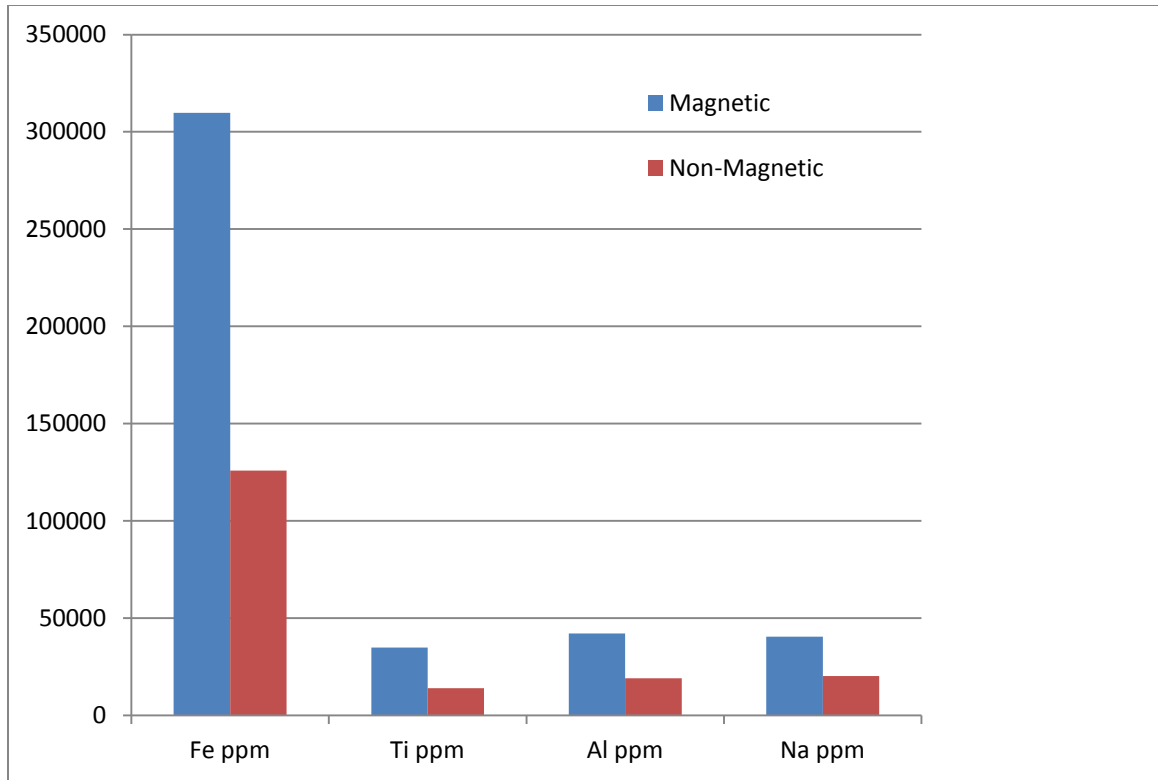


Figure A-7: Higher Intensity Magnetic Separation Test 2 Analysis

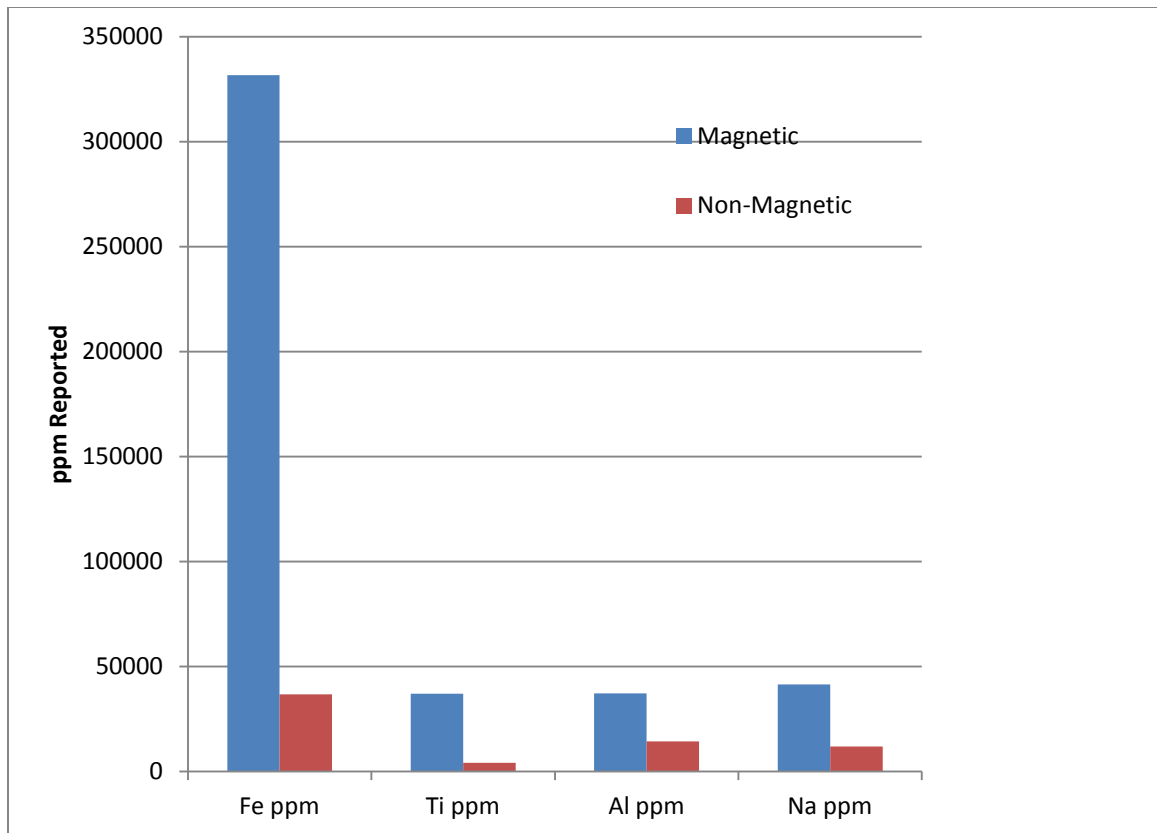


Figure A-8: Lower Intensity Magnetic Separation Test 2 Analysis

APPENDIX B – SODIUM CARBONATE ROASTS WITH WATER WASH

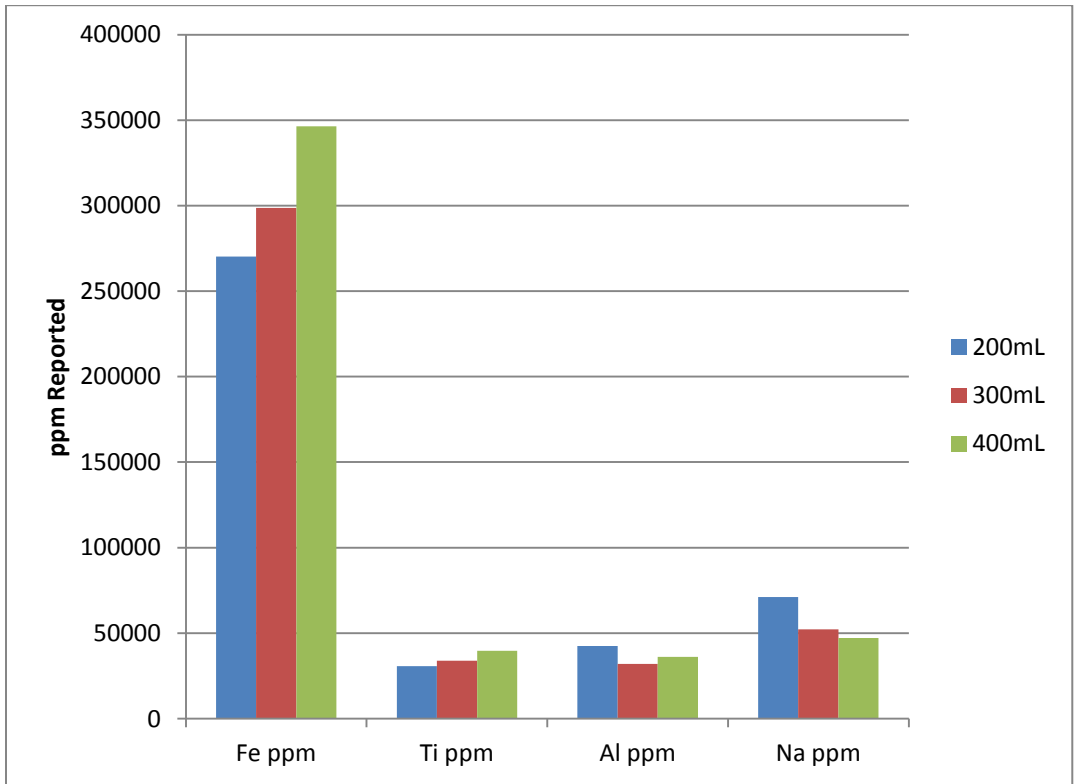


Figure B-9: 50% Excess Sodium Carbonate Roast Water Wash Solids Analysis

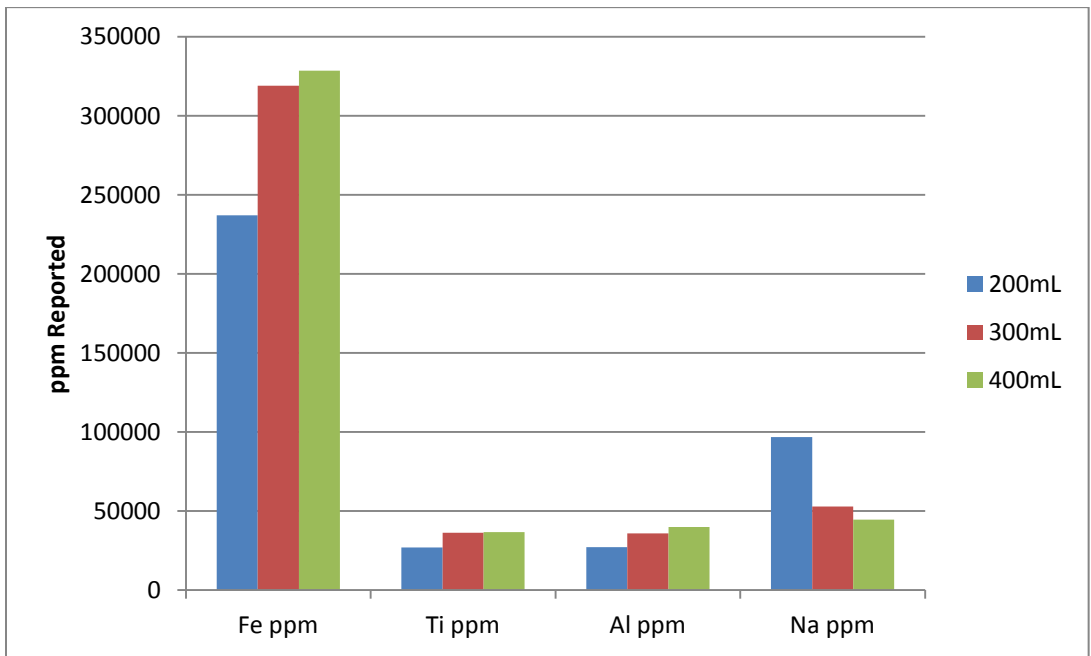


Figure B-10: 100% Excess Sodium Carbonate Roast Water Wash Solids Analysis

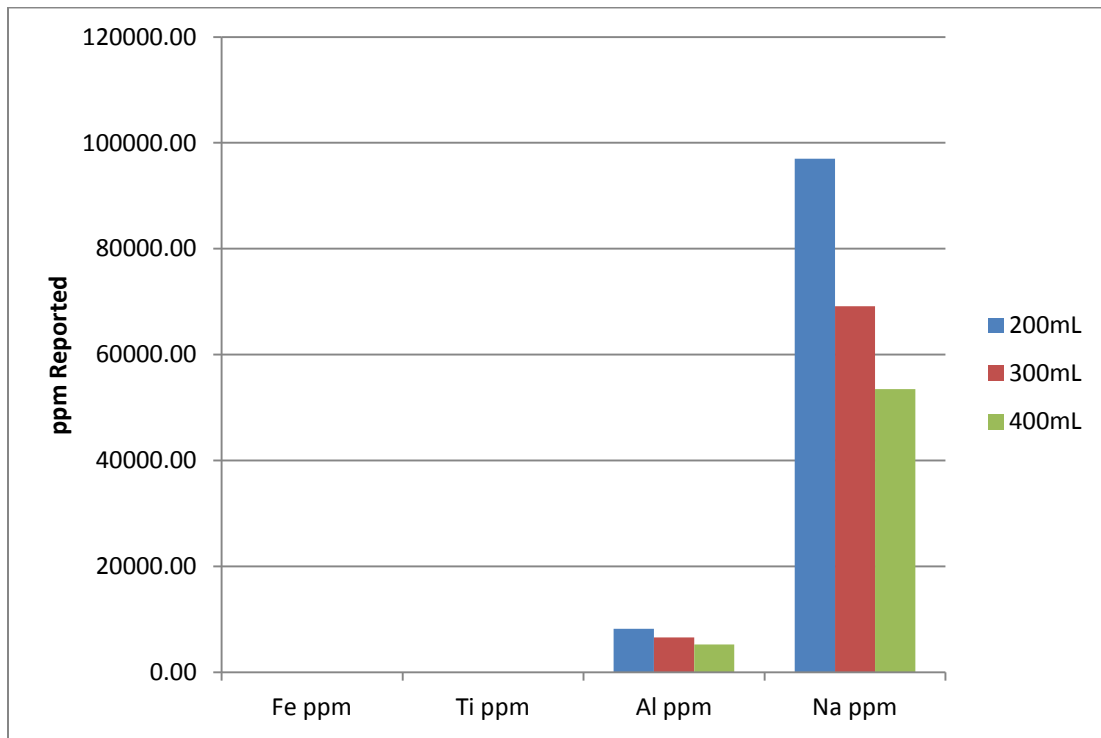


Figure B-11: 50% Excess Sodium Carbonate Roast Water Wash Liquids Analysis

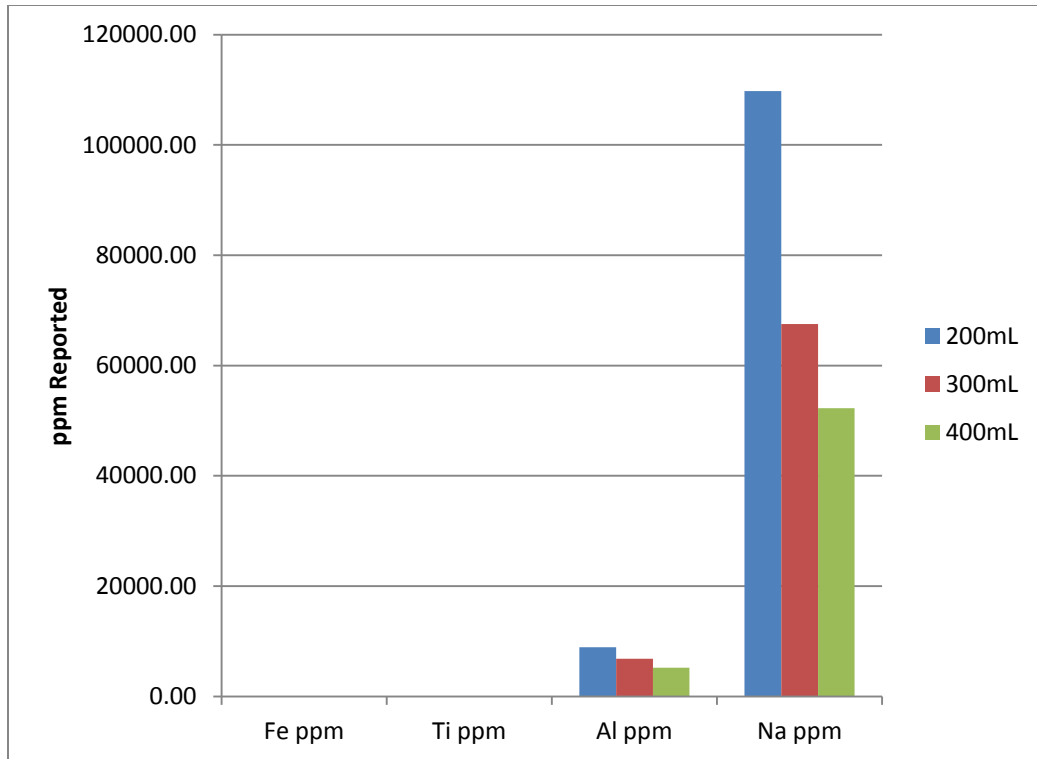


Figure B-12: 100% Excess Sodium Carbonate Roast Water Wash Liquids Analysis

APPENDIX C – CARBON ROASTS AND MAGNETIC SEPARATION

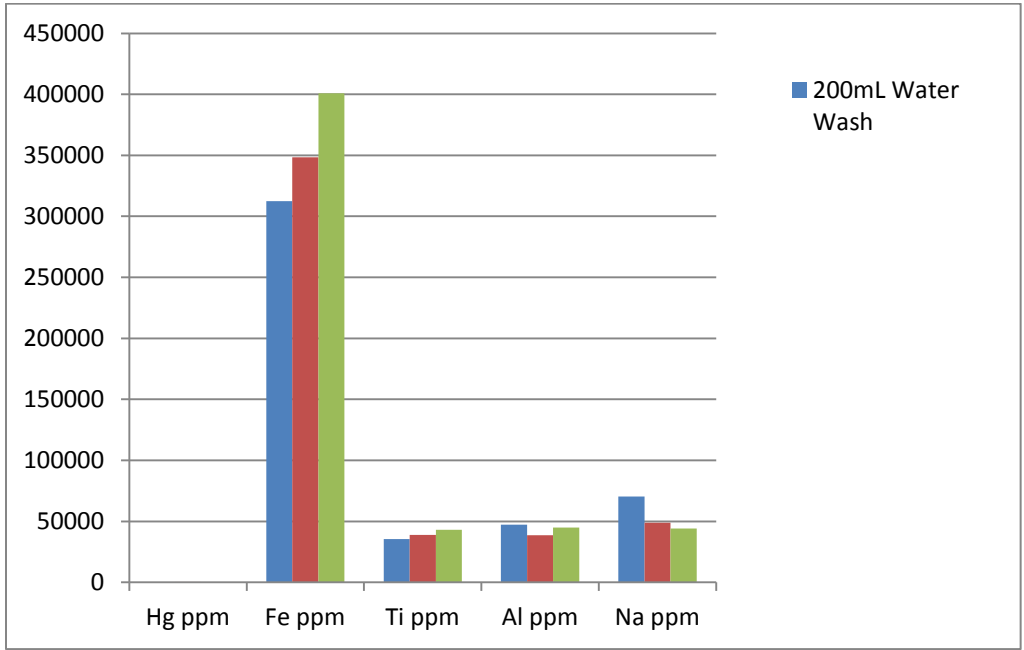


Figure C-13: From Dried Water Wash of 50% Excess Sodium Carbonate Roast and 50% Excess Carbon Roast, Magnetic Fraction

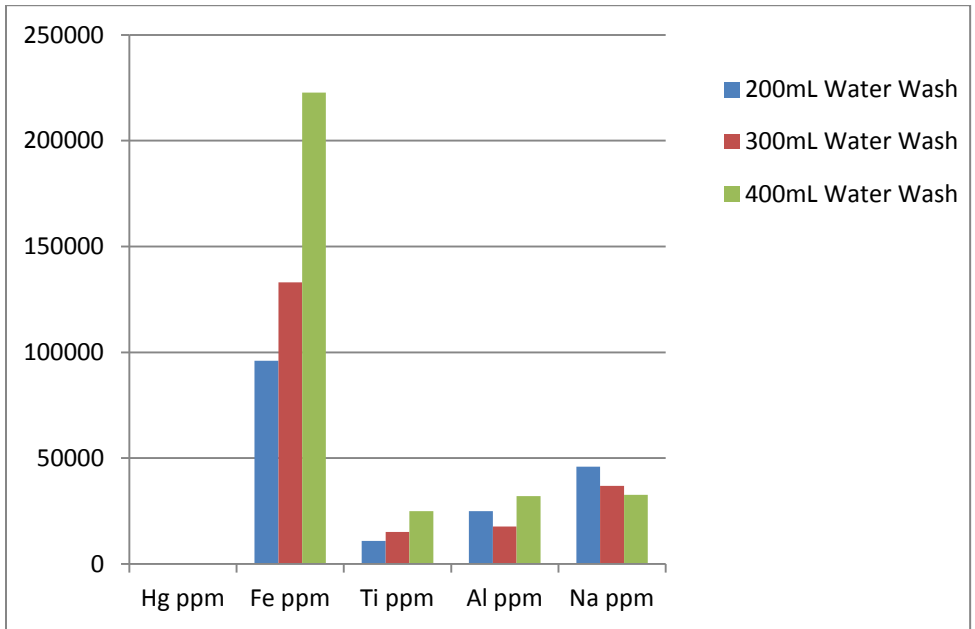


Figure C-14: From Dried Water Wash of 50% Excess Sodium Carbonate Roast and 50% Excess Carbon Roast, Non-Magnetic Fraction

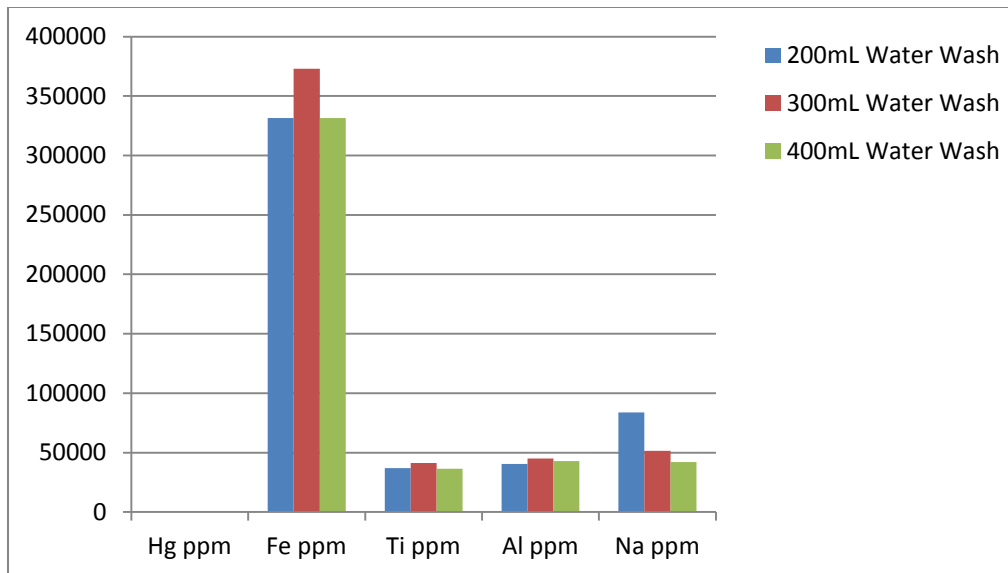


Figure C-15: From Dried Water Wash of 100% Excess Sodium Carbonate Roast and 50% Excess Carbon Roast, Magnetic Fraction

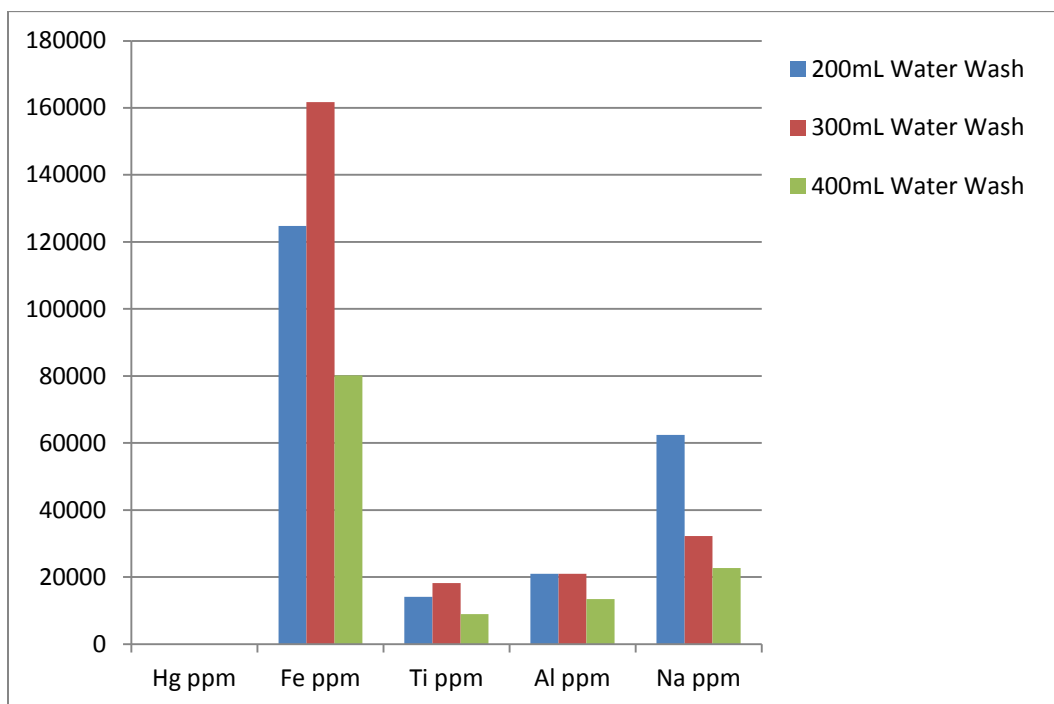


Figure C-16: From Dried Water Wash of 100% Excess Sodium Carbonate Roast and 50% Excess Carbon Roast, Non-Magnetic Fraction

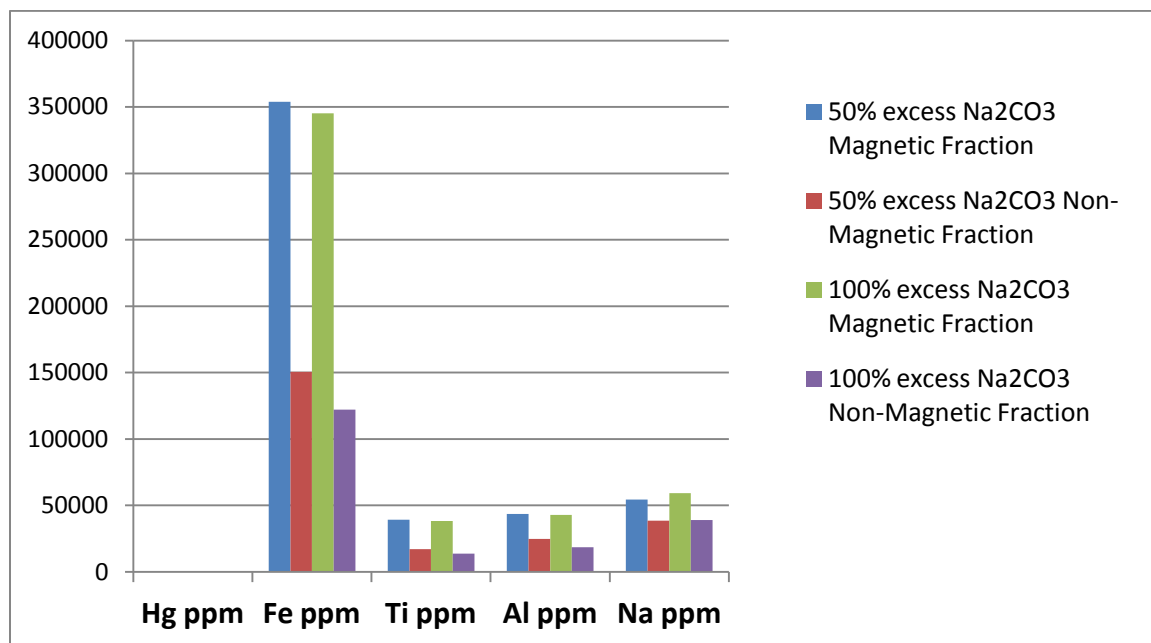


Figure C-17: Summary of Carbon Roasts and Magnetic Separation

APPENDIX D – FINAL WATER WASH RESULTS

Test Name	Amount Excess Na ₂ CO ₃ in Roast	Dry Solids	Liquid	Time Agitated
P81	75%	10g	40mL	60 min
P82	75%	10g	40mL	90 min
P83	75%	10g	40mL	120 min
P84	25%	10g	40mL	60 min
P85	25%	10g	40mL	90 min
P86	25%	10g	40mL	120 min

Table D-1: Final Water Wash Conditions

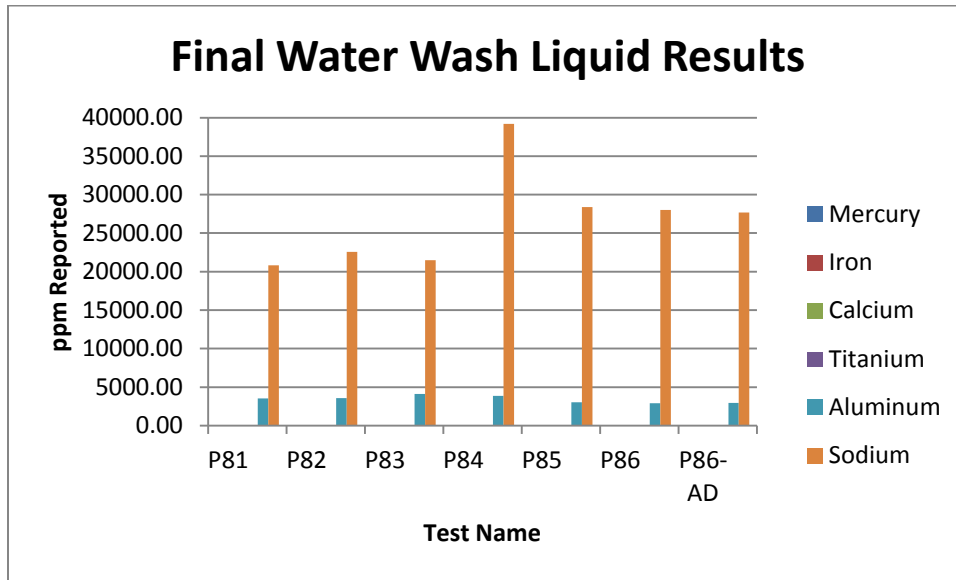


Figure D-18: Final Water Wash Liquid Results All Elements

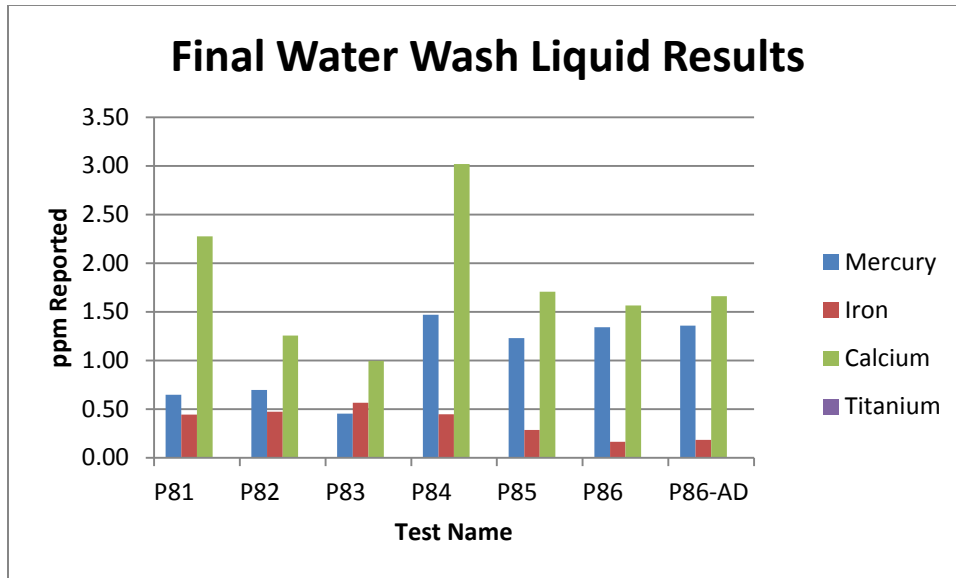


Figure D-19: Final Water Wash Liquid Results Excluding Al and Na

Table D-2: Final Water Wash Liquid Results

	Hg ppm	Fe ppm	Ca ppm	Ti ppm	Al ppm	Na ppm
Liquids						
P81	0.65	0.44	2.27	DL	3537	20831
P82	0.70	0.47	1.25	DL	3561	22547
P83	0.45	0.56	0.99	DL	4125	21480
P84	1.47	0.44	3.02	DL	3862	39190
P85	1.23	0.28	1.71	DL	3042	28405

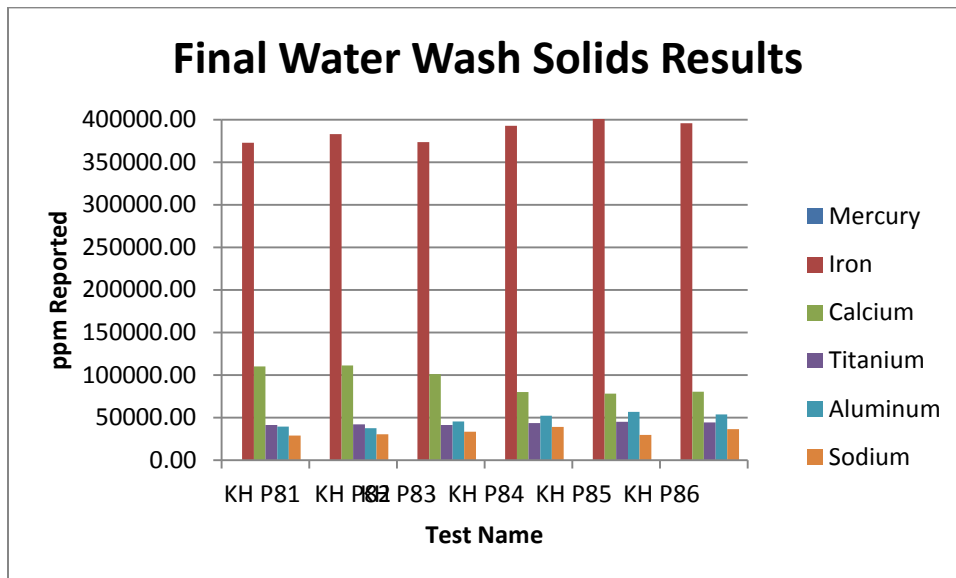


Figure D-20: Final Water Wash Solids Results All Elements

Table D-3: Final Water Wash Solid Results

solids	Hg ppm	Fe ppm	Ca ppm	Ti ppm	Al ppm	Na ppm
P81	DL	372890	109820	41011	39179	28706
P82	DL	382922	111285	41950	37309	30242
P83	DL	373717	100835	41288	45346	33242
P84	DL	392726	79888	43403	51965	39005
P85	DL	407807	78063	44944	56429	29623
P86	0.00	395580	80424	44103	53522	36406

APPENDIX E – FINAL MAGNETIC SEPARATION RESULTS

Table E-4: Final Water Wash Conditions

Test Name	Magnetic	Non Magnetic	Total Weight	% Magnetic
p88	4.16	0.78	4.94	84.21
p89	4.79	0.21	5.00	95.80
p90	4.61	0.29	4.90	94.08
p91	4.50	0.43	4.93	91.28
p92	4.23	0.73	4.96	85.28

APPENDIX F – FINAL SMELTING PHOTOGRAPHS



Figure F-21: Final Smelting Top View of Products Broken into Quarters



Figure F-22: Final Smelting Side View of Products Broken into Quarters



Figure F-23: Final Smelting Fe Buttons

APPENDIX G – SCANNING ELECTRON MICROSCOPE RESULTS

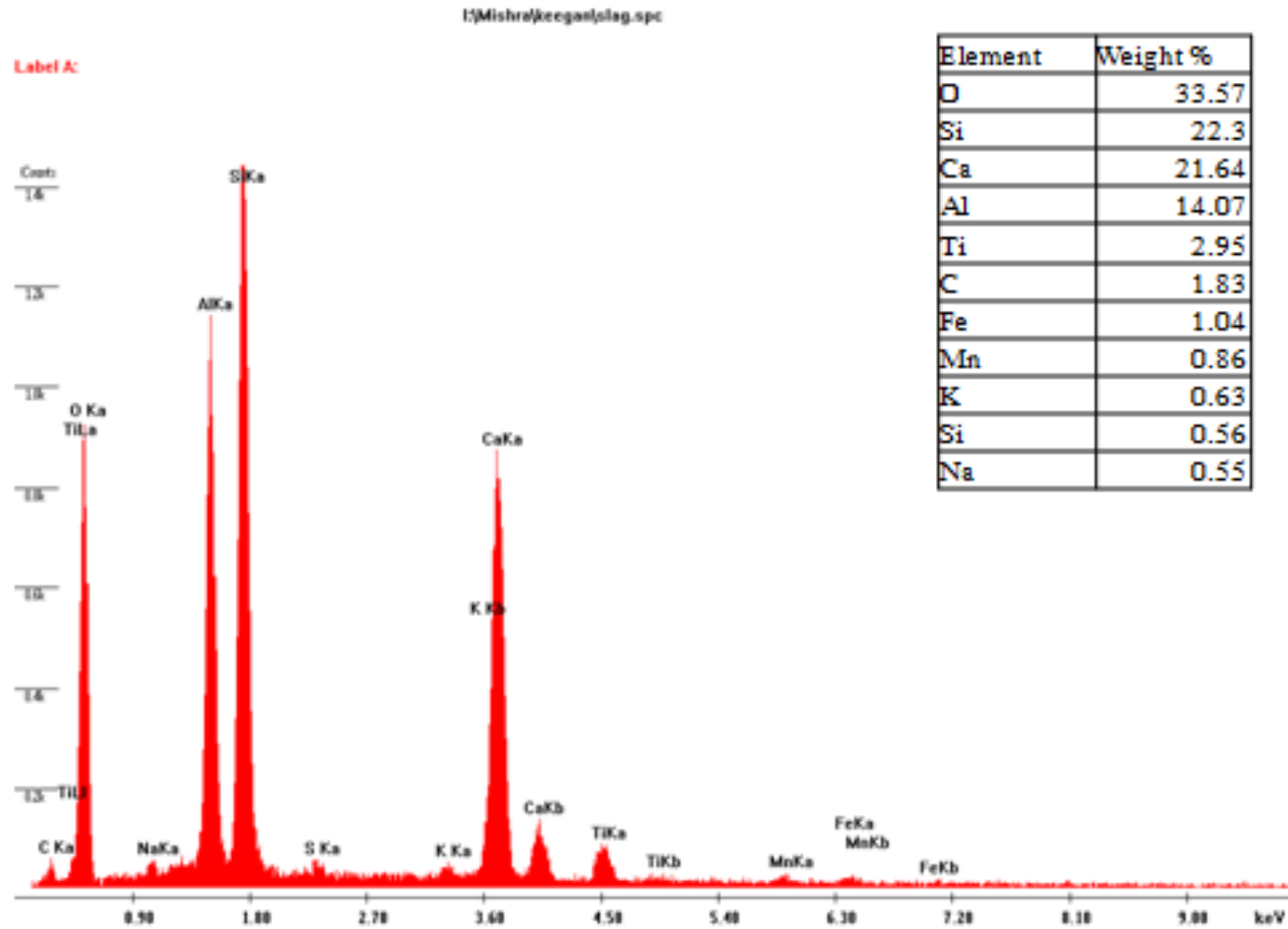


Figure G-24: Slag SEM XRay Peaks

I:\Mishra\keegan\button.spc

Label A:

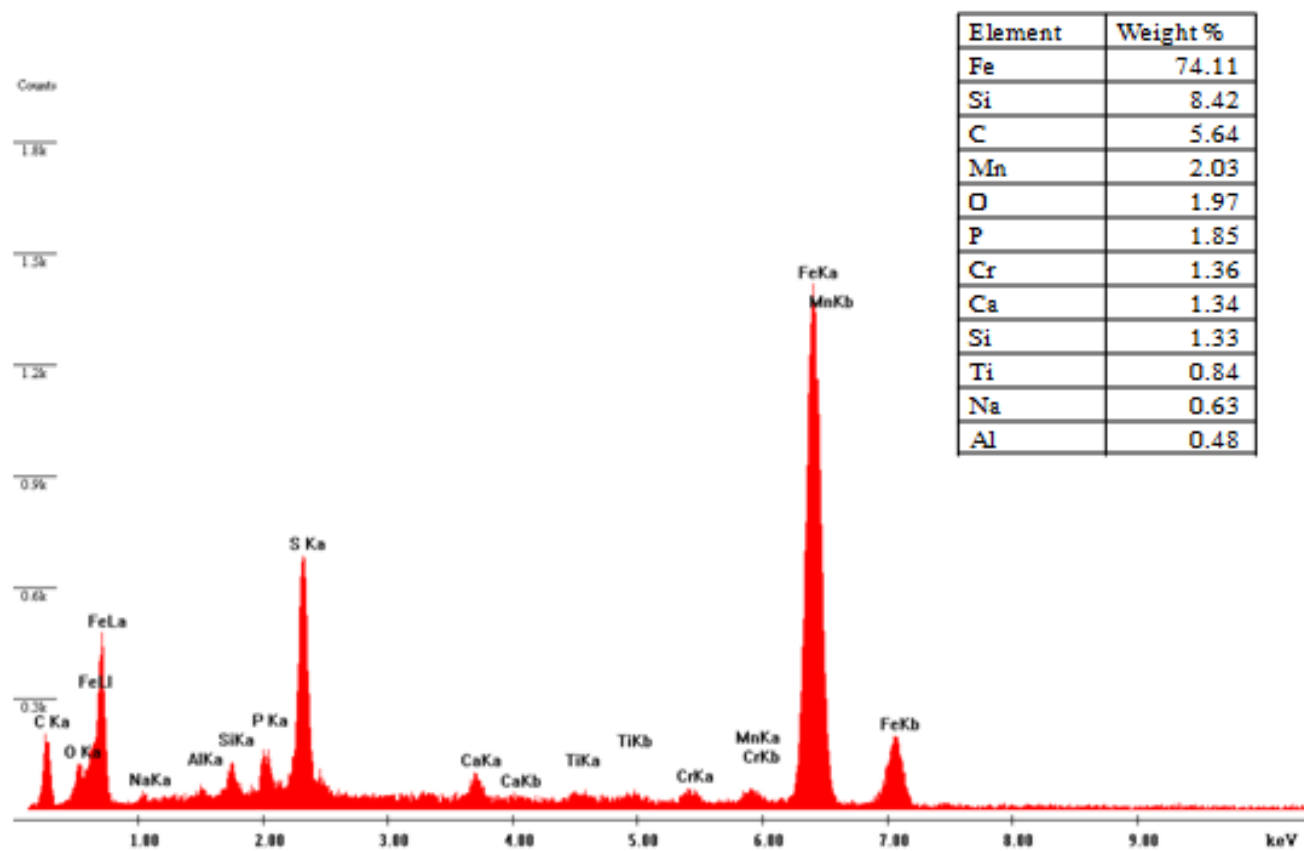


Figure G-25: Iron Button SEM XRay Peaks